

# BIBLIOGRAPHY

*Edited by*

Z. KOPAL

*University of Manchester, England*

M. MOUTSOULAS

*University of Athens, Greece*

J. W. SALISBURY

*Air Force Cambridge Research Laboratories, Bedford, Mass., U.S.A.*

and

F. B. WARANIUS

*Lunar Science Institute, Houston, Tex., U.S.A.*

## **1. Motion of the Moon in Space and Dynamics of the Earth-Moon System; Lunar Astronautics**

Arrhenius, G., Alfvén, H., and Fitzgerald, R.: 'Asteroid and Comet Exploration', NASA-CR-2291.

Exploration of Venus, Mars, and the Moon have had two major scientific objectives. One was to clarify the processes which control planetary evolution. The fulfillment of this purpose, although far from complete, was eminently successful in generating entirely new perspectives on the growth and differentiation of Earth. The second objective, particularly prominent in the planning of the lunar exploration, was to augment the understanding of the virtually unknown preplanetary history of the solar system. This would include the fundamental questions of the origin, emplacement, and state of matter gathered around the Sun and some planets. Preplanetary history also inquires into the problems of fractionation, condensation, and non-gravitation aggregation of circumsolar and circumplanetary matter.

Averbukh, A. I., Volokhov, Yu. D., and Koroleva, L. S.: 'Aiming Procedure in a Flight from the Moon to the Earth', *Cosmic Res.* **11**, 359–369.

The basic characteristics of the association of trajectories of flight from the Moon to the Earth, the conditions of landing at a given point on the Earth, and the necessary starting velocities are determined in the present article, and an evaluation of the dispersion is derived.

Egorov, V. A., Zolotukhina, N. I., and Teslenko, N. A.: 'Choice of Return Trajectory to Earth from Orbit of Artificial Moon Satellite', *Cosmic Res.* **11**, 350–358.

A solution is obtained for the problem of finding a return trajectory to Earth for a given time of descent from the orbit of an artificial Moon satellite when three given conditions are fulfilled at perigee. These conditions are satisfied through the choice of three components of the characteristic velocity for the transfer maneuver from the lunar orbit to the return trajectory. Motion within the Moon's sphere of influence is examined in a selenocentric coordinate system; outside this sphere, geocentric coordinates are used. The internal problem is solved both in the momentum and in the exact formulation (assuming the thrust vector is constant) and it joins the external problem through iteration over the three components of the selenocentric escape velocity from the sphere of influence (or, more exactly, of the corresponding velocity 'at infinity').

Giacaglia, G. E. O.: 'Lunar Perturbations on Artificial Satellites of the Earth', SAO Special Report 352.

Lunisolar perturbations for general terms of the disturbing function were derived by Kaula. However, his formulas use equatorial elements for the Moon and do not give a definite algorithm for computational procedures. As Kozai suggested, both inclination and node of the Moon's orbit with respect to the equator of the Earth are not simple functions of time, while the same elements with respect to the ecliptic are well approximated by a constant and a linear function of time, respectively. In the present work, we obtain the disturbing function for the Moon's perturbations using ecliptic elements for the Moon and equatorial elements for the satellite. Secular, long-period, and short-period perturbations are then computed, with the expressions kept in closed form in both inclination and eccentricity of the satellite. Alternative expressions for short-period perturbations of high satellites are also given, assuming small values of the eccentricity. The Moon's position is specified by the inclination, node, argument of perigee, true (or mean) longitude, and its radius vector from the center of the Earth. We can then apply the results to numerical integration by using coordinates of the Moon from ephemeris tapes or to analytical representation by using results from lunar theory, with the Moon's motion represented by a precessing and rotating elliptical orbit.

Lancaster, J. E.: 'Application of Matched Asymptotic Expansions to Lunar and Interplanetary Trajectories; Volume 1, Technical Discussion', NASA-CR-2255.

Previously published asymptotic solutions for lunar and interplanetary trajectories have been modified and combined to formulate a general analytical solution to the problem on  $N$ -bodies. The earlier first-order solutions, derived by the method of matched asymptotic expansions, have been extended to second order for the purpose of obtaining increased accuracy. The derivation of the second-order solution is summarized by showing the essential steps, some in functional form. The general asymptotic solution has been used as a basis for formulating a number of analytical two-point boundary value solutions. These include Earth-to-Moon, one- and two-impulse Moon-to-Earth, and interplanetary solutions. The results show that the accuracies of the asymptotic solutions range from an order of magnitude better than conic approximations to that of numerical integration itself. Also, since no iterations are required, the asymptotic boundary value solutions are obtained in a fraction of the time required for comparable numerically integrated solutions. The subject of minimizing the second-order error is discussed, and recommendations made for further work directed toward achieving a uniform accuracy in all applications.

Lancaster, J. E.: 'Application of Matched Asymptotic Expansions to Lunar and Interplanetary Trajectories; Volume 2: Derivations of Second-Order Asymptotic Boundary Value Solutions', NASA-CR-2256.

Previously published asymptotic solutions for lunar and interplanetary trajectories have been modified and combined to formulate a general analytical solution to the problem of  $N$ -bodies. The earlier first-order solutions, derived by the method of matched asymptotic expansions, have been extended to second order for the purpose of obtaining increased accuracy. The complete derivation of the second-order solution, including the application of a rigorous matching principle, is given. It is shown that the outer and inner expansions can be matched in a region of order  $\mu$  to the  $\alpha$  power, where  $\frac{2}{3} < \alpha < \frac{1}{2}$ , and  $\mu$  (the Moon/Earth or planet/Sun mass ratio) is much less than one. The second-order asymptotic solution has been used as a basis for formulating a number of analytical two-point boundary value solutions. These include Earth-to-Moon, one- and two-impulse Moon-to-Earth, and interplanetary solutions. Each is presented as an explicit analytical solution which does not require iterative steps to satisfy the boundary conditions. The complete derivation of each solution is shown, as well as instructions for numerical evaluation.

Mulholland, J. D., Shelus, P. J., and Silverberg, E. C.: 'Location of Lunakhod 2 from Laser Ranging Observations', *Cospar Inform. Bull.* **68**, 27-32.

The data thus far obtained by laser ranging on Lunakhod 2 are not capable of yielding very reliable positional determinations because of their sparseness. It has seemed possible, in spite of this, to give some general indication of the locations of the vehicle during its first two lunar nights and, perhaps more reliably, a measure of its net displacement during the intervening day. It would have been possible to produce systems of isochrones around the solution sites, corresponding to specifying one or more constraints on the solutions, but this did not seem profitable in view of the rover's continued motion.

It cannot be over-emphasized how encouraging our results are, considering the very short spans covered by the observations. On this basis, it appears quite reasonable to suppose that regular tracking of a reflector over a major fraction of one lunation would give a usable fix on the coordinates, given a good ephemeris. On the other hand, the results clearly illustrate the critical importance of a high quality lunar ephemeris to the interpretation of sparse data.

Oesterwinter, C. and Cohen, C. J.: 'New Orbital Elements for Moon and Planets', AD-755164.

A simultaneous solution is made for the orbital elements of Moon and planets. A modern Cowell integrator is used for orbit computations, and least-squares fits are made to some 40000 optical observations taken since 1913. The model includes relativistic terms, the leading zonal harmonics of Earth and Moon, the precession of the lunar equator, and the tidal couple between Earth and Moon. The solution also yields an extrapolation of the atomic time scale back to 1912.5. This solution is believed to be the only simultaneous improvement of the orbits of Moon and planets. The simultaneity is found to be an essential feature in separating the Moon's mean motion, the lunar tidal deceleration, and the corrections to the Earth rotation rate. It is now possible to refer all astronomical events of the past 60 years to a time with uniform rate, namely the atomic clock system. Considering the long baseline, this model should facilitate the prediction of fast variables, such as the lunar longitude, with considerably increased confidence.

Sharma, R. P. and Muldrew, D. B.: 'A Lunar Effect in the Occurrence of Conjugate Echoes on Topside Sounder Ionograms', *J. Geophys. Res.* **78**, 8251-8260.

Radio waves, transmitted by the Alouette 2 and Isis 1 satellites, can become trapped in magnetic field aligned ionization ducts, which can extend between the northern and southern hemispheres of the Earth. In a set of data containing  $1.8 \times 10^5$  ionograms recorded at five low-latitude telemetry stations from December 1965 to November 1971, conjugate echoes were observed on 4.5% of the ionograms. The frequency of occurrence of these echoes has a lunar semimonthly oscillation about the 4.5% average with an amplitude of  $(0.63 \pm 0.13)\%$  and with maximums at lunar ages of 4.9 and 16.9 hr (6 and 21 days after new moon). This oscillation occurs in independent blocks of data at very nearly the same lunar ages. The effect appears to depend on longitude, since it is found to be strongest in the data recorded at the American telemetry stations, intermediate at the African and Hawaiian stations, and weakest at the Asian and Australian stations. This effect is strongest for data recorded at the Quito telemetry station, where for data recorded between December 1965 and December 1966 a lunar semimonthly oscillation of amplitude  $(3.0 \pm 0.2)\%$  was found in the percentage occurrence of conjugate echoes. This semimonthly variation probably indicates that lunar tidal induced electric fields in the dynamo region have some influence in the production or duration of conjugate ducts; it is surprising, however, that no lunar diurnal or semidiurnal variation in occurrence frequency of conjugate ducts was found.

Williams, G. E.: 'Geotectonic Cycles, Lunar Evolution, and the Dynamics of the Earth-Moon System', *Mod. Geology* **4**, 159-183.

The concept of secular change in the obliquity of the ecliptic ( $\epsilon$ ), and the 'Prominence Hypothesis' for the origin of the solar system, previously deduced from study of the Earth's 'soft-rock' geological record, are the basis for new models of lunar evolution and cyclic tectonism on Earth.

It is envisaged that the Earth's spin axis changes attitude with respect to the ecliptic plane with a period of *c.* 2500 m.y., whilst the Moon maintains an orbit close to the ecliptic plane. By this model,

two independent lunar torques have thus been applied to the outer parts of the spinning Earth in regularly recurring cycles: (1) a *tidal torque*, due to the pull of the Moon on the Earth's tidal bulge, peaking when the Moon is in equatorial orbit ( $\epsilon = 0^\circ, 180^\circ$ ); and (2) a *precessional torque*, due to the pull of the Moon on the Earth's equatorial bulge, peaking when the Moon is in polar orbit ( $\epsilon = 90^\circ, 270^\circ$ ). Tidal and precessional torques have therefore peaked alternately about every 620 m.y., commencing with a peak tidal torque *c.* 3850 m.y. ago ( $\epsilon = 180^\circ$ ), and continuing through *c.* 3250 m.y. ( $270^\circ$ ), 2600 m.y. ( $0^\circ$ ), 2000 m.y. ( $90^\circ$ ), 1350 m.y. ( $180^\circ$ ), 750 m.y. ( $270^\circ$ ) and 130 m.y. ( $0^\circ$ ).

There was probably a close approach of the Moon between *c.* 3850 and 3250 m.y. ago, when the Moon was in effective retrograde orbit and the Earth possessed a rapid spin. Since then the Moon may have moved outward at varying rates dependent on the value of  $\epsilon$ .

This model plausibly explains major features of lunar evolution and structure: (1) an initial hot Moon; (2) antipodal concentration of radioactive lunar crust; (3) lunar remanent magnetism; (4) time of major impact cratering; and (5) mare volcanism, which correlates with the probable close approach of the Moon between *c.* 3850 and 3250 m.y. ago.

The major episodes or 'modes' of crustal tension on Earth are also explained by the model of a dynamic Earth-Moon system. The formation of Archaean greenstone belts *c.*  $3250 \pm 250$  m.y. ago, the continental disruption and diastrophism of the Archaean-Proterozoic transition *c.*  $2600 \pm 200$  m.y. ago, the continental fragmentation, through formation, dyke intrusion, and mafic and alkaline magmatism of the Proterozoic (*c.*  $2000 \pm 200, 1350 \pm 200$  and  $750 \pm 150$  m.y. ago), and the breakup and dispersal of Pangaea during the Mesozoic all correlate with the proposed scheme of peak tidal and precessional torques. Global diastrophism was particularly marked *c.* 2600 and 130 m.y. ago, when the Moon was in prograde, equatorial orbit ( $\epsilon \simeq 0^\circ$ ). The close agreement between theory and geological observation forcefully argues that the periodicity of crustal tension reflects the proposed vicissitudes of the Earth-Moon system. It is considered that during intervals of minimal lunar torque dispersed continents reassembled by means of inertial plate-motions resulting from deceleration of the Earth's rotation by an internal 'brake.'

The present model of a dynamic Earth-Moon system amply confirms Sutton's concept of the 'chelogenic cycle,' and offers new insights into major problems of planetology and cosmology.

## 2. Motion of the Moon About Its Centre of Gravity (Librations)

Peale, S. J.: 'Some Effects of Elasticity on Lunar Rotation', NASA-CR-132046.

A general Hamiltonian function for a rotating Moon in the field of the Earth is expanded in terms of parameters orienting the spin angular momentum relative to the principal axes of the Moon and relative to coordinate axes fixed in the orbit plane. The effects of elastic distortion are included as modifications of the moment of inertia tensor, where the magnitude of the distortion is parameterized by the Love number.

## 4. Internal Structure of the Moon

Anderson, D. L.: 'The Moon as a High Temperature Condensate', NASA-CR-132209.

The accretion during condensation mechanism is used to explain the differences in composition of the terrestrial planets and the Moon. Many of the properties of the Moon, including the enrichment in Ca, Al, Ti, U, Th, Ba, Sr and the REE and the depletion in Fe, Rb, K, Na and other volatiles can be understood if the Moon represents a high temperature condensate from the solar nebula. Thermodynamic calculations show that Ca, Al and Ti rich compounds condense first in a cooling nebula. The high temperature mineralogy is gehlenite, spinel perovskite, Ca-Al-rich pyroxenes and anorthite. The model is consistent with extensive early melting, shallow melting at 3 AE and with presently high speed internal temperatures it is predicted that the outer 250 km is rich in plagioclase and FeO. The low iron content of the interior in this model raises the interior temperatures estimated from electrical conductivity by some  $800^\circ\text{C}$ . The lunar crust is 80% gabbroic anorthosite, 20% basalt and is about 250-270 km thick. The lunar mantle is probably composed of spinel, merwinite and diopside with a density of 3.4 g/cu cm.

Kovach, R. L. and Watkins, J. S.: 'The Structure of the Lunar Crust at the Apollo 17 Site', *Proceedings of the Fourth Lunar Science Conference, Geochim. Cosmochim. Acta* **3**, Suppl. 4, 2549–2560.

A seismic profiling experiment was successfully executed on the lunar surface during the Apollo 17 mission allowing a determination of the structure of the lunar crust to a depth of several kilometers. The most outstanding feature of the seismic velocity variation, in the Taurus-Littrow region, is the stepwise increase with depth. A total thickness of about 1200 m for the infilling mare basalts at the 17 landing site is also indicated from the seismic results. The apparent velocity is high (about  $4 \text{ km s}^{-1}$  for  $P$  waves) in the material below the basalts.

Latham, G., Dorman, J., Duennebie, F., Ewing, M., Lammlein, D., and Nakamura, Y.: 'Moonquakes, Meteoroids, and the State of the Lunar Interior', *Proceedings of the Fourth Lunar Science Conference, Geochim. Cosmochim. Acta* **3**, Suppl. 4, 2515–2527.

Analysis of data returned from the four stations of the Apollo Seismic Network has revealed that the lunar interior can be divided into two major zones: a rigid, dynamically inactive outer shell, about 1000 km thick (the lunar lithosphere); and a relatively weak central zone (the lunar asthenosphere) in which partial melting is probable. The transition between these two zones is gradual. Seismic activity within the Moon is far below that of the Earth. The small moonquakes that do occur originate near the base of the lithosphere, and appear to fall within two major belts. Tidal energy appears to be an important, if not the dominant, source of energy released as moonquakes. A secular component of moonquake energy release may result from slight thermal expansion or contraction of the Moon, weak convection in the asthenosphere, or secular recession of the Moon from the Earth. Lack of shallow moonquake activity implies that the Moon is neither expanding nor contracting at an appreciable rate at present. The mass flux of meteoroids that collide with the Moon to produce detectable seismic signals, appears to be between 1 and 3 orders of magnitude lower than that predicted from Earth-based measurements. The largest meteoroid impacts have occurred each year during the months of April through July. This clustering suggests the presence of a distinct meteoroid population of as yet unexplained origin.

Wang, H., Todd, T., Richter, D., and Simmons, G.: 'Elastic Properties of Plagioclase Aggregates and Seismic Velocities in the Moon', *Proceedings of the Fourth Lunar Science Conference, Geochim. Cosmochim. Acta* **3**, Suppl. 4, 2663–2671.

The compressional velocities of Apollo 16 gabbroic anorthosites in which the cracks have been closed match the seismic velocity of  $7 \text{ km s}^{-1}$  in the 25 to 65 km depth region of the Moon beneath the Imbrium Basin. The intrinsic velocities of plagioclase aggregates indicate that a velocity of  $7 \text{ km s}^{-1}$  in a highly calcic gabbroic anorthosite is consistent only with a very small pyroxene component. Because mare basalts and gabbroic-anorthosites both have intrinsic velocities of  $7 \text{ km s}^{-1}$ , the laboratory velocity data do not require a compositional change from basalt to anorthosite at the 25 km discontinuity. The laboratory velocity data only imply that the 25 km seismic discontinuity is one of micro-crack density. The physical rather than the chemical or mineralogical state is constrained.

Watkins, J. S. and Kovach, R. L.: 'Seismic Investigation of the Lunar Regolith', *Proceedings of the Fourth Lunar Science Conference, Geochim. Cosmochim. Acta* **3**, Suppl. 4, 2561–2574.

Seismic investigation of the lunar regolith shows that the regolith consists of a layer with an average velocity of  $105 \text{ m s}^{-1}$ . Seismically determined regolith thicknesses in the highlands average 10 m, about twice the thickness deduced from astronaut observations and photographs from the maria. The difference in thickness is thought to be due to a depositional rate about one order of magnitude greater during the interval between formation of the circular maria and the extrusion of mare basalts than during the post-extrusion interval.

Seismic velocities observed in the regolith indicate that the regolith consists primarily of impact derived ejecta. The regolith at the Apollo 17 site is anomalously thick, probably because the site is in

the midst of a crater field and because of irregularities in the surface of the underlying subfloor basalt. The Apollo 17 seismic data do not support the compacted powder model of the lunar near surface but show that the lunar crust to a depth of over 1 km consists of horizontal or subhorizontal strata comprised of breccia, lava flows, and rock.

### 5. Thermal and Stress History of the Moon

Albee, A. L., Gancarz, A. J., and Chodos, A. A.: 'Metamorphism of Apollo 16 and 17 and Luna 20 Metaclastic Rocks at about 3.95 AE: Samples 61156, 64423, 14-2, 65015, 67483, 15-2, 76055, 22006, and 22007', *Proceedings of the Fourth Lunar Science Conference, Geochim. Cosmochim. Acta* 1, Suppl. 4, 569-595.

Isotopically-dated metamorphic rocks from the Apollo 16 and 17 and Luna 20 landing sites exhibit not only similar petrographic and mineralogic characteristics, but also a limited spread of recrystallization ages at about 3.95 b.y. The rocks are typically rich in plagioclase, low-Ca pyroxene and olivine and include a variety of rock and mineral clasts. These clasts clearly indicate a polymict origin. The most probable protolith is an agglutinate of mineral and rock fragments cemented by glass, which in some samples was of KREEP composition. High-temperature metamorphism, probably accompanied by some partial melting, resulted in an intergranular reaction responsible for the development of (1) coarser matrix material, (2) reaction rims on clasts, and (3) a poikilitic texture. Such metaclastic rocks with recrystallization ages of about 3.95 b.y. appear to blanket large portions of the Moon and are critical to deciphering early lunar history.

Bence, A. E., Papike, J. J., Sueno, S., and Delano, J. W.: 'Pyroxene Poikiloblastic Rocks from the Lunar Highlands', *Proceedings of the Fourth Lunar Science Conference, Geochim. Cosmochim. Acta* 1, Suppl. 4, 597-611.

The results of detailed petrographic, X-ray, electron microprobe, ion probe, and  $^{40}\text{Ar}/^{39}\text{Ar}$  age studies of pyroxene poikiloblastic breccias, an important lunar highlands lithology, are interpreted to indicate that high grade metamorphic recrystallization occurred over wide regions of the Moon at about 4.0 G.y. This metamorphism was probably related to a period of high meteorite influx at that time. The temperatures achieved were highly variable but in some cases were sufficiently intense to cause varying degrees of partial melting of the precursor highlands breccias. A complete spectrum of metamorphic grades from only slight recrystallization to virtually complete melting would be expected in such a model. Such a spectrum is observed in the Apollo 16 rocks.

Birck, J. L. and Allegre, C. J.: 'Ages, Rb-87 Sr-87 of Soil and Rock Fragments Brought from the Lunar Mountains by Luna 20', NASA-TT-F-14981.

Results are reported on Rb-87 and Sr-87 found in fragments from the Luna 20 mission. The results show a low radiogenic character, but clearly demonstrate the presence of high K components. A model for lunar evolution is presented.

Chao, E. C. T.: 'The Petrology of 76055, 10, a Thermally Metamorphosed Fragment-Laden Olivine Micronorite Hornfels', *Proceedings of the Fourth Lunar Science Conference, Geochim. Cosmochim. Acta* 1, Suppl. 4, 719-732.

Polished thin section 76055,10 is that of an olivine-bearing micronorite hornfels with abundant xenocrysts and xenoliths. It consists of two parts: a large clast of olivine micronorite hornfels with well-developed porphyroblastic texture, surrounded by highly vesicular olivine micronorite hornfels with incipient development of the porphyroblastic textures. This rock contains xenoliths of granulated dunite, xenocryst-laden olivine-plagioclase rocks, granulated and recrystallized anorthosite, annealed shock-vitrified plagioclase glass, and well polygonized anorthosite.

Pink spinels with radial anorthite rims occur in both the clast and the surrounding matrix. Many anorthite xenocrysts inside the clast have overgrowths of anorthite separated by a ring of olivine blebs. Olivine and porphyroblasts of orthopyroxenes in the clast are generally slightly more magnesian than those in the surrounding matrix. Plagioclase inside the clast is also slightly more calcic than that outside. The clast is richer in plagioclase and olivine whereas orthopyroxene is more predominant in the matrix. Nickel-iron particles are present in both parts. Apparently only armalcolite is present inside the clast whereas in addition to armalcolite with sieve texture, some ilmenite cores surrounded by armalcolite still exist in the surrounding matrix.

The texture of this rock is metamorphic, probably the result of sustained reheating and annealing. The clast and the surrounding matrix were heated to temperatures probably in excess of 1000°C, assuming an oxygen fugacity of between  $10^{-12}$  to  $10^{-15}$  bars.

It is possible that 76055 itself is a clast enclosed in or in contact with some other melt rock. It was not shocked by impact after the thermal metamorphism.  $^{40}\text{Ar}/^{39}\text{Ar}$  age of 4.0 b.y. dates its last metamorphic episode.

Crawford, M. L.: 'Crystallization of Plagioclase in Mare Basalts', *Proceedings of the Fourth Lunar Science Conference, Geochim. Cosmochim. Acta* 1, Suppl. 4, 705-717.

A detailed study has been made of the morphology, zoning and major- and minor-element chemistry of plagioclase in mare basalt 12021 and for comparison, in several other mare basalts. Two types of plagioclase can be distinguished based on growth rate as expressed by the formation of hollow as opposed to lath-shaped crystals. The liquidus plagioclase is the most sodic part of the hollow crystals and is more sodic than the lath-shaped crystals. Hollow grains show oscillatory zoning, whereas the lath-shaped grains show normal zoning. The ratios  $\text{FeO}/(\text{FeO} + \text{MgO})$  and  $\text{K}_2\text{O}/(\text{K}_2\text{O} + \text{Na}_2\text{O})$  increased in both types of plagioclase as they grew, and these ratios can be used as a guide to the crystallization history of the plagioclase. The  $\text{FeO}/(\text{FeO} + \text{MgO})$  ratios are similar to those of coprecipitating pyroxene. The cause of the excess of Si and deficiency of Al for mare plagioclases may be a function of cooling rate or composition and structure of the melt. The data presented here suggest the onset of plagioclase nucleation is primarily controlled by magma composition, and the point at which the magma becomes supersaturated with plagioclase.

Cukierman, M., Klein, L., Scherer, G., Hopper, R. W., and Uhlmann, D. R.: 'Viscous Flow and Crystallization Behavior of Selected Lunar Compositions', *Proceedings of the Fourth Lunar Science Conference, Geochim. Cosmochim. Acta* 3, Suppl. 4, 2685-2696.

The flow characteristics of lunar compositions 15555 and 68502 have been determined over a wide range of viscosity. The temperature ranges covered by the measurements are 1201-1410°C and 622-695°C for the 15555 composition and 1261-1515°C and 725-840°C for 68502 composition. Reliable data could not be obtained over the intermediate ranges of temperature because of the occurrence of crystallization. The experimental data in the high temperature regions are found to be in close agreement with predictions of the semi-empirical model of Bottinga and Weill. The results on these compositions are compared with previous data on other lunar compositions and on anorthite; and the importance of the flow behavior in interpreting lunar flows and phase morphologies is emphasized.

Data are also reported on the kinetics of crystallization of the 15555 composition over the temperature interval from 700 to 1020°C. The growth rate data are combined with the viscosity data to construct a reduced growth rate vs. undercooling relation. The form of this relation, which exhibits positive curvature, is suggestive of growth by a surface nucleation mechanism; but a plot of logarithm (growth rate  $\times$  viscosity) vs  $1/T\Delta T$  does not display the straight-line form expected by the standard models for such a growth mechanism. It does, however, have the form suggested by recent computer simulations of crystal growth. The combined data are also used to construct a time-temperature-transformation curve corresponding to a barely-detectable degree of crystallinity. From this curve, the cooling rate required to form a glass of composition 15555 and the maximum thickness obtainable as a glass are estimated. This composition is found to be more difficult than previously investigated lunar compositions to form as a glass; and it is unlikely that specimens of this or closely similar compositions can be obtained as amorphous solids for sizes larger than about 0.5 cm.

Delano, J. W., Bence, A. E., Papike, J. J., and Cameron, K. L.: 'Petrology of the 2–4 mm Soil Fraction from the Descartes Region of the Moon and Stratigraphic Implications', *Proceedings of the Fourth Lunar Science Conference, Geochim. Cosmochim. Acta* **1**, Suppl. 4, 537–551.

Three hundred forty-two thin sections of 2–4 mm soil fragments from 8 of the 10 Apollo 16 sampling stations have been examined by optical petrographic and electron microprobe techniques. No fewer than twenty-eight fragments were studied from each station. A lithologic classification based on textural and chemical data has been devised and subsequently correlated with  $^{40}\text{Ar}/^{39}\text{Ar}$  age determinations. The data indicate that the Apollo 16 landing site is a geologically old and complex highland region consisting of stratified, impact generated, base surge deposits overlying a lower dark-colored layer dominated by 4.0 b.y. old volcanic rock debris. The most abundant rock types observed are microbreccias, although nearly 20% of the 2–4 mm samples are volcanic in origin. No major lithologic differences have been observed to exist between the Cayley Plain and Stone Mountain. A mare basalt sample, probably derived from Mare Nectaris, indicates that both the mineralogy and time of crystallization of mare basalts within Mare Nectaris, Tranquillitatis, and Serenitatis are very similar.

The inferred subsurface structure at the Apollo 16 landing site suggests that at least most of the presently observed lunar basins were excavated less than about 4.0 b.y. ago.

Dowty, E., Kell, K., and Prinz, M.: 'Major-Element Vapor Fractionation on the Lunar Surface: An Unusual Lithic Fragment from the Luna 20 Fines', *Earth Planetary Sci. Letters* **21**, 91–96.

A 250- $\mu\text{m}$  fragment in the Luna 20 fines has a very fine-grained 'igneous' texture and has the composition (wt. %):  $\text{SiO}_2$ , 41.1;  $\text{TiO}_2$ , 0.35;  $\text{Al}_2\text{O}_3$ , 27.2;  $\text{Cr}_2\text{O}_3$ , 0.14;  $\text{FeO}$ , 4.2;  $\text{MnO}$ , 0.06;  $\text{MgO}$ , 8.5;  $\text{CaO}$ , 17.8;  $\text{Na}_2\text{O}$ , 0.05; and  $\text{K}_2\text{O} < 0.02$ . It contains  $\sim 65\%$  plagioclase  $\text{An}_{99-100}$ ,  $\sim 15\%$  olivine  $\text{Fo}_{90}$ ,  $\sim 2\%$  Mg–Al spinel and the remainder an unusual interstitial phase with composition  $\text{SiO}_2$ , 34.8;  $\text{TiO}_2$ , 1.78;  $\text{Al}_2\text{O}_3$ , 18.3;  $\text{Cr}_2\text{O}_3$ , 0.04;  $\text{FeO}$ , 14.1;  $\text{MnO}$ , 0.22;  $\text{MgO}$ , 5.0;  $\text{CaO}$ , 24.1;  $\text{Na}_2\text{O}$ , 0.34;  $\text{K}_2\text{O} < 0.02$ . This fragment probably represents a portion of a normal highland rock (anorthositic norite) which was heated to a very high temperature by impact, lost volatiles including  $\text{SiO}_2$ , and then partially crystallized. The observed phases and their inferred crystallization sequence are consistent with experimental results in the system  $\text{CaO} \pm \text{MgO} \pm \text{Al}_2\text{O}_3 \pm \text{SiO}_2$ , assuming the unusual phase to be a residual glass. This type of internal fractionation, leading to silica depletion in the residuum, is different from that normally observed in lunar rocks and is attributed to slightly lower bulk  $\text{SiO}_2$  resulting from vapor fractionation due to impact (which also results in lower  $\text{Na}_2\text{O}$  and other volatiles). Because differentiation of the type shown by this fragment is rare in lunar materials, we infer that such major-element vapor fractionation is uncommon on the surface of the Moon. The experimental  $\text{CaO} - \text{MgO} - \text{Al}_2\text{O}_3 - \text{SiO}_2$  phase relations also have a bearing on the lunar model proposed by D. L. Anderson in 1973: his 'refractory' original lunar composition would differentiate to produce silica deficient liquids, like the unusual phase in our fragment, rather than the normal lunar crustal rocks.

Frick, U., Beaur, H., Funk, H., Phinney, D., Schäfer, C., Schultz, L., and Signer, P.: 'Diffusion Properties of Light Noble Gases in Lunar Fines', *Proceedings of the Fourth Lunar Science Conference, Geochim. Cosmochim. Acta* **2**, Suppl. 4, 1978–2002.

Diffusion properties of He, Ne, and Ar in several green glass fractions and one olivine separate of lunar soil 15421 have been studied in linear heating experiments, complimented by bulk measurements. From the release patterns, a solar origin of practically all  $^{36}\text{Ar}$  from both components can be deduced. Evaluation of thermal history influences were attempted by investigating green glass samples tempered for 47 h at 600°C. In this process all gases normally released up to 600°C are lost, but above about 700°C the release patterns of the gases from the tempered and not tempered samples are very similar. The linear 'reheating' technique, as a sequence of linear heatings on the same sample, gives results which substantiate this observation. The study of samples bombarded with 2 keV Ar ions, to simulate the proposed retrapping mechanism for the excess  $^{40}\text{Ar}$ , reveals the fundamental difference between the release patterns of artificially implanted and "natural"  $^{40}\text{Ar}$ . As a consequence a different mechanism to understand the excess  $^{40}\text{Ar}$  must be considered. This matter will be discussed in a separate



paper. Extensive model calculations based on Fick's diffusion law, the Arrhenius equation, and simple geometry were carried out. The results show that applications or deductions on the ground of a simple diffusion model with one activation energy have to be met with great caution. Measurements on authigenic quartz serve as an independent check of our interpretations.

Ghose, S. and Wan, C.: 'Luna 20 Pyroxenes: Evidence for a Complex Thermal History', *Proceedings of the Fourth Lunar Science Conference, Geochim. Cosmochim. Acta* **1**, Suppl. 4, 901–907.

X-ray diffraction and microprobe study of a pigeonite grain,  $\text{Wo}_7\text{En}_{60}\text{Fs}_{33}$  from the Luna 20 regolith show exsolved coarse augite lamellae parallel to (001) and (100), a finer set of second generation augite lamellae parallel to (001) and rods of exsolved chromite spinel nearly parallel and perpendicular to (001); in addition, the clinobronzite in the pigeonite is partially inverted to bronzite. These features indicate a fairly slow cooling in a relatively shallow magma chamber. This pigeonite most likely comes from the original lunar crust.

Orthopyroxene grains from the Luna 20 regolith show exsolved fine augite lamellae in twinned orientation parallel to (100). In addition, diffuse X-ray diffraction streaks parallel to  $a^*$  connecting Bragg reflections indicate stacking faults parallel to (100). The intensity distribution in the diffuse streaks around a Bragg reflection is asymmetric, the intensity being high in positions expected for clinobronzite, indicating the possible presence of very fine clinobronzite lamellae. Site occupancy refinement in connection with the crystal structure analysis of a Luna 20 orthopyroxene ( $\text{En}_{70}\text{Fs}_{26}\text{Wo}_4$ ) indicates a very high degree of cation disorder ( $K_D = 0.216$ ) and a cation equilibration temperature of  $\sim 900^\circ\text{C}$ . These features in the orthopyroxene grain indicate a post-crystallization shock-effect due to meteorite impact, which erased the earlier crystallographic record.

Gooley, R. C., Brett, R., and Warner, J. L.: 'Crystallization History of Metal Particles in Apollo 16 Rake Samples', *Proceedings of the Fourth Lunar Science Conference, Geochim. Cosmochim. Acta* **1**, Suppl. 4, 799–810.

Electron microprobe analyses for Fe, Co, Ni, S, and P have been carried out on the metal and associated troilite, schreibersite, and rare cohenite in the Apollo 16 rake samples from Stations 1, 4, and 13. The Co/Ni ratios of most of the metal are within the limits of meteoritic metal as defined by Goldstein and Yakowitz. The large abundance of schreibersite in all of the lithic types except the poikilitic rocks suggests that much of it may be of lunar origin. The near-absence of schreibersite in the poikilitic rocks may be a result of P diffusion from the metal to the surrounding silicate at low temperature. Application of the compositional data for the coexisting metal-schreibersite pairs to isotherms in the system Fe–Ni–P indicates a sequence of progressively lower temperatures of equilibration (and probably a corresponding sequence of slower cooling rates) of these phases from the devitrified glasses, to the mesostasis-rich rocks, to the diabases, to the poikilitic rocks.

Grieve, R. A. F. and Plant, A. G.: 'Partial Melting on the Lunar Surface, as Observed in Glass Coated Apollo 16 Samples', *Proceedings of the Fourth Lunar Science Conference, Geochim. Cosmochim. Acta* **1**, Suppl. 4, 667–679.

Apollo 16 samples 64455,35, a crystalline highland basalt, and 65075,9, a recrystallized anorthositic gabbro breccia with clasts of gabbroic anorthositic microbreccia, have adhering glass coats and injection veins of highland basalt composition. The coatings represent splashed on impact melted material of similar composition to that of the crystalline rocks and not the fusion products of earlier surfaces of the samples.

Heat supplied by the splash glass has been sufficient to produce zones of partial melting within the crystalline portions of the samples. The analytical data indicate a possible genetic relationship, on a small scale, between anorthositic and Fra Mauro basalt compositions through the low pressure partial melting of materials with highland basalt composition. The partial melts have major element compositions similar to Fra Mauro basalts, but with slightly lower FeO (5.8–9.3), while the residual crystalline materials are relatively anorthositic, being enriched in the plagioclase component. Variation

in the degree of melting and the composition of the parent lithologies has produced only minor compositional differences in areas of partial melt within and between samples.

Schreibersite is found with a variety of textures and in all areas of the samples examined. However, the alteration of Fe metal to a rusty component is confined to the crystalline portions of the samples and is not observed in either the partial melt zones or the glass coatings.

Grove, T. L., Walker, D., Longhi, J., Stolper, E., and Hays, J. F.: 'Petrology of Rock 12002 and Origin of Picritic Basalts at Oceanus Procellarum', *Proceedings of the Fourth Lunar Science Conference, Geochim. Cosmochim. Acta* **1**, Suppl. 4, 995-1011.

Rock 12002 is a member of the Apollo 12 picritic basalt suite. Experimental olivine-liquid equilibria combined with petrographic observations indicate that 12002 may represent a primary liquid composition. As shown by high pressure experiments, liquids capable of producing the picritic suite can be generated by the partial melting of an olivine + clinopyroxene lunar interior at a depth of 300 km. The crystallization sequence inferred from petrographic observations has been reproduced experimentally at low pressures. Chemical variations similar to those in natural pyroxenes have been partially reproduced in equilibration experiments and suggest a two-stage cooling history for 12002.

Hays, J. F.: 'Melting Behavior and Phase Relations in the Lunar Interior' (Final Report), Hoffman Lab. Harvard Univ. Cambridge, Mass.

Phase equilibrium experiments at both high and low pressures on lunar samples and synthetic compositions are reported as well as related petrographic studies of lunar rock samples. The objectives were to trace the origins of rocks found on the lunar surface, to characterize the nature of the lunar interior and to locate and identify the sources of lunar magmas.

Helz, R. T. and Appleman, D. E.: 'Mineralogy, Petrology, and Crystallization History of Apollo 16 Rock 68415', *Proceedings of the Fourth Lunar Science Conference, Geochim. Cosmochim. Acta* **1**, Suppl. 4, 643-659.

Rock 68415 consists of 79.3% plagioclase, 4.8% olivine, 4.4% augite, 10.3% pigeonite, plus minor amounts of opaques, phosphates and potassic granitic glass. In spite of the extremely high percentage of plagioclase in the mode, its dominant texture is that of a basalt or diabase. Phenocrysts are rare.

Rock 68415 is not exclusively igneous in texture, however; the rock contains 2-5% of coarse, anhedral feldspar grains and aggregates of feldspar, which appear to be xenocrystic or xenolithic. These grains are mostly untwinned, with irregular patterns of fractures and extinction. They appear to have been derived from a fairly coarse-grained anorthosite which had been shocked and then partially annealed.

The igneous-looking material which makes up 95-98% of rock 68415 is chemically hybrid. The Wo percentage in the bulk normative pyroxene is 12-13 weight percent, a value intermediate between the 2-6% characteristic of the noritic suite and the 17-26% typical of the mare basalts. Trace element and isotopic data provide further evidence that rock 68415 is chemically hybrid.

The hybrid, but very An-rich chemistry of rock 68415, its seriate diabasic texture, its extremely high liquidus temperature, and the presence of unassimilated xenolithic material all suggest that rock 68415 was produced by impact melting of a soil or breccia containing more than one lunar rock type, followed by very rapid cooling. The anhedral feldspar appears to have been picked up after the thermal peak. The presence of this material may account for the anomalously high radiogenic Ar in the plagioclase separate as compared with the bulk rock.

Hodges, F. N. and Kushiro, I.: 'Petrology of Apollo 16 Lunar Highland Rocks', *Proceedings of the Fourth Lunar Science Conference, Geochim. Cosmochim. Acta* **1**, Suppl. 4, 1033-1048.

Petrographic observation, electron microprobe analyses and high-pressure melting experiments car-

ried out on four Apollo 16 samples indicate that these highland rocks are the result of complex magmatic differentiation, followed by large-scale impact, subsequent remelting and recrystallization. Cataclastic anorthosite 60025 probably formed by accumulation of calcic plagioclase; small amounts of trapped, interstitial liquid crystallized mostly to plagioclase, augite, hypersthene, and pigeonite. Subsolidus re-equilibration, prior to brecciation, resulted in the breakdown of pigeonite to augite and relatively iron-rich hypersthene. Rock 60315, a recrystallized breccia probably formed near the base of a large impact ejecta blanket, is characterized by large poikilitic grains of orthopyroxene. The initial matrix material of the breccia, possibly derived in part from considerable depths, must have contained a small amount of interstitial silicate melt. Crystallization of orthopyroxene poikiloblasts concentrated the melt, into which K, Ti, Fe (relative to Mg) and minor elements were fractionated. Zones of greater melt concentration crystallized with a well developed diabasic texture. The compositions of coexisting pyroxenes suggest a crystallization temperature near 1100°C. Rock 68416, a fine-grained intersertal feldspathic basalt, was most likely formed by rapid crystallization, probably of an impact-melted plagioclase cumulate. Spinel troctolite 62295, one of the most magnesium lunar samples returned, was probably formed by rapid crystallization of a basic magma which may have been derived by partial melting of a plagioclase-bearing peridotite under anhydrous conditions. The presence of xenocrystic calcic plagioclase and chromian spinel suggests contamination by pre-existing anorthositic material. Magma similar in composition to 62295, or one nearer the low-pressure three-phase boundary olivine-spinel-plagioclase, may be parental to a wide variety of highland rocks including anorthosite, feldspathic basalt, and gabbroic anorthosite. Presence of a wide compositional gap between highland-type rocks and mare basalts, the significant difference in Fe/Mg ratios of liquidus olivine and pyroxene in the two rock types over a wide pressure range, and the general paucity of pyroxene component in highland rocks indicate that highland-type rocks and mare basalts were derived from distinctly different source materials.

Hollister, L. S.: 'Sample 67955: A Description and a Problem', *Proceedings of the Fourth Lunar Science Conference, Geochim. Cosmochim. Acta* 1, Suppl. 4, 633–641.

Clasts in breccia sample 67955 contain relatively coarse olivine and plagioclase in part enveloped by poikilitic hypersthene and diopside. This distinctive texture is concluded to result from high temperature crystallization in the presence of a fluid phase, probably a silicate melt. A problem posed by this rock is whether the bulk chemistry, characterized by a high Mg/Fe ratio but low total Fe + Mg, is the result of primary igneous processes on the Moon or whether it is the residual end product of a multiple distillation process resulting from repeated meteorite impacts.

Housley, R. M., Grant, R. W., and Paton, N. E.: 'Origin and Characteristics of Excess Fe Metal in Lunar Glass Welded Aggregates', *Proceedings of the Fourth Lunar Science Conference, Geochim. Cosmochim. Acta* 3, Suppl. 4, 2737–2749.

We show that the characteristic features of lunar glass welded aggregates including their irregular shapes, vesicularity and content of submicron Fe metal in the welding glass can be explained by a model in which they are predominantly formed by micrometeorite impacts into the solar wind saturated topmost surface of the regolith. The Fe metal is reduced from silicates by the solar wind gases. Other possible mechanisms of Fe metal formation are discussed and shown to play at most minor roles.

We also show that surface tension forces control vesicularity and that the low gravity and high vacuum conditions prevailing on the Moon are unimportant. Consequences of this surface tension control to possible lunar eruptive volcanism and to the  $^{40}\text{Ar}$ - $^{39}\text{Ar}$  dating of impact events are discussed.

We have studied the Fe metal particles in the welding glass by transmission electron microscopy and found them to be single crystal spheres mostly less than 250  $\mu\text{m}$  in diam. The implications of these results with respect to the magnetic and microwave resonance properties of fines and breccias are discussed.

Hubbard, N. J., Rhodes, J. M., Gast, P. W., Bansal, B. M., Shih, C.-Y., Wiesmann, H., and Nyquist,

L. E.: 'Lunar Rock Types: The Role of Plagioclase in Non-Mare and Highland Rock Types', *Proceedings of the Fourth Lunar Science Conference, Geochim. Cosmochim. Acta* 2, Suppl. 4, 1297-1312.

Some non-mare and highland rock types (14310 type KREEP and very high  $\text{Al}_2\text{O}_3$  basalts) have the internal chemical variations expected for a plagioclase-liquid system. The observed Eu variations in these rock types suggest a  $D_{\text{Eu}1/p}$  of 0.6 to 0.7. The Sr variations suggest a  $D_{\text{Sr}1/p}$  of about 0.6, with values as low as 0.35 suggested for some materials from sample 14063. Common Apollo 14 KREEP and Apollo 15 KREEP do not show internal Sr, Eu,  $\text{Al}_2\text{O}_3$  variations consistent with the  $D_{\text{Eu},\text{Sr}1/p}$  values derived for 14310 type KREEP. Major element and experimental data indicate that olivine or pyroxene is a large, perhaps dominant, controller of chemical variations within common Apollo 14 KREEP. The application of these distribution coefficients to pure anorthosites like 15415 yields the model dependent conclusion that the silicate liquids with which such anorthosites may have been chemically equilibrated have not yet been analyzed and perhaps not directly sampled. If instead we allow  $D_{\text{Eu}1/p}$  to be greater than 1.0, we may require higher temperatures or perhaps higher  $\text{Po}_2$  when pure anorthosites formed relative to the time when KREEP and VHA basalts formed.

Khodak, Yu. A. and Likhosherstnykh, G. U.: 'Lunar Geology' (transl. into English from *Izv. Akad. Nauk S.S.S.R., Ser. Geol.* No 11 (1972), 3-14 and *Mat. Metody v Geol.* No 2 (1971/1972), 104-110), Joint Publications Research Service-59895.

Articles are presented on the possible evolution and petrochemical differentiation of the Moon and on tides as an energy factor in the geological activity on the Moon.

Lowman, P. D.: 'The Geologic Evolution of the Moon', NASA-TM-X-65939.

A synthesis of pre- and post-Apollo 11 studies is presented to produce an outline of the Moon's geologic evolution from three lines of evidence: (1) relative ages of lunar landforms and rock types, (2) absolute ages of returned lunar samples, and (3) petrography, chemistry, and isotopic ratios of lunar rocks and soils. It is assumed that the ray craters, circular mare basins, and most intermediate circular landforms are primarily of impact origin, although many other landforms are volcanic or of hybrid origin. The Moon's evolution is divided into four main stages, each including several distinct but overlapping events or processes.

Macedougall, D., Rajan, R. S., Hutcheon, I. D., and Price, P. B.: 'Irradiation History and Accretionary Processes in Lunar and Meteoritic Breccias', *Proceedings of the Fourth Lunar Science Conference, Geochim. Cosmochim. Acta* 3, Suppl. 4, 2319-2336.

Particle track studies reveal an abundant record of fossil solar flare tracks in breccia components. Metamorphic events govern the degree to which this record is preserved, and studies of phases with different track retentivities allow limits to be placed on temperatures reached during a rock's history. The least affected breccias have never experienced temperatures as great as  $\sim 300^\circ\text{C}$ . Two breccias which contain xenon from spontaneous fission of  $\text{Pu}^{244}$  (14301 and 14318) and  $\text{Xe}^{129}$  (14301 only) have never been heated above  $\sim 700^\circ\text{C}$ . This and evidence for a surface irradiation of some of the breccia components support the surface implantation model for the origin of the xenon in these breccias. Green glass spheres in 15086 have not been heated above  $\sim 300^\circ\text{C}$  during or after breccia formation yet have retained fission tracks for less than 0.7 G.y. Argon ages of  $\sim 3.5$  G.y. for similar green glass are at least five times as great and may indicate that the glass was not completely outgassed at its formation. Similarities between solar flare track retention in lunar breccias and gas-rich meteorites indicate that the latter may have been compacted in the regoliths of small bodies.

MacDougall, J. D.: 'Particle Track Records in Natural Solids from Oceans on Earth and Moon', Ph.D. Thesis, Univ. Microfilms Order, No. 73-865.

Several earth science problems which involve charged particle tracks are discussed. These include: the dating of rocks from the ocean floor; the dating of components of oceans sediments; and the investigation of kinetic processes in the lunar regolith. Methods are described for processing small amounts of material, for increasing contrast through use of dyes and metal plating of tracks, and for increasing resolution through use of an electron microscope replica technique. Attention is given to problems of fission track dating natural glasses: use of proper etching solutions, accurate neutron flux measurements, and absolute calibration of the dating method.

Nakamura, Y.: 'Origin of Sector-Zoning of Igneous Clinopyroxenes', *Amer. Mineralogist* **58**, 986-990.

A protosite is defined as a partially formed structural site on a crystal surface. When a crystal grows rapidly from a magma, portosites but not structural sites are in equilibrium with the magma. The geometry of each protosite on each growth surface differs from that of the corresponding true structural site in variable degree. The geometry of the  $M(1)$  and  $M(2)$  protosites on  $\{100\}$  surfaces of augite deviate most from the true structural sites, and are effectively the most flexible. Consequently the composition of the  $\{100\}$  sector can deviate most prominently from the equilibrium composition. Several types of sector-zoning are interpreted, based on this concept of protosites.

Ridley, W. I., Reid, A. M., Warner, J. L., Brown, R. W., Gooley, R., and Donaldson, C.: 'Glass Compositions in Apollo 16 Soils 60501 and 61221', *Proceedings of the Fourth Lunar Science Conference, Geochim. Cosmochim. Acta* **1**, Suppl. 4, 309-321.

Major element analyses have been made of 303 glasses in two Apollo 16 soils, 60501 and 61221. Averages of preferred glass compositions are used as a guide to the nature of the major rock types contributing to these soils. The major glass groups in 60501 have the composition of Highland basalt (anorthositic gabbro), gabbroic anorthosite, low K Fra Mauro basalt (high alumina basalt), and anorthosite. Soil 61221 differs from any other soil we have studied in that 57% of the glasses have plagioclase compositions and may be either melted anorthosites or maskelynites. The abundances of glass groups in the two soils are similar except for the prominence of the gabbroic anorthosite group in 60501 and for the overwhelming abundance of glasses of plagioclase composition in 61221. In both soils glasses of Fra Mauro basalt (KREEP basalt) and mare basalt compositions are present but rare. The data indicate similarities in types, but differences in abundances, between the rocks of the Cayley-Descartes Highlands and those from the Apollonius Highlands, sampled by the Luna 20 mission.

Sato, M., Hickling, N. L., and McLane, J. E.: 'Oxygen Fugacity Values of Apollo 12, 14, and 15 Lunar Samples and Reduced State of Lunar Magmas'. *Proceedings of the Fourth Lunar Science Conference, Geochim. Cosmochim. Acta* **1**, Suppl. 4, 1061-1079.

The oxygen fugacity values of lunar samples were measured directly with an improved solid-electrolyte oxygen cell between 1000 and 1200°C with an accuracy mostly better than 0.2 log  $f_{O_2}$  unit. The bulk rock  $f_{O_2}$  values of basaltic igneous rocks 12009, 12053, 15058, and 15595 ranged from  $10^{-15.4}$  to  $10^{-15.7}$  at 1000°C and from  $10^{-12.3}$  to  $10^{-12.8}$  at 1200°C. Those of microbreccia 14321 also fell in this range, but the change of oxygen fugacity with temperature was irregular in the first heating cycle in comparison to the smooth changes observed with the basaltic igneous rocks. Two different samples of rock 14310 also showed similar  $f_{O_2}$  values below 1170°C, but exhibited irreversible sudden rise in  $f_{O_2}$  at this temperature for reasons yet to be determined. The data on the phenocryst olivine and the groundmass of basalt 12009 do not conclusively indicate progressive reduction of the lunar magma during cooling. For possible reduction of the lunar magmas during ascent and extrusion, the reaction of reduced carbon with the magmas as the result of pressure decrease and the loss of sulfur as gas from the magmas are suggested to be plausible mechanisms of reduction.

Schaeffer, O. A. and Husain, L.: 'Early Lunar History: Ages of 2 to 4 mm Soil Fragments from the Lunar Highlands', *Proceedings of the Fourth Lunar Science Conference, Geochim. Cosmochim. Acta* **2**, Suppl. 4, 1847-1863.

The  $^{40}\text{Ar}$ - $^{39}\text{Ar}$  stepwise-heating technique was used to determine the ages of twenty-one 2 to 4 mm soil fragments from Apollo 16 Stations 6, 8, 11, and 13. These include all six major petrographic rock types found among Apollo 16 samples. An Apollo 11 type basalt fragment, with an age 3.79 G.y., may be material from Mare Nectaris. Twelve of the fragments have ages in the range of 3.95–4.06 G.y. These samples, representing all major rock types, most likely date the Cayley Formation. Four fragments have ages older than 4.1 G.y. These represent the oldest lunar material found. A light matrix breccia which has an age of  $4.26 \pm 0.05$  G.y. is evidence for the earliest lunar crust. The light matrix breccia fragments must have been formed by the bombardment of an ancient, perhaps the original lunar anorthositic crust. The light matrix breccias have ages in the range of 4.04 to 4.26 G.y. indicating a continuous activity in the early evolution of the Moon.

The cosmic ray exposure ages were determined for all samples from  $^{38}\text{Ar}$  produced by spallation of Ca. The exposure ages fall into two distinct groups. The samples from Stations 11 and 13 give an age for North Ray Crater of  $35 \pm 3$  m.y. The samples from Stations 6 and 8 give a mean age of  $140 \pm 10$  m.y. indicating that South Ray Crater was formed 140 m.y. ago or there is no debris from South Ray Crater in the 2 to 4 mm size fragments at Stations 6 and 8.

Simonds, C. H., Warner, J. L., and Phinney, W. C.: 'Petrology of Apollo 16 Poikilitic Rocks', *Proceedings of the Fourth Lunar Science Conference, Geochim. Cosmochim. Acta* 1, Suppl. 4, 613–632.

Poikilitic rocks, virtually all with low K-KREEP composition are found in all non-mare suites of lunar samples. Most of these rocks have low calcium pyroxene oikocrysts enclosing many chadacrysts of feldspar. The poikilitic rocks are proposed to form by crystallization of an impact generated partial melt with over 70% liquid. The protolith is gas bearing polymict breccias and/or soil. The key to forming a poikilitic texture is to rapidly chill a low K-KREEP melt a few tens of degrees, so that abundant feldspar and olivine grains are nucleated. The melt then cools more slowly due to the presence of an insulating layer of material. Slow cooling through the plagioclase-olivine-pyroxene peritectic, allows few pyroxene nuclei to form. Continuous pyroxene growth is possible due to ease of silica transport through the abundant (> 50%) remaining melt. A number of observations support this hypothesis: (1) The euhedral shape of feldspar chadacrysts, not expected for subsolidus melt crystallization or solid state recrystallization. (2) Flow alignment of feldspar chadacrysts. (3) Large spherical pores, which appear to have formed in a liquid. (4) Preservation of only refractory olivine and plagioclase relics and the lack of pyroxene which had a lower melting point than olivine or plagioclase. (5) Relic feldspar is more anorthite rich, i.e., more refractory than matrix feldspar. (6) Resorbed olivine in pyroxene oikocrysts. (7) Normally zoned oikocrysts. (8) High temperature ( $\sim 1200^\circ$ ) partition coefficients for Fe and Mg between low Ca pyroxene and augite. (9) Concentration of late crystallizing ilmenite, phosphate and high K phases between oikocrysts. (10) The compositional correlation with poikilitic texture. (11) The abundance of impact melted rocks with higher melting points than the low K-KREEP composition.

Steele, I. M. and Smith, J. V.: 'Mineralogy and Petrology of Some Apollo 16 Rocks and Fines: General Petrologic Model of Moon', *Proceedings of the Fourth Lunar Science Conference, Geochim. Cosmochim. Acta* 1, Suppl. 4, 519–536.

Apollo 16 rake samples from Stations 8 and 11, and 1–2 mm fines from Station 1 are dominated by plagioclase-rich breccia with textures and compositions affected by metamorphism and recrystallization. Feldspar-rich basalts are rare. Minor elements in plagioclase clasts in breccia indicate little contribution from KREEP- and MARE-type basalt. Olivines and pyroxenes from breccias and igneous rocks are Mg-rich ( $mg > 0.6$ ) with essentially no Fe-enrichment trend. Unique are a KREEP clast in 67749 with Fe-rich pyroxene, plagioclase ( $\text{An}_{65}$ ), phosphates, and K-feldspar; and a pyroxene ( $\text{En}_{77}\text{Wo}_4\text{Fs}_{19}$ )-olivine ( $\text{Fo}_{72}$ )-plagioclase ( $\text{An}_{86-92}$ ) clast in 67667. Early proposals of widespread early melting of most or all of the Moon are now considered seriously, and Mg/Fe data for experimental olivine-liquid and olivine-orthopyroxene equilibria are used as constraints to examine compositional data for rocks, glasses and fragments in the light of specific models for crystal-liquid differentiation. A complication for simple early differentiation is suggested by an apparent negative correlation between the An-content of plagioclase and Fo content of coexisting olivine in igneous

rocks of the ANT suite; one possible explanation involves general outgassing during an early turbulent period of formation of the crust.

Storzer, D., Poupeau, G., and Krättschmer, W.: 'Track-Exposure and Formation Ages of Some Lunar Samples', *Proceedings of the Fourth Lunar Science Conference, Geochim. Cosmochim. Acta* **3**, Suppl. 4, 2363–2377.

The etchable ranges of 9.6 MeV/nucleon Fe-ion tracks in various detector materials are longer than previously assumed. They depend strongly on the etching conditions. This implies that the available cosmic ray track production rates have a high uncertainty and are correct only by order of magnitude. Using conventional track production rates, apparent track-exposure ages were determined for Apollo 15, 16, and 17 and Luna 16 samples in the age range between  $10^1$  y.r. and  $10^7$  y.r. Fission track analyses in lunar glass spherules among green ones of Apollo 15, brown ones of Apollo 15, Luna 16, 20 and orange ones of Apollo 17 indicate that these spherules were formed in the early history of the Moon and that they are probably related to the excavation of the lunar mare basins.

Sweet, J. R., White, W. B., White, E. W., and Roy, R.: 'Structural and Mineralogical Investigations of Lunar Glasses and Terrestrial Glasses by Raman Spectroscopy', *Proceedings of the Fourth Lunar Science Conference, Geochim. Cosmochim. Acta* **1**, Suppl. 4, 389–396.

Raman spectra of most examples of lunar glass are featureless except for the Rayleigh tail and occasional sharp fine structure. The fine structure is shown to be due to specific mineral inclusions and can be used to identify the separated crystalline phases. By comparison with spectra of common terrestrial glasses (obsidians, tektites, and fulgurites) and by comparison with several synthetic glasses it is shown that the featureless spectrum of most lunar glass is due to intermediate range structural disorder. The only lunar glasses so far examined that are sufficiently ordered to produce glass-like spectral features are the extremely high  $Al_2O_3$  anorthosite glasses.

Takeda, H.: 'Inverted Pigeonites from a Clast of Rock 15459 and Basaltic Achondrites', *Proceedings of the Fourth Lunar Science Conference, Geochim. Cosmochim. Acta* **1**, Suppl. 4, 875–885.

A highly fractured clast of anorthositic gabbro in rock 15459 has a granulitic texture and contains pyroxene and plagioclase grains up to 1 mm in diameter. X-ray single crystal diffraction studies, electron microprobe analyses and optical microscopic examination of these pyroxenes have indicated that there are orthopyroxenes with coarse exsolution lamellae of augite on (100), and that they may be inverted pigeonites. Comparisons of orientational and compositional relationships between lunar, terrestrial and meteoritic inverted pigeonites suggest a possible mechanism of inversion from orthopyroxene to pigeonite under various crystallization and cooling conditions. It appears that the 15459 anorthositic gabbro containing such pyroxenes represents further evidence that very slowly cooled rocks exist in the lunar highlands.

Taylor, L. A., McCallister, R. H., and Sardi, O.: 'Cooling Histories of Lunar Rocks Based on Opaque Mineral Geothermometers', *Proceedings of the Fourth Lunar Science Conference, Geochim. Cosmochim. Acta* **1**, Suppl. 4, 819–828.

The application of experimentally derived data on (1) the Zr partitioning between coexisting ilmenite and ulvöspinel and (2) the Ti partitioning between coexisting troilite and ilmenite has allowed the discernment of differences in subsolidus cooling histories of lunar rocks – e.g., the Apollo 15 Type 1 Mare basalts. The rocks which show Zr partitionings reequilibrated to lower temperature (i.e.,  $< 950^\circ C$ ), as a result of slow cooling, also show evidence for subsolidus reduction of ulvöspinel to ilmenite + native Fe. It is suggested that the presence of ulvöspinel reduction is not evidence *a priori* that these rocks have undergone more reducing conditions than the other Apollo 15 Mare basalts; it may only indicate that the cooling rates were slower in that subsolidus temperature range (i.e.,

$\ll 900^\circ\text{C}$ ) where  $f_{\text{O}_2}$  values were favorable for ulvöspinel reduction. The rocks with higher temperature Zr partitionings and no ulvöspinel reduction may have cooled under the same fugacity conditions but at a faster rate. The conclusions to be reached by application of both the Zr and Ti partitioning geothermometers are in complete agreement with Bence *et al*, who first suggested that 12052 cooled faster at subsolidus temperatures than 12021.

Walker, D., Grove, T. L., Longhi, J., Stolper, E. M., and Hays, J. F.: 'Origin of Lunar Feldspathic Rocks', *Earth Planetary Sci. Letters* **20**, 325–336.

Melting experiments and petrographic studies of lunar feldspathic rocks reveal possible genetic relationships among several compositionally and mineralogically distinct groups of lunar rocks and soil fragments. Dry, low  $\text{PO}_2$  partial melting of crustal anorthositic norites of the anorthositic-noritic-troctolitic (ANT) suite produces liquids of the KREEP-Fra Mauro basalt type; dry, low  $\text{PO}_2$  partial melting of pink spinel troctolite (PST) produces liquids of the 'very high alumina basalt' or micro-troctolite type.

Both ANT and PST are probable components of the primitive terra crust. If crystal fractionation in a cooling basaltic liquid could have produced such a crust, it would also produce a mafic interior capable of yielding mare basalts by later remelting at depth.

Walker, D., Longhi, J., Grove, T. L., Stolper, E., and Hays, J. F.: 'Experimental Petrology and Origin of Rocks from the Descartes Highlands', *Proceedings of the Fourth Lunar Science Conference*, *Geochim. Cosmochim. Acta* **1**, Suppl. 4, 1013–1032.

Petrographic studies of Apollo 16 samples indicate that rocks 62295 and 68415 are crystallization products of highly aluminous melts, 60025 is a shocked, crushed and partially annealed plagioclase cumulate. 60315 is a recrystallized noritic breccia of disputed origin. 60335 is a feldspathic basalt filled with xenoliths and xenocrysts of anorthosite, breccia, and anorthite. The  $\text{Fe}/(\text{Fe} + \text{Mg})$  of plagioclase appears to be a relative crystallization index.

Low pressure melting experiments with controlled  $\text{PO}_2$  indicate that the igneous samples crystallized at oxygen fugacities well below the  $\text{Fe}/\text{FeO}$  buffer. Crystallization experiments at various pressures suggest that the 62295 and 68415 compositions were produced by partial or complete melting of lunar crustal materials, and not by partial melting of the deep lunar interior.

Warner, J. L., Simonds, C. H., and Phinney, W. C.: 'Apollo 16 Rocks: Classification and Petrogenetic Model', *Proceedings of the Fourth Lunar Science Conference*, *Geochim. Cosmochim. Acta* **1**, Suppl. 4, 481–504.

The Apollo 16 rocks include cataclastic anorthosites, two varieties of unequilibrated breccia, two varieties of partly- to fully-equilibrated breccia, and a sequence of partially melted breccias. The latter, which dominate the Apollo 16 collection, include glass, devitrified glass, mesostasis-olivine-plagioclase rock, mesostasis-rich basalt, basalt, and poikilitic rocks. All sequence members contain vesicles and relics of plagioclase, olivine, pink spinel, and lithic fragments. Their equilibrated matrices define a series from glass, to a plagioclase-olivine-mesostasis assemblage displaying spherulitic and skeletal shaped crystals, through a plagioclase-pyroxene-olivine assemblage displaying euhedral shaped crystals. Such data suggest that the sequence lithologies were derived from breccias or soils that were partially melted in an impact event. The product of the melting was a liquid that contained the solid material that we now observe as the relics. The range in mineralogy and texture in the sequence lithologies is due to different cooling rates – the glass end of the sequence cooled rapidly whereas the crystalline end cooled more slowly.

Weiblen, P. W. and Roedder, E.: 'Petrology of Melt Inclusions in Apollo Samples 15598 and 62295, and of Clasts in 67915 and Several Lunar Soils', *Proceedings of the Fourth Lunar Science Conference*, *Geochim. Cosmochim. Acta* **1**, Suppl. 4, 681–703.



We present 188 analyses of silicate melt inclusions and their host and associated phases (olivine including fayalite, pyroxene, plagioclase, hyalophane, ilmenite, ulvöspinel, spinel, chromite, taenite, kamacite, and schreibersite) from Apollo 15 porphyritic olivine basalt 15598, soils 15302, 15472, 15532, and 15602, and from Apollo 16 spinel troctolite 62295, soils 63502, 61242, 66082, and breccia 67915.

Inclusions in mare basalt and highlands rocks, ranging from those in early olivine and intermediate plagioclase, to late stage interstitial inclusions, show an evolutionary change in composition. Postulated crystallization sequences are consistent with textures, trends on variation diagrams, and preliminary petrologic mixing calculations. For mare basalts the sequence is olivine, ilmenite, and plagioclase, followed by pyroxene. The sequence for a very high aluminum basalt, 62295, is spinel, olivine, and a minor undetermined titanium bearing phase followed by plagioclase, leaving a residual melt of 40% normative quartz, 27% feldspar, 27% pyroxene, and 6% ilmenite. Late-stage melts in mare basalts but not 62295 split into immiscible high-iron and high-silica liquids.

Unusual fragments found in soil samples include: in 15472, an anorthositic clast consisting of chromian pleonaste and ilmenite in  $An_{96}$  plagioclase, possibly from a deep source, and glass with 65% normative ilmenite, presumably a shock fusion crust; in 15532, 11, a variolitic pyroxene porphyry showing a crystallization sequence of Fe-Ni metal, Mg-Al chromite, augite, plagioclase, and a residuum of immiscible high-silica and high-iron melts (in part crystallized to hyalophane, silica, apatite (x), and hedenbergitic pyroxene).

Polymict breccia 67915 contains clasts of metal, sulfide, or spinel, and a 70  $\mu\text{m}$  zircon crystal, but consists principally of clasts of a finely crushed, very pure mixture of plagioclase, pyroxene, and olivine or silica, corresponding to gabbroic, quartz or olivine normative anorthosites, in various textural states. It is cut by unusual shock glass veinlets ( $\sim 100 \mu\text{m}$  wide) that were apparently so hot on injection that plagioclase in the vein walls was made isotropic. Six clasts were found of a crystalline rock type – sodic ferrogabbro – not heretofore described from the lunar samples. They consist mainly of hedenbergitic pyroxene (maximum 31% En), alkalic plagioclase (up to  $Ab_{85}$  and  $Or_8$ ), ilmenite, and cristobalite, plus minor amounts of several other phases.

Wenk, H. R., Müller, W. F., and Thomas, G.: 'Antiphase Domains in Lunar Plagioclase', *Proceedings of the Fourth Lunar Science Conference, Geochim. Cosmochim. Acta* **1**, Suppl. 4, 909–923.

The paper is a compilation of data on antiphase domains in lunar plagioclase. New observations and reports in the literature are tabulated and discussed. In the pattern which emerges (but is still very incomplete) it appears that *b*-domains which, except for the  $An_{82}$  bytownite from the Stillwater complex, have only been observed in lunar feldspars occurring in the anorthite range  $An_{80}$  to 95. Especially in the sodium rich part there seems to be a close relation between an exsolution structure and *b*-APB's. *c*-APB's are found in anorthites  $An_{95}$  to 100 and for a given *An*-content they are larger for metamorphic than for volcanic anorthites. Near  $An_{95}$ , *c*- and *b*-domains can be observed in the same crystal, *c*-domains disappear when heated above 1200°C; they are not affected by heating below 600°C. This implies that calcic anorthite without *c*-domains must have been rapidly quenched from high temperatures. The domain structure of anorthite in lunar rocks indicates that no generalizations can be made and that the cooling history of each specimen has to be analyzed separately.

Woolum, D. S.: 'Neutron Capture: A Tracer in the Evolution of the Lunar Surface', *Amer. Phys. Soc.* **18**, 1574–1973.

In-situ measurements of the neutron-induced fission-rate of  $U^{235}$  and the neutron capture rate of  $B^{10}$  were made to a depth of  $\sim 400 \text{ g cm}^{-2}$  by the Apollo 17 Lunar Neutron Probe Experiment. The results are in reasonable agreement with prior theoretical calculations, with the profiles rising sharply from the surface to a broad maximum (at  $\sim 140 \text{ g cm}^{-2}$ ) and then declining less dramatically at greater depths. Neutron capture profiles are unique in the lunar particle exposure record, where the production rate profiles of other cosmic ray primaries and secondaries peak much closer to the surface. Inferences drawn from the extensive lunar sample neutron capture data, concerning the dynamic processes and evolution of the lunar surface, will be discussed.

## 6. Chemical Composition of the Moon

Adams, J. A. S., Barretto, P. M. C., Clark, R. B., and Fryer, G. E.: 'Radon-222 Emanation Characteristics of Lunar Fines', *Proceedings of the Fourth Lunar Science Conference, Geochim. Cosmochim. Acta* 2, Suppl. 4, 2097–2104.

Bulk radon emanation rates are reported for 8 lunar dust samples (150,2183, 68501,13, 10084,107, 10084,83, 12070,14,845, 10084,257, 10084,557, and 64501,8) and one small sample of KREEP glass particles (12033,73). The bulk emanation rates are low (less than 1%) in each case. It is concluded that the lunar dust contributes little radon to its surroundings because of its low and uniformly distributed uranium content, its glassy state for the most part, and the possibility of radon being adsorbed on the glassy and/or radiation damaged surfaces. Breccias and other lunar rock types, as well as highly uraniferous minerals are still unknown as to their bulk and grain radon emanation rates.

Adler, I., Trombka, J. I., Schmadebeck, R., Lowman, P., Blodget, H., Yin, L., Eller, E., Podwysocki, M., Weidner, J. R., Bickel, A. L., Lum, R. K. L., Gerard, J., Gorenstein, P., Bjorkholm, P., and Harris, B.: 'Results of the Apollo 15 and 16 X-Ray Experiment', *Proceedings of the Fourth Lunar Science Conference, Geochim. Cosmochim. Acta* 3, Suppl. 4, 2783–2791.

Except for some minor modifications the Apollo 16 X-ray fluorescence experiment was similar to that flown aboard Apollo 15. The Apollo 16 provided data for a number of features not previously covered such as Mare Cognitum, Mare Nubium, Ptolemaeus, Descartes, Mendeleev as well as other areas. Many data points were obtained by the X-ray experiments so that comparisons could be drawn between Apollo 15 and 16 flights. The agreement was generally within about 10%. Al Si concentration ratios ranged from 0.38% in Mare Cognitum to 0.67% in the Descartes area highlands. A comparison of the Apollo 16 data Al Si values with optical albedo values along the ground tracks showed the same positive correlation as in the Apollo 15 flight. A reexamination of the detector and collimator geometries showed that the spatial resolution was better by almost a factor of two than the initial estimates. The data are presently being examined using smaller integration intervals in an effort to prepare concentration contours and enhanced spatial resolution.

Akella, J. and Boyd, F. R.: 'Partitioning of Ti and Al Between Coexisting Silicates, Oxides, and Liquids', *Proceedings of the Fourth Lunar Science Conference, Geochim. Cosmochim. Acta* 1, Suppl. 4, 1049–1059.

Coexisting Ti-rich oxides and silicates have been equilibrated over a range of temperatures and pressures and analyzed with an electron microprobe. In subsolidus runs clinopyroxenes in equilibrium with ilmenite contain 1–5 weight percent TiO<sub>2</sub>, with the most Ti-rich pyroxenes crystallizing in an intermediate pressure range (5–20 kbar). In the melting interval, clinopyroxenes containing up to 6.5 weight percent TiO<sub>2</sub> coexist with Ti-rich liquids. The Ti and Al contents of pyroxenes in equilibrium with ilmenite are not much affected by moderate variations in bulk Mg/(Mg + Fe). However, in the melting interval, increase in the silica activity of the liquid produces a large decrease in the Ti and Al contents of coexisting clinopyroxenes. Ilmenite melts at the solidus in a range of bulk compositions, and in runs at atmospheric pressure, liquids quenched to glass from temperatures just above the solidus have compositions similar to high-Ti mare basalts. It is suggested that the large difference in TiO<sub>2</sub> content between the high-Ti mare basalts and the low-Ti mare basalts was caused by the presence of ilmenite in the source rocks of the former and the absence of ilmenite in the latter.

Allen, R. O., Jovanovic, S., and Reed, G. W.: 'Geochemistry of Primordial Pb, Bi, and Zn in Apollo 15 Samples', *Proceedings of the Fourth Lunar Science Conference, Geochim. Cosmochim. Acta* 2, Suppl. 4, 1169–1175.

Primordial Pb as <sup>204</sup>Pb is present in Apollo 15 samples in concentrations ranging from <0.2 ppb in basalts to 6 ppb in soils. An acid soluble, pH 5–6, readily volatile component of this Pb is present,

possibly as  $\text{Pb Br}_2$ ; the remainder is correlated with the metal content of the sample. Leachable Bi and  $^{204}\text{Pb}$  are correlated; residual Bi is probably present in a phosphate, possibly apatite. Zn is also highly leachable; residual Zn and  $^{204}\text{Pb}$  are correlated.

Baedecker, P. A., Chou, C.-L., Grudewicz, E. B., and Wasson, J. T.: 'Volatile and Siderophilic Trace Elements in Apollo 15 Samples: Geochemical Implications and Characterization of the Long-Lived and Short-Lived Extralunar Materials', *Proceedings of the Fourth Lunar Science Conference, Geochim. Cosmochim. Acta* 2, Suppl. 4, 1177-1195.

The concentrations of Ni, Ge, Ir, and Au in six mature Apollo 15 soils indicate a 1.37% extralunar component. This is 20% higher than that at the Apollo 12 site, and probably indicates contamination of these soils by older regolith from the Apennine Front. Three Apollo 15 soils are immature, as indicated by low siderophile contents. Ni/Ir, Ge/Ir, and Au/Ir ratios in the extralunar components of mature soils increase monotonically with increasing concentration of extralunar materials. This variation reflects a small difference in composition between the long-lived and short-lived populations of extralunar materials. The same ratios change in the same direction and by roughly comparable amounts between the Allende CV and Orgeuil CI chondrites. It seems likely that both types of extralunar materials are primitive (chondritic) in nature, and that they differ as a result of the same type of nebular fractionation which has affected the CV chondrites. Breccia 15205 consists of KREEP nearly uncontaminated by extralunar materials, and provides upper limits on the Ni, Ge, Ir, and Au contents of Apollo 15 KREEP materials. The Ga/Al ratio is a factor of two lower in lunar anorthosites than in lunar basalts, and about a factor of 4 lower in the lunar crust than in the terrestrial crust. A strong correlation between Zn and Cd in lunar soils is mainly due to the high contents of these elements in the highlands regolith, probably reflecting a higher rate of release of magmatic volatiles during the early history of the Moon. Several Apollo 15 soils seem to have escaped contamination by In; the lowest concentrations ( $3.1\text{--}3.7\text{ ng g}^{-1}$ ) are too high to be understood in terms of a Cl-like extralunar component, and suggest that In, like Zn and Cd, may be atmophilic.

Barnes, I. L., Garner, E. L., Gramlich, J. W., Machlan, L. A., Moody, J. R., Moore, L. J., Murphy, T. J., and Shields, W. R.: 'Isotopic Abundance Ratios and Concentrations of Selected Elements in Some Apollo 15 and Apollo 16 Samples', *Proceedings of the Fourth Lunar Science Conference, Geochim. Cosmochim. Acta* 2, Suppl. 4, 1197-1207.

The elements Pb, U, Th, Rb, Sr, K, Cr, and Ni have been determined on a series of Apollo 15 and 16 rocks and soils. The elements U, Rb, Cr, and Ni show isotopic abundances identical with those of terrestrial materials in both types of samples but the  $^{39}\text{K}/^{41}\text{K}$  ratio is fractionated by about 1% in the soils and the extreme reversed discordancy of the Pb - U - Th ages in the Apollo 16 soils indicated that lead has also been fractionated in these.

The breccia 60335,36 has concordant Pb - U - Th model ages of 4075 MY and the basalt 15495,59 shows one slightly discordant age of around 4480 MY. The Rb - Sr model ages are in good agreement with the Pb - U - Th model ages.

Basford, J. R., Dragon, J. C., Pepin, R. O., Coscio, M. R., and Murthy, V. R.: 'Krypton and Xenon in Lunar Fines', *Proceedings of the Fourth Lunar Science Conference, Geochim. Cosmochim. Acta* 2, Suppl. 4, 1915-1955.

Lunar krypton and xenon are variable superpositions of gas components derived principally from ion bombardment and *in situ* spallation, and in smaller amounts from indigenous gases and *in situ* radioactive decay. Data from grain-size separates, stepwise heating fractions and bulk analyses of twenty samples of fines and breccias from five lunar sites are used to define three-isotope and ordinate intercept correlations, in what is hoped to be a statistically valid approach to the problem of resolving the lunar heavy rare gas system. This approach divides naturally into the separate study of surface correlated and volume correlated gases, in which characteristic primary components are respectively solar wind and spallogenic Kr and Xe. Surface correlated krypton follows two principal isotopic

patterns, the first closely resembling terrestrial Kr, to within 1 part/thousand at all isotopes in one case, and the second apparently fractionated with respect to the terrestrial isotopic composition by  $\sim -0.25\%$ /mass number. The composition of surface correlated Xe is significantly variable from sample to sample; the systematics of the variations provide evidence for the presence of specific components tentatively attributed to neutron capture in iodine, decay of extinct  $^{129}\text{I}$ , and spontaneous fission of  $^{244}\text{Pu}$ . A surprising correlation of excess concentrations of  $^{128}\text{Xe}$  and  $^{129}\text{Xe}$  in four samples suggests, in a crude model, that Xe retention ages of some of the fines may approach the age of the Moon. Volume correlated Kr appears to be dominated by galactic cosmic ray spallation, but volume correlated Xe is shown to contain a variable mixture of two isotopically distinct components from different sources. Assumption that the second volume component is fissionogenic leads to derivation of a spallation spectrum for lunar fines which is in generally excellent agreement with measurements in lunar rocks, and to an isotopic composition for the fission Xe which approaches that from  $^{244}\text{Pu}$  but does not quite agree with it within error.

Behrmann, C., Crozaz, G., Drozd, R., Hohenberg, C., Ralston, C., Walker, R., and Yuhas, D.: 'Cosmic-Ray Exposure History of North Ray and South Ray Material', *Proceedings of the Fourth Lunar Science Conference, Geochim. Cosmochim. Acta* 2, Suppl. 4, 1957-1974.

Cosmic-ray exposure ages for two breccias 68815 and 69935 in the vicinity of South Ray Crater give consistent values of  $2.0 \pm 0.2$  m.y. when measured by the  $^{81}\text{Kr} - \text{Kr}$ ,  $^{22}\text{Na} - \text{Ne}$ , and particle track methods. These also agree with estimates of exposure ages made by others using microcrater counts on six rocks in the same vicinity including 69935. It is likely that this represents the age of South Ray Crater. Soils from stations close to South Ray Crater appear to be mature, well-irradiated materials containing little, if any, of a 2 m.y. component. Reviewing various lines of evidence, we conclude that there are no compelling reasons to believe that so-called South Ray soils contain a large fraction of South Ray ejecta. However, if they do contain such ejecta, this material must have been well irradiated *in situ* prior to being thrown out in the South Ray event. A chip from a large boulder on the rim of North Ray Crater gives a  $^{81}\text{Kr} - \text{Kr}$  age of  $50.6 \pm 3.8$  m.y. Similar ages are found by the  $^{22}\text{Na} - \text{Ne}$  and the particle track methods (assuming an erosion rate of  $\gtrsim 1$  mm/m.y.) The agreement of this result with other data on large North Ray boulders fixes the age of North Ray Crater as 50 m.y.

Bjorkholm, P. J., Golub, L., and Gorenstein, P.: 'Distribution of  $^{222}\text{Rn}$  and  $^{210}\text{Po}$  on the Lunar Surface as Observed by the Alpha Particle Spectrometer', *Proceedings of the Fourth Lunar Science Conference, Geochim. Cosmochim. Acta* 3, Suppl. 4, 2793-2802.

The distribution of  $^{222}\text{Rn}$  and her daughter products has been observed from orbit during the Apollo 15 and Apollo 16 missions. Decays of  $^{222}\text{Rn}$  were observed locally over the crater Aristarchus and more generally over Oceanus Procellarum and Mare Imbrium. Decays of  $^{210}\text{Po}$  (a delayed daughter of  $^{222}\text{Rn}$ ) were observed over most of the eastern hemisphere on both missions. All observations indicate a lack of radioactive equilibrium between  $^{222}\text{Rn}$  and  $^{210}\text{Po}$  implying a time dependent process for the production of radon at the lunar surface. In addition, the  $^{210}\text{Po}$  shows a remarkable correlation with the Mare edges.

Bogard, D. D., and Nyquist, L. E.: ' $^{40}\text{Ar}/^{36}\text{Ar}$  Variations in Apollo 15 and 16 Regolith', *Proceedings of the Fourth Lunar Science Conference, Geochim. Cosmochim. Acta* 2, Suppl. 4, 1975-1985.

Values of  $^{40}\text{Ar}/^{36}\text{Ar}$  have been determined for a large number of Apollo 15 and Apollo 16 fines, including samples from a range of depths in the Apollo 15 and 16 deep drill cores. Most of the  $^{40}\text{Ar}$  in these samples is 'excess  $^{40}\text{Ar}$ ' in that it has not been produced by *in situ* decay of K. Values of  $^{40}\text{Ar}/^{36}\text{Ar}$  range from 0.74 to 4.35 and demonstrate that the regolith is not well mixed over depths of several cm or over surface distances greater than  $\sim 100$  m. However, fines collected over surface distances of less than a few tens of meters tend to possess similar ratios. Values of  $^{40}\text{Ar}/^{36}\text{Ar}$  in the Apollo 15 drill core increase with depth by nearly a factor of four (0.74 to 2.86) in the 0-80 cm depth range, then decrease for greater depths. Values of  $^{40}\text{Ar}/^{36}\text{Ar}$  in the Apollo 16 drill core are nearly

constant at  $\sim 1.3$ , except for the deepest sample analyzed ( $\sim 2.7$ ). Concentrations of glass-bonded agglutinate particles in the fines tend to correlate with lower  $^{40}\text{Ar}/^{36}\text{Ar}$ , and may indicate that dynamic regolith processes also affect the trapped  $^{40}\text{Ar}/^{36}\text{Ar}$ .

Bogard, D. D., Nyquist, L. E., Hirsch, W. C., and Moore, D. R.: 'Trapped Solar and Cosmogenic Noble Gas Abundances in Apollo 15 and 16 Deep Drill Samples', *Earth Planetary Sci. Letters* **21**, 52–69.

Abundances and isotopic compositions of all the stable noble gases have been measured in 19 different depths of the Apollo 15 deep drill core, 7 different depths of the Apollo 16 deep drill core, and in several surface fines and breccias. All samples analyzed from both drill cores contain large concentration of solar wind implanted gases, which demonstrates that even the deepest layers of both cores have experienced a lunar surface history. For the Apollo 15 core samples, trapped He concentrations are constant to within a factor of two; elemental ratios show even greater similarities with mean values of  $^4\text{He}/^{22}\text{Ne} = 683 \pm 44$ ,  $^{22}\text{Ne}/^{36}\text{Ar} = 0.439 \pm 0.057$ ,  $^{36}\text{Ar}/^{84}\text{Kr} = 1.60 \pm 0.11 \cdot 10^3$ , and  $^{84}\text{Kr}/^{132}\text{Xe} = 5.92 \pm 0.74$ . Apollo 16 core samples show distinctly lower  $^4\text{He}$  contents,  $^4\text{He}/^{22}\text{Ne}$  ( $567 \pm 74$ ), and  $^{22}\text{Ne}/^{36}\text{Ar}$  ( $0.229 \pm 0.024$ ), but their heavy-element ratios are essentially identical to Apollo 15 core samples. Apollo 16 surface fines also show lower values of  $^4\text{He}/^{22}\text{Ne}$  and  $^{22}\text{Ne}/^{36}\text{Ar}$ . This phenomenon is attributed to greater fractionation during gas loss because of the higher plagioclase contents of Apollo 16 fines. Of these four elemental ratios as measured in both cores, only the  $^{22}\text{Ne}/^{36}\text{Ar}$  for the Apollo 15 core shows an apparent depth dependence. No unambiguous evidence was seen in these core materials of appreciable variations in the composition of the solar wind. Calculated concentrations of cosmic ray-produced  $^{21}\text{Ne}$ ,  $^{80}\text{Kr}$ , and  $^{126}\text{Xe}$  for the Apollo 15 core showed nearly flat (within factor of two) depth profiles, but with smaller random concentration variations over depths of a few cm. These data are not consistent with a short-term core accretion model from non-irradiated regolith. The Apollo 15 core data are consistent with a combined accretion plus static time of a few hundred million years, and also indicate variable pre-accretion irradiation of core material. The lack of large variations in solar wind gas contents across core layers is also consistent with appreciable pre-accretion irradiation. Depth profiles of cosmogenic gases in the Apollo 16 core show considerably larger concentrations of cosmogenic gases below  $\sim 65$  cm depth than above. This pattern may be interpreted either as an accretionary process, or by a more recent deposition of regolith to the upper  $\sim 70$  cm of the core. Cosmogenic gas concentrations of several Apollo 16 fines and breccias are consistent with ages of North Ray Crater and South Ray Crater of  $\sim 50 \times 10^6$  and  $\sim 2 \times 10^6$  yr, respectively.

Brecher, A., Vaughan, D. J., Burns, R. G., and Morash, K. R.: 'Magnetic and Mössbauer Studies of Apollo 16 Rock Chips 60315.51 and 62295.27', *Proceedings of the Fourth Lunar Sciences Conference, Geochim. Cosmochim. Acta* **3**, Suppl. 4, 2991–3001.

Analysis of the Mössbauer spectra of two Apollo 16 rocks showed that 60315.51 is much richer in iron metal and troilite, but poorer in olivine, than 62295.27. The values of magnetic parameters, derived from hysteresis loops at 175 and 300 K, indicate the high metal contents and the predominance of coarse multidomain grains in both rocks. These coexist with a superparamagnetic grain fraction in 60315 and with a small single-domain grain fraction in 62295. The high  $\text{Fe}^0/\text{Fe}^{2+}$  ratios, the non-linear acquisition of laboratory thermoremanence and the drastic changes in magnetic parameters upon heating, support the proposed formation of both rocks from the lunar regolith, with incorporation of shocked meteoritic metal grains during high-temperature impact events and simultaneous acquisition of magnetic remanence. Values estimated for ancient lunar magnetic fields by comparing the natural remanence with laboratory thermoremanence acquired in fields of 0.05 and 0.5 Oe, range from 0.01 to  $> 1$  Oe. However, changes in the samples during heating in the laboratory may invalidate such paleointensity estimates.

Brito, U., Lalou, C., Valladas, G., Ceva, T., and Visocekas, R.: 'Thermoluminescence of Lunar Fines (Apollo 12, 14, and 15) and Lunar Rock (Apollo 15)', *Proceedings of the Fourth Lunar Science Conference, Geochim. Cosmochim. Acta* **3**, Suppl. 4, 2453–2458.

A study is made of the spectrum of the thermoluminescent emission of fines samples of Apollo 12, 14, and 15 missions and rock sample of Apollo 15 mission. Differences in intensity of the whole TL from one site to another have been found that may be explained by differences in mineralogical composition. In the Apollo 15 drill core sample, the percentage of TL carriers seems different from one level to another. To make precise studies of TL gradients, it is necessary to work with normalized TL on mineralogical separates.

Brown, G. E. and Prewitt, C. T.: 'High-Temperature Crystal Chemistry of Hortonolite', *Amer. Mineralogist* **58**, 577–587.

The crystal structure of a hortonolite ( $\text{Fa}_{31}$ ) has been refined from intensity data collected at 24°, 375° and 710°C. Significant ordering of  $\text{Fe}^{2+}$  on  $M(1)$  was detected [ $K_D = 1.19(3)$ ] and did not change over the temperature range studied. Mean  $M$ -O distances and octahedral volumes increase linearly from 24°–710°C whereas mean tetrahedral distances and volumes show no significant changes. Octahedral distortions increase differentially as a function of temperature with  $M(1)$  distortion increasing at a faster rate than  $M(2)$  distortion. A consideration of these distortions over the temperature range studied helps in understanding recent Mössbauer spectra of olivines as well as the observed relative enrichment of  $\text{Fe}^{2+}$  on the  $M(1)$  site in some olivines.

Structural refinements of another lunar olivine ( $\text{Fa}_{18}$ ) from rock 12018 and a terrestrial metamorphic olivine ( $\text{Fa}_{29}$ ) show them to be significantly ordered [ $K_D = 1.15(3)$ ] and disordered [ $K_D = 1.02(4)$ ], respectively. However, the X-ray site populations for 12018 olivine disclose considerably less ordering [ $K_D = 1.15(3)$ ] than that [ $K_D = 1.75$ ] determined by Virgo and Hafner (1972) using Mössbauer spectroscopy on a more Fe-rich olivine also from lunar rock 12018. This suggests that the earlier-crystallizing Mg-rich olivines are less ordered than the later-crystallizing Fe-rich olivines.

Brown, G. E. and Wechsler, B. A.: 'Crystallography of Pigeonites from Basaltic Vitrophyre 15597', *Proceedings of the Fourth Lunar Science Conference, Geochim. Cosmochim. Acta* **1**, Suppl. 4, 887–900.

Pigeonite crystals from lunar rock chip 15597,28, a pyroxene vitrophyre, have been examined using precession camera, four-circle diffractometer and microprobe. These crystals are (1) typically zoned with respect to Mg, Fe, Ca, and Al, (2) mantled with augite sharing (100), (3) without exsolution of augite on (001) or (100), and (4) sometimes twinned on (100) on both coarse and fine scales. The structure of a moderately zoned pigeonite crystal ( $\sim \text{Wo}_6\text{En}_{68}\text{Fs}_{26}$ ), with  $\sim 10\%$  by volume of (100) epitaxial augite, was refined to an R-factor of 0.051. The intracrystalline Fe/Mg distribution coefficient,  $K_D$ , is near 0.12, indicating moderate disorder between the octahedral sites and an approximate equilibration temperature of  $\sim 650^\circ\text{C}$ . Analysis of Si—O bond lengths indicates that the 0.05 tetrahedral Al is located in the B-chain. Class  $b$  X-ray reflections are not significantly more diffuse than adjacent class  $a$  reflections, suggesting domains larger in size than those in Mull pigeonite, a terrestrial pigeonite set in a glassy andesite with domains estimated to be  $\sim 200 \text{ \AA}$  in diam. Rock 15597 is believed to have arrived at the lunar surface in an essentially undifferentiated, liquid state and was probably separated from the main magma body and quenched to low temperature in or on the lunar regolith. During the metastable crystallization of 15597 pyroxenes under supercooled conditions, reheating through the release of the heat of crystallization may have raised the temperature up to  $\sim 950^\circ\text{C}$  and allowed relatively slow cooling as is suggested by sharp class  $b$  reflections and a  $K_D$  of 0.12.

Brown, G. M., Peckett, A., Phillips, R., and Emeleus, C. H.: 'Mineral-Chemical Variations in the Apollo 16 Magnesian-Feldspathic Highland Rocks', *Proceedings of the Fourth Lunar Science Conference, Geochim. Cosmochim. Acta* **1**, Suppl. 4, 505–518.

Most of the feldspathic rocks studied from the Descartes region are characterized by high Mg:Fe ratios. These include quench-textured spinel troctolite, plagioclase-phyric troctolite and gabbro, and troctolitic fragments in a breccia. Highly magnesian olivines and spinels are associated with high

Mg:Fe ratios in ilmenites and plagioclases. The low chromium contents of these magnesian rocks may be complementary to the high chromium in the ferriferous Fra Mauro basalts. A disrupted pluton, fractionated to less magnesian compositions, has probably yielded the coarsely exsolved pyroxene suite found in one feldspathic breccia. Fractional crystallization of feldspathic magmas early in the evolution of the crust may be reflected in the sequence from olivine (troctolitic) through orthopyroxene (noritic) to pigeonite augite (gabbroic) feldspathic rocks. Although impact melting and recrystallization may be of local significance, evidence from one breccia suggests that the ease of melting is proportional to the aluminum content of the impacted rock. Under such conditions, the troctolitic fragments are the least affected.

Brunfelt, A. O., Heier, K. S., Nilssen, B., and Sundvoll, B.: 'Geochemistry of Apollo 15 and 16 Materials', *Proceedings of the Fourth Lunar Science Conference, Geochim. Cosmochim. Acta* 2, Suppl. 4, 1209–1218.

Neutron activation analysis data are given for two soils, three breccias and one rock sample from the Apollo 16 and 17 missions together with analytical data on separated soil fractions. These results and data on Apollo 15 and 16 soils, breccias, rocks and minerals previously published by us, are discussed together with results from microprobe analyses of some mineral fractions. Apollo 15 soils and breccias can be derived from a mixture of mare and non-mare (KREEP) basalts and anorthositic rocks, the mare basalt content decreasing with decreasing distance from the Apennine Front. On the basis of chemical and mineral composition the Apollo 15 mare basalts are considered to be derived from at least two distinct lava flows. The Apollo 16 regolith is very homogeneous presumably representing material from the Cayley Formation only. Apollo 16 soils and breccias exhibit a marked enrichment in Al and Ca, and depletion in Mg and Fe compared to those from the other landing sites, reflecting the higher anorthosite content of the highland rocks. KREEP basalts similar to sample 14310 from the Fra Mauro landing site are present. The high Ni and Co contents in Apollo 16 breccias together with the unusually high contents of the volatile elements Cl, Zn and In in breccia 66095 may indicate a higher percentage of admixture of an extra-lunar component in the Descartes area than at the other landing sites.

Burns, R. G., Vaughan, D. J., Abu-Eid, R. M., Witner, M., and Morawski, A.: 'Spectral Evidence for Cr<sup>3+</sup>, Ti<sup>3+</sup>, and Fe<sup>3+</sup> rather than Cr<sup>2+</sup> and Fe<sup>3+</sup> in Lunar Ferromagnesian Silicates', *Proceedings of the Fourth Lunar Science Conference, Geochim. Cosmochim. Acta* 1, Suppl. 4, 983–994.

Fe<sup>3+</sup> and Cr<sup>2+</sup> ions were not detected in absorption spectral measurements of zoned pyroxene phenocrysts in rock 15058. However, peaks assigned to Cr<sup>3+</sup>, Ti<sup>3+</sup>, and Fe<sup>2+</sup> ions were resolved in the pigeonite cores and augite mantles. Mössbauer spectroscopy of these regions also revealed no evidence for Fe<sup>3+</sup> ions. Correlations with spectral data for synthetic Cr(II) – Cr(III) forsterite indicated the presence of Cr<sup>3+</sup> in olivines from rock 15555 and earlier Apollo samples, whereas Cr<sup>2+</sup> spectral features were not observed in lunar olivine spectra. The incompatibility of Cr<sup>2+</sup> and Fe<sup>3+</sup> ions and their implied coexistence in appreciable amounts in other lunar ferromagnesian silicates led to a critical review of earlier spectral measurements. It is concluded that the upper detectability limit of Fe<sup>3+</sup> ions by Mössbauer spectroscopy (< 1% of the total iron) precludes the detection of Fe<sup>3+</sup> spectral features in lunar ferromagnesian silicates amidst Fe<sup>2+</sup>, Cr<sup>3+</sup>, and Ti<sup>3+</sup> peaks. The overlap of Cr<sup>2+</sup> and Fe<sup>2+</sup> crystal field bands renders the detection of Cr<sup>2+</sup> ions difficult when Cr/Fe ratios are low in lunar olivines and pyroxenes.

Cadenhead, D. A., Jones, B. R., Buerger, W. G., and Stetter, J. R.: 'Solar Wind and Terrestrial Atmosphere Effects on Lunar Sample Surface Composition', *Proceedings of the Fourth Lunar Science Conference, Geochim. Cosmochim. Acta* 3, Suppl. 4, 2391–2401.

Samples returned from the Apollo missions have been shown to have undergone a partial surface oxidation with the degree of oxidation being dependent on the intensity and duration of exposure to a terrestrial or other oxidizing atmosphere. Exposure to atomic hydrogen at room temperature, or

molecular hydrogen above 100°C results in a surface reduction. The adsorption of water vapor on a test sample was found to be only slightly dependent on the state of surface oxidation, a situation consistent with the formation of hydroxyl groups on the surface when a sample is exposed to hydrogen. That hydroxyl groups are indeed formed is substantiated by the release of water vapor (and by release of heavy water following exposure to deuterium) indicating that water vapor can be synthesized from solar wind hydrogen and sample oxygen. Observation of trace amounts of methane indicate that the reduction process is by no means restricted to the formation of water vapor.

Cadogan, P. H., Eglinton, G., Gowar, A. P., Jull, A. J. T., Maxwell, J. R., and Pillinger, C. T.: 'Location of Methane and Carbide in Apollo 11 and 16 Lunar Fines', *Proceedings of the Fourth Lunar Science Conference, Geochim. Cosmochim. Acta* 2, Suppl. 4, 1493-1508.

The methane and carbide concentrations of visually-selected fractions, and of fractions selected according to density, magnetic susceptibility and density magnetic susceptibility from samples of 10086 and 60501, 17 sieved lunar fines have been measured by methods involving deuterated acid dissolution. The finest grains (0.5-10  $\mu\text{m}$ ), which adhere to the surface of larger particles, contain the highest concentrations of both species. Of the larger particles, breccias and glassy agglutinates contain the highest proportions of carbide and  $\text{CH}_4$ ; these particles are aggregates of finer grains. A sequence of events involving synthesis of carbon species and their subsequent redistribution is described, in which very fine grains, containing high concentrations of solar wind carbon, are considered as the major reaction sites; meteorite impact provides the energy source for synthesis and redistribution of carbon species. The direct contribution of carbide by meteorites is small; metal-rich grains of presumed meteoritic origin are low in carbide and there is little evidence of vapor deposition of carbide. A contribution from meteorite carbon to the carbide *via* an indirect mechanism involving the synthesis of free iron cannot be dismissed.

Cameron, K. L. and Delano, J. W.: 'Petrology of Apollo 15 Consortium Breccia 15465', *Proceedings of the Fourth Lunar Science Conference, Geochim. Cosmochim. Acta* 1, Suppl. 4, 461-466.

Specimen 15465 was collected on the Apennine Front at Spur Crater. The portion of this rock that was allocated to the consortium (15465,7) is a fine-grained soil breccia consisting of clasts of monomineralic grains, glass fragments, and crystalline rock fragments set in a dark matrix composed predominantly of fine particles of brown glass. The two most abundant types of non-mare crystalline rock fragments are KREEP basalt and recrystallized norite. KREEP basalt fragments appear to be relatively more abundant in 15465.7 than in most other samples from Spur Crater and the soils from Stations 2 and 6. The relative abundance of KREEP suggests that 15465,7 may contain a significant contribution of Aristillus-Autolycus ray material.

Carter, J. L.: 'Scanning Electron Microscopy, Non-Dispersive X-ray Analysis and Electron Microprobe Studies of Lunar Soil, Rocks and Microbreccia' (Progress Report), NASA-CR-131870.

Silicate glass of composition similar to brown lunar glass was reduced with carbon and hydrogen. The typical complex iron sulfide and metallic iron mound formed by reduction with carbon is zoned. Its interior is metallic iron or a mixture of iron sulfide and metallic iron. The outer layer is pure metallic iron which is generally discontinuous, but the surface of the mound next to the silicate host is iron sulfide. This type of mound commonly has a waist of metallic iron and a void beneath it. The silicate surface of the void is covered with droplets or stringers of iron sulfide. The complex iron sulfide and metallic iron mounds formed by reduction with hydrogen generally are zoned. The outer layer is iron sulfide or a mixture of iron sulfide and metallic iron but the interior is metallic iron and iron sulfide, and the mound material next to the silicate host is iron sulfide. On the surface of some complex mounds, globules of silicate material are present. In one example, the globules consist of particles of aluminum oxide surrounded by silicate material. In turn, the margin of the globules is surrounded by iron sulfide. Dimples are present and surface of the dimples is covered by dendritic sheaths of iron sulfide and isolated metallic iron globules.



Chang, S., Mack, R., Gibson, E. K., and Moore, G. W.: 'Simulated Solar Wind Implantation of Carbon and Nitrogen Ions into Terrestrial Basalt and Lunar Fines', *Proceedings of the Fourth Lunar Science Conference, Geochim. Cosmochim. Acta* 2, Suppl. 4, 1509-1522.

Carbon-13 and nitrogen-15 ions were implanted in targets of terrestrial basalt and lunar fines under simulated solar wind conditions. Vacuum pyrolysis of irradiated basalt and lunar fines released the implanted  $^{13}\text{C}$  concurrently as  $^{13}\text{CO}$  and  $^{13}\text{CO}_2$  with  $^{13}\text{CO}$  predominating by a factor of 10. With the basalt target, the  $^{13}\text{CO}$  evolved at 950°–1150°C with a peak in the gas release pattern at about 1050°C. A poorly resolved bimodal pattern of  $^{13}\text{CO}$  evolution was obtained with the irradiated lunar fines from 700°–1150°C with a minor peak at 850° and a major one at 1050°C. Implanted  $^{15}\text{N}$  was released from lunar fines in bimodal fashion as  $^{15}\text{N}_2$  over the range 500°–1150°C with a major peak at 800°C and a minor one at 1050°C. The gas evolution patterns of implanted  $^{13}\text{C}$  and  $^{15}\text{N}$  are compared with those of  $^{12}\text{CO}$  and  $^{14}\text{N}_2$  released simultaneously from the lunar fines targets. The pattern of CO evolution in lunar fines suggests post-irradiation chemical alteration of solar wind carbon. The relevance of solar wind carbon and nitrogen concentrations in lunar fines to the estimation of the ratios of these elements in the solar wind is considered.

Chyi, L. L. and Ehmann, W. D.: 'Zirconium and Hafnium Abundances in Some Lunar Materials and Implications of their Ratios', *Proceedings of the Fourth Lunar Science Conference, Geochim. Cosmochim. Acta* 2, Suppl. 4, 1219-1226.

A new rapid and precise analytical procedure for Zr and Hf has been applied to the study of lunar materials. The results indicate that the Zr/Hf ratios in lunar materials vary in a narrow range from 36.6 to 51.3 while their respective contents vary by a factor of 40. There is a strong Zr, Hf, and major element correlation. This correlation and the Zr and Hf systematics suggest that lunar materials fall into two groups. One group characterized by high Zr and Hf contents and higher Zr/Hf ratios corresponds to materials with a high KREEP content; the other characterized by low Zr and Hf contents and lower Zr/Hf ratios corresponds to materials with high Ti, Fe, Mn, and Mg contents. We believe that the modest Zr and Hf fractionation we observe is related to the extent of stabilization of the metals in the early titanium minerals and a charge disparity under extremely reduced conditions in which Zr exists as 3+, while Hf remains as 4+.

Clanton, U. S., McKay, D. S., Laughon, R. B., and Ladle, G. H.: 'Iron Crystals in Lunar Breccias', *Proceedings of the Fourth Lunar Science Conference, Geochim. Cosmochim. Acta* 1, Suppl. 4, 925-931.

Many of the vugs in the highly recrystallized breccias from Apollos 14, 15, and 16 contain euhedral iron crystals. Three populations have been recognized based on crystal habit. In the first group the trapezohedron predominates and the cube faces are smaller. The second group is characterized by the cube as the dominant form; trapezohedron and tetrahexahedron faces are smaller and about equally developed. The dominant habit of the third group is the octahedron with smaller but equally developed cube and dodecahedron faces. Iron has been mobilized and redistributed in a vapor phase. The euhedral crystals, the abundant growth steps, and the open network of substrate crystals clearly support the concept of growth from a vapor-phase.

Clark, R. S. and Keith, J. E.: 'Determination of Natural and Cosmic Ray Induced Radionuclides in Apollo 16 Lunar Samples', *Proceedings of the Fourth Lunar Science Conference, Geochim. Cosmochim. Acta* 2, Suppl. 4, 2105-2113.

Natural and cosmic ray induced radionuclides have been determined in 22 rocks and 16 soils from the Apollo 16 mission by non-destructive gamma-ray spectroscopy. The natural and cosmic ray-induced radioactivities vary considerably in this set of samples; for example, potassium varies from 0.0114% to 0.284%. Samples 67935,5 and 67936,18 are probably unsaturated in  $^{26}\text{Al}$ . These samples were collected from the border of a large spall zone on Outhouse Rock at Station 11, and are heavily shocked. It is probable that this spall zone was formed within the last few hundred thousand years.

Clayton, R. N., Hurd, J. M., and Mayeda, T. K.: 'Oxygen Isotopic Compositions of Apollo 15, 16, and 17 Samples, and their Bearing on Lunar Origin and Petrogenesis', *Proceedings of the Fourth Lunar Science Conference, Geochim. Cosmochim. Acta* 2, Suppl. 4, 1535–1542.

Crystalline rocks from the Apollo 15 and 16 collections, and lithic clasts in breccias, have mineral-pair oxygen isotopic fractionations consistent with equilibration at temperatures near 1100°C. Metaclastic rock 65015 has a somewhat larger plagioclase-ilmenite fractionation, indicating metamorphism at about 100°C. Isotopic compositions of Apollo 16 breccias fall within a very narrow range. The dispersion of  $\delta O^{18}$  values for all lunar rocks is so small that it must be concluded that the oxygen isotopic composition of the lunar interior is known with considerable certainty. The isotopic evidence favors a ferromagnesian composition rather than a Ca – Al silicate composition for the interior.

Cuttitta, F., Rose, H. J., Annell, C. S., Carron, M. K., Christian, R. P., Ligon, D. T., Dwornik, E. J., Wright, T. L., and Greenland, L. P.: 'Chemistry of Twenty-One Igneous Rocks and Soils Returned by the Apollo 15 Mission', *Proceedings of the Fourth Lunar Science Conference, Geochim. Cosmochim. Acta* 2, Suppl. 4, 1081–1096.

The major, minor and trace element compositions of 14 igneous rocks and 7 soils returned by the Apollo 15 mission have been determined. These rocks comprise two chemically defined groups: Vesicular, porphyritic basalts (olivine normative), and vuggy, medium-grained gabbros (quartz normative). The rocks are characterized by the lowest refractory and volatile element content of any lunar igneous rocks returned by previous missions.

Effects reflecting magma chamber zoning as a result of temperature gradients are evident in the Apollo 15 rocks (e.g., gabbro 15065). However, simple fractionation from a homogeneous magmatic source does not adequately explain all the compositional differences seen among lunar basalts. These studies also indicate that the Apollo 15 rocks represent several parent magmas rather than a single magmatic event.

Our data indicate that the chemical composition of lunar soils depends largely on the geographical locations from whence they were obtained. The highland soils from the Apennine Front have smaller proportions of the KREEP basalt and meteoritic components than the Fra Mauro highland soils.

DesMarais, D. J., Hayes, J. M., and Meinschein, W. G.: 'Accumulation of Carbon in Lunar Soils', *Nature* 246, 65–68.

Analyses of the carbon compounds released by pyrolysis from size fractions and particle separates of lunar soils indicate that the rate at which extralunar carbon is accumulated is slow compared to the rate at which it is redistributed among the different particle types by the cycle of particle erosion and aggregation. Consequently, much of the carbon acquired from the solar wind and meteorites has been modified by the energetic events that cycle lunar soils.

DesMarais, D. J., Hayes, J. M., and Meinschein, W. G.: 'The Distribution in Lunar Soil of Carbon Released by Pyrolysis', *Proceedings of the Fourth Lunar Science Conference, Geochim. Cosmochim. Acta* 2, Suppl. 4, 1543–1558.

The carbon contents of various lunar soil particle types and sieve fractions of Apollo 15 and 16 samples have been determined by the pyrolysis method. The mineral, glass, and high-grade breccia fragments in the soils examined contain relatively low amounts of carbon (approximately 8, 25, and 25  $\mu\text{g C/g}$  sample respectively in 149–250  $\mu\text{m}$  grains). Most low-grade breccias and all agglutinates examined have high carbon contents (approximately 52 and 80  $\mu\text{g C/g}$  ample respectively), and agglutinate abundance is indicative of the carbon content and maturity of a soil.

The distribution of carbon with respect to particle size in mature soils generally reveals a minimum in carbon content at about 100  $\mu\text{m}$  particle diameter. At smaller particle diameters, carbon content is directly proportional to particle surface area and therefore increases with the ratio (surface area)/(particle mass). At particle diameters larger than 100  $\mu\text{m}$ , carbon-rich aggregates become more

abundant. A model relating the cycle of comminution and aggregation of soil particles to the redistribution of surface implanted carbon is developed. The rate of soil cycling appears to be rapid compared to the rates of carbon accumulation. Quantitative interpretation of the distribution of carbon among particle types and sizes in sample 68501,37 indicates the presence in this soil of a coarse-grained carbon poor diluent, presumably ejecta from South Ray Crater.

Dowty, E., Prinz, M., and Keil, K.: 'Composition, Mineralogy, and Petrology of 28 Mare Basalts from Apollo 15 Rake Samples', *Proceedings of the Fourth Lunar Science Conference, Geochim. Cosmochim. Acta* **1**, Suppl. 4, 423-444.

Twenty-eight mare basalts from three Apollo 15 rake sample sections are divided into five groups. *Pyroxene-phyric basalts* (6 specimens) have high SiO<sub>2</sub> (46.9-49.2%) and low FeO (19.0-22.3%) and TiO<sub>2</sub> (1.2-2.3%) with respect to the other groups; they are equivalent to the 'quartz-normative' group of others. They contain zoned pyroxene and occasionally a few olivine phenocrysts in a finer groundmass of acicular pyroxene and plagioclase. They are distinct mineralogically from other groups in that they contain plagioclase with lower anorthite content (average An<sub>89.1</sub>), ilmenite with lower MgO (average 0.2%) and spinel with a wider compositional gap between chromite and ulvöspinel and a closer approach of each to these end-members.

Two olivine-bearing groups are rather similar compositionally and mineralogically and together are equivalent to the "olivine-normative" group of others. Both have relatively low SiO<sub>2</sub> (43.8-46.7%), and high FeO (21.3-24.3%) and TiO<sub>2</sub> (1.3-3.1%). However, *olivine-phyric basalts* (7 specimens) have low MgO (7.7-10.5%) and contain skeletal or amoeboid olivine phenocrysts in a groundmass of sub-equant pyroxene grains enclosed in sub-radiating plagioclase laths; there are no pyroxene phenocrysts. *Olivine microgabbros* (12 specimens), on the other hand, have higher MgO (9.3-12.7%) and contain large crystals of both olivine and pyroxene in more-or-less gabbroic, though variable, textures. The olivine-phyric basalts generally have olivine which is more magnesian than that in olivine microgabbros (frequency maximum at about Fo<sub>61</sub> vs Fo<sub>51</sub>), slightly less magnesian pyroxene, and less anorthitic feldspar (average An<sub>90.0</sub> vs An<sub>91.2</sub>; ilmenite compositions are similar (average 1.0% MgO).

These three rock groups occur at two stations. Hadley Rille and St. George, and probably represent at least three different units which are near the mare surface at the Apollo 15 site and at least two magmas, represented by pyroxene-phyric basalt and olivine-bearing rocks; the two olivine-bearing groups might be related by subsurface differentiation.

Two additional rock groups are present only in the sample from Spur Crater, and may represent units which are from deeper levels in the mare or from a more distant source. *Feldspathic peridotites* (2 specimens) are similar texturally to olivine microgabbros, but have very high modal olivine (30-34%), high bulk MgO (16.9-18.1%), and low SiO<sub>2</sub> (41.4-41.8%). Olivine and pyroxene show relatively little iron enrichment and maximum forsterite in olivine (Fo<sub>68</sub>) is no greater than that in the other groups; hence, these rocks are probably cumulates from a liquid with Mg/(Mg + Fe) similar to that of the olivine-bearing groups. *Feldspathic microgabbro* (one specimen) has low FeO (17.2%) and high Al<sub>2</sub>O<sub>3</sub> (10.9%), with abundant plagioclase (36% modally vs ≤ 30% for other rocks). No olivine is present and large pyroxene and plagioclase laths show sub-parallel alignment. Spinel has restricted composition (chromian ulvöspinel), and metal has low nickel (< 3% vs averages of 4.5-6.5 for other groups). This group may represent a pyroxene and, possibly, plagioclase cumulate from a more typical mare basalt liquid, such as the olivine-phyric basalt, or may have crystallized from a liquid derived from a more feldspathic source rock.

Drake, J. C. and Klein, C.: 'Lithic Fragments and Glasses in Microbreccia 15086: Their Chemistry and Occurrence', *Proceedings of the Fourth Lunar Science Conference, Geochim. Cosmochim. Acta* **1**, Suppl. 4, 467-479.

A polished thin section of microbreccia 15086, which was collected at Station 1 during Apollo 15 traverses, has been extensively studied using electron microprobe and standard petrographic techniques. A small amount of fragmental material from this same microbreccia was used for a complete chemical bulk analysis. 291 glasses, 58 pyroxenes, 27 feldspars, 4 olivines and 12 lithic fragments were analyzed with the electron microprobe. Rounded glass particles exhibit a single preferred composi-

tion, identical with that of the 'green glass' common in Apollo 15 regolith materials. Angular glasses and large irregular patches of glass have six distinct preferred compositions: (1) green glass, (2) Highland basalt, (3) Fra Mauro basalt, (4) low K, low Mg, high Fe, high Al glass, (5) Mare basalt, and (6) anorthosite. Lithic fragments include various texturally distinct members of the pyroxene-phyric group, hyalo-ophitic basalt, microgabbros, and recrystallized rocks of variable composition. No unrecrystallized breccia fragments were observed. Compositions of minerals in the lithic fragments are similar to those of individual mineral clasts.

Drake, M. J., Stoesser, J. W., and Goles, G. G.: 'A Unified Approach to a Fragmental Problem: Petrological and Geochemical Studies of Lithic Fragments from Apollo 15 Soils', *Earth Planetary Sci. Letters* 20, 425-439.

We report the results of a petrological-(nondestructive) geochemical investigation of some lithic fragments separated from Apollo 15 soil samples. Three groups of non-mare materials are recognized on the basis of REE concentrations, viz. KREEP-rich, KREEP-intermediate, and KREEP-poor rocks. These groups may be discrete rather than gradational. Within the group of KREEP-rich rocks three subtypes are recognized. These subtypes do not appear to be simply related to one another. Apollo 15 mare basalts have the lowest REE concentrations observed thus far. All mare basalts analyzed in this study display small negative Eu anomalies.

Duncan, A. R., Erlank, A. J., Willis, J. P., and Ahrens, L. H.: 'Composition and Inter-Relationships of Some Apollo 16 Samples', *Proceedings of the Fourth Lunar Science Conference, Geochim. Cosmochim. Acta* 2, Suppl. 4, 1097-1113.

Data are presented on 20 elements in three Apollo 16 soils (60501, 65501, and 67481), two breccias (67016, two portions of 67915), and three metaigneous rocks (61016, 65015, and 66095). Abundances of 14 of these elements in 19 Apollo 16 soils have been compiled by combining our data with those of other workers. Two compositional groups can be distinguished, one of which is closely associated with ejecta from North Ray Crater. A subtle but systematic compositional change from north to south across the EVA traverse area has been revealed by multivariate analysis and is attributed to mixing between compositionally distinct North Ray and South Ray ejecta blankets. We consider both the Cayley and Descartes formations to be ejecta blankets, with their contact dipping at a shallow angle beneath the Cayley plains. The proximity of North Ray Crater to the Cayley-Descartes boundary thus implies that the North Ray ejecta blanket is dominantly Descartes material. The compositions of what we consider typical Cayley and Descartes soils are presented in the form of putative component proportions derived from compositional mixing models.

Inter-element relationships between the incompatible elements K, Zr, Nb, Ba, Y, and P are examined in the light of our Apollo 16 data and that we have previously obtained in lunar materials and stony meteorites. Some of these relationships are not as well developed as we have previously noted because of the probable cumulate character of some Apollo 16 samples. Volatile-involatile element relationships do not support large scale volatilization of K from lunar lavas, nor are they compatible with volatility dependant inhomogeneous accretion processes. Refractory inter-element relationships in stony meteorites are similar, sometimes closely so, to those in lunar materials, and it appears that the Moon and stony meteorite parent bodies inherited the same high temperature fraction which became mixed with different proportions of low temperature fraction(s). The enrichment of refractory elements in KREEP materials is best explained by fractionation processes operative within the Moon.

Eberhardt, P., Geiss, J., Graf, H., Grögler, N., Krähenbühl, U., Schwaller, H., and Stettler, A.: 'Noble Gas Investigations of Lunar Rocks 10017 and 10071', *Geochim. Cosmochim. Acta* 38, 97-120.

The noble gases He, Ne, Ar, Kr and Xe and also K and Ba were measured in the Apollo 11 igneous rocks 10017 and 10071, and in an ilmenite and two feldspar concentrates separated from rock 10071. Whole rock K/Ar ages of rocks 10017 and 10071 are  $(2350 \pm 60) \times 10^6$  yr and  $(2880 \pm 60) \times 10^6$  yr, respectively. The two feldspar concentrates of rock 10071 have distinctly higher ages:  $(3260 \pm 60) \times$

$\times 10^6$  yr and  $(3350 \pm 70) \times 10^6$  yr. These ages are still 10% lower than the Rb/Sr age obtained by Papanastassiou *et al.* and some Ar<sup>40</sup> diffusion loss must have occurred even in the relatively coarse-grained feldspar.<sup>7</sup>

The relative abundance patterns of spallation Ne, Ar, Kr and Xe are in agreement with the ratios predicted from meteoritic production rates. However, diffusion loss of spallation He<sup>3</sup> is evident in the whole rock samples, and even more in the feldspar concentrates. The ilmenite shows little or no diffusion loss. The isotopic composition of spallation Kr and Xe is similar to the one observed in meteorites. Small, systematic differences in the spallation Kr spectra of rocks 10017 and 10071 are due to variations in the irradiation hardness (shielding). The Kr spallation spectra in the mineral concentrates are different from the whole rock spectra and also show individual variations, reflecting the differences in target element composition. The relative abundance of cosmic ray produced Xe<sup>131</sup> differs by nearly 50% in the two rocks. The other Xe isotopes show no variations of similar magnitude. The origin of the Xe<sup>131</sup> yield variability is discussed.

Kr<sup>81</sup> was measured in all the samples investigated. The Kr<sup>81</sup>/Kr exposure ages of rocks 10017 and 10071 are  $(480 \pm 25) \times 10^6$  yr and  $(350 \pm 15) \times 10^6$  yr, respectively. Exposure ages derived from spallation Ne<sup>21</sup>, Ar<sup>38</sup>, Kr<sup>83</sup> and Xe<sup>126</sup> are essentially in agreement with the Kr<sup>81</sup>/Kr ages. The age of rock 10071 might be somewhat low because of a possible recent exposure of our sample to solar flare particles.

Eldridge, J. S., O'Kelley, G. D., and Northcutt, K. J.: 'Radionuclide Concentrations in Apollo 16 Lunar Samples Determined by Nondestructive Gamma-Ray Spectrometry', *Proceedings of the Fourth Lunar Science Conference, Geochim. Cosmochim. Acta* 2, Suppl. 4, 2115–2122.

A gamma-ray spectrometer system with high sensitivity and low background was used to determine concentrations of K, Th, U, <sup>26</sup>Al, and <sup>22</sup>Na in eleven soil samples: 61161, 61181, 61281, 61501, 62241, 63501, 64801, 65901, 66031, 67941, and 68501. In addition those same radioelements and radionuclides were determined in fifteen rock samples: 60135, 60315, 61016, 6120, 61135, 61155, 61156, 61175, 61195, 61295, 62295, 65095, 66035, 66075, 67055, and 67937.

The K, Th, and U contents of all the soils are strikingly similar, with average concentrations of 940, 1.95, and 0.54 ppm for K, Th, and U, respectively. Rock 60315 was found to have high concentrations of primordial radioelements, characteristic of KREEP basalts.

Aluminum-26 concentrations in Apollo 16 samples are considerably higher than Apollo 15 samples due to the higher Al<sub>2</sub>O<sub>3</sub> content of the Descartes materials. Two rocks and three soils appear to have short exposure ages as determined by low ratios of <sup>26</sup>Al to <sup>22</sup>Na compared to other samples in this suite.

Potassium-uranium systematics for Apollo 16 samples again show the uniqueness of lunar materials compared to terrestrial and meteoritic samples.

Eldridge, J. S., O'Kelley, G. D., Northcutt, K. J., and Schonfeld, E.: 'Non-Destructive Determination of Radionuclides in Lunar Samples Using a Large Low-Background Gamma-Ray Spectrometer and a Novel Application of Least-Squares Fitting', *Nucl. Instruments Methods* 112, 319–322; also NASA-TM-X-69581.

Dual-parameter  $\gamma$ -ray spectrometer systems with large-volume NaI(Tl) crystals and ultra-low backgrounds have been used for the non-destructive determination of K, Th, U, and cosmic-ray produced radionuclides in 60 lunar samples. The total mass of samples measured with these systems is  $\sim 28$  kg, and the individual sample masses varied from 2 to 2300 g. Samples from Apollo 11, 12, 14, 15 and 16 missions have been measured. Operation of the spectrometers in a coincidence mode and analyzing singles- and coincidence-spectra permits the simultaneous determination of 8–10 radionuclides in each lunar sample.

Epstein, S. and Taylor, H. P.: 'The Isotopic Composition and Concentration of Water, Hydrogen, and Carbon in Some Apollo 15 and 16 Soils and in the Apollo 17 Orange Soil', *Proceedings of the Fourth Lunar Science Conference, Geochim. Cosmochim. Acta* 2, Suppl. 4, 1559–1575.

Samples 15021, 64421, 65513, 61221, and 74220 were analyzed for their water, carbon, and hydrogen contents and their isotopic composition. The H<sub>2</sub>O contents of the Apollo 16 samples are on the average significantly higher than for the samples from other sites, whereas the H<sub>2</sub>O content of 74220 (orange soil) is the lowest yet observed on a lunar soil sample. By considering lunar soils from all the Apollo sites which exhibit a wide range in H<sub>2</sub>O/H<sub>2</sub> ratios, it is possible to show that the  $\delta D$  of the 'lunar water' approaches an asymptotic value of about  $-125\text{‰}$  at high H<sub>2</sub>O/H<sub>2</sub> ratios. A  $\delta D$  of about  $-125$  is thus considered to be typical of the "lunar water" in all lunar soils analyzed by us to date. Such a  $\delta D$  value is characteristic of terrestrial meteoric waters, and suggests that these small amounts of H<sub>2</sub>O represent terrestrial contamination.

The H<sub>2</sub> concentrations and isotopic compositions in 15021, 64421, and 65513 (14 to 31  $\mu\text{moles H}_2/\text{g}$  and  $\delta D = -710$  to  $-805$ ) are very similar to data obtained on previously analyzed lunar soils. Sample 61221, however, has a low H<sub>2</sub> content (3.9  $\mu\text{moles/g}$ ), compatible with the fact that it is a trench sample that has had a short exposure time at the lunar surface. Sample 74220 is unlike any other lunar soil yet analyzed in that it contains only 0.1  $\mu\text{moles H}_2/\text{g}$ . The hydrogen in all these samples appears to be dominantly of solar wind origin. The H<sub>2</sub>/rare gas ratios in the Apollo 16 samples are roughly a factor of three higher than that for Apollo 11 and 12 soils.

Except for samples 61221 and 74220 the new data on the isotopic composition and concentration of carbon lie within the range of the previously analyzed lunar soils and breccias, Apollo 16 sample 61221,8 is unusual in that it has a remarkably low  $\delta C^{13}$  value ( $-13.9$  for a sample containing as much as 97 ppm carbon. This carbon may be of meteoritic origin. Contrary to data reported by Gibson and Moore we did not find any HCN gas in 61221.

Sample 74220 is also very unusual in that our carbon analysis is the lowest yet reported in any lunar soil or basalt ( $\sim 3.5$  ppm). The  $\delta C^{13}$  value in 74220 ( $-7.2$ ) is unusually high for a lunar sample containing so little carbon.

Evensen, N. M., Murthy, V. R., and Coscio, M. R.: 'Rb-Sr Ages of Some Mare Basalts and the Isotopic and Trace Element Systematics in Lunar Fines', *Proceedings of the Fourth Lunar Science Conference, Geochim. Cosmochim. Acta* 2, Suppl. 4, 1707-1724.

Mare basalt 15016 from Hadley Rille has been dated at  $3.29 \pm 0.05$  AE with  $(^{87}\text{Sr}/^{86}\text{Sr})_1 = 0.69914 \pm 0.00005$  by the Rb-Sr internal isochron method. In age and trace element chemistry it is very similar to sample 15555 which we have previously studied. Basalt 70035 from Taurus-Littrow has a Rb-Sr age of  $3.82 \pm 0.06$  AE and  $(^{87}\text{Sr}/^{86}\text{Sr})_1 = 0.69923 \pm 0.00003$ . This the oldest mare basalt we have dated and may represent an earlier flow in an extended Serengetis-Tranquillitatis mare flooding episode previously sampled at the Tranquillity site. Flooding of the lunar maria may have proceeded in two or more episodes between 3.1 and 3.8 AE ago, rather than continuously during that period.

The age of rock 70035, and our studies of size fractions of the dark mantle soil 75081 provide no evidence for major volcanism or other thermal event at this site more recent than 3.8 AE ago.

It has been postulated by others that in addition to material derived from the local rocks, an 'exotic component' must be present in the lunar soils to explain their radiogenic nature and the trace element abundances. Measurements of K, Rb, Sr and Ba abundances and  $^{87}\text{Sr}/^{86}\text{Sr}$  ratios in various grain size fractions of soils from the Apollo 11, 15, and 17 missions demonstrate that the exotic component is concentrated in the finer grain sizes of these soils. We suggest that this observation, together with the nature of the material sampled by Apollo 14 and the decrease in proportion of exotic component with increasing distance from the Apollo 14 site, point to the Fra Mauro Formation as the source of the exotic component. Transport from the Fra Mauro site to more distant regions would result in progressive breakup of the material and to a decrease in its relative abundance. Additionally, the systematics of the soils appear to require a differential comminution mechanism in which production of soils from the local rocks results in concentration of the more trace element rich phases into the finer grained fractions. The observed scatter in model ages of the lunar soils may be satisfactorily explained by a combination of these mechanisms.

From these and other considerations, we suggest that there is at present no definitive evidence for a global radioactive crust on the Moon, or 'hot spots' distributed uniformly over the lunar surface.

Fields, P. R., Diamond, H., Metta, D. N., and Rokor, D. J.: 'Reaction Products of Lunar Uranium

and Cosmic Rays', *Proceedings of the Fourth Lunar Science Conference, Geochim. Cosmochim. Acta* 2, 2123-2130.

A possible grouping of  $^{236}\text{U}$ : $^{238}\text{U}$  ratios around  $5 \times 10^{-9}$ , tentatively ascribed to the reaction  $^{235}\text{U}(n, \gamma)^{236}\text{U}$ , leads to an estimate of the average thermal neutron exposure that is higher than would be expected from current models. The cosmic ray-induced fission rate for uranium in most of the observed samples is an order of magnitude greater than the spontaneous fission rate. The thermal neutron exposure age of 14259 is calculated.  $^{237}\text{Np}$  has now been preceived in 6 lunar samples; some  $^{237}\text{Np}$ : $^{238}\text{U}$  ratios may measure the high energy neutron flux required for  $^{238}\text{U}(n, 2n)$  reactions. Here too, more neutrons would be needed than are provided in current models. No  $^{244}\text{Pu}$ ,  $^{239}\text{Pu}$ , or  $^{238}\text{Pu}$  has been observed. The uranium and thorium contents of 15021,105 are  $1.16 \pm 0.03$  and  $4.75 \pm 0.08$  ppm; for 15271,80 they are  $1.18 \pm 0.02$  and  $4.29 \pm 0.08$  ppm.

Finkel, R. C.: 'Depth Profiles of Galactic Cosmic Ray Produced Radionuclides in Lunar Samples', Ph.D. Thesis California Univ., San Diego, Univ. Microfilms Order No. 72-33082.

The concentrations of several cosmogenic radionuclides as a function of depth were analyzed by radiochemical means in lunar samples from the Apollo missions. A chemical separation procedure, which relied heavily on ion exchange techniques, was used to separate the following elements from samples of lunar soil and rock: Be, Na, Al, Cl, V, Mn, Fe, Co, and Ni. This procedure and the subsequent radiochemical purification of these elements is described. Atomic absorption techniques for monitoring the separative procedure and for analyzing the lunar materials are discussed.

Fireman, E. L., D'Amico, J., and DeFelice, J.: 'Radioactivities vs Depth in Apollo 16 and 17 Soil', *Proceedings of the Fourth Lunar Science Conference, Geochim. Cosmochim. Acta* 2, Supp. 4, 2131-2143.

$\text{Ar}^{37}$ ,  $\text{Ar}^{39}$ , and  $\text{H}^3$  radioactivities were measured at a number of depths for Apollo 16 and 17 soil. From the  $\text{Ar}^{37}$  measurements, the intensities of the 4 August and 19 April 1972 solar flares integrated over  $2\pi$  solid angle were determined to be  $(168 \pm 6) \times 10^7$  protons ( $> 50$  MeV)/ $\text{cm}^2$ , respectively. The 4 August 1972 flare was 50 times more intense than the large flare of 24 January 1971, which was determined from  $\text{Ar}^{37}$  measurements in Apollo 14 material and also from satellite measurements to be  $(3.3 \pm 0.4) \times 10^7$  protons ( $> 50$  MeV)/ $\text{cm}^2$ . The 4 August 1972 flare caused excess  $\text{Ar}^{37}$  activation in depths as large as  $15 \text{ g cm}^{-2}$ , indicating a hard differential energy spectrum ( $\sim 1/E^{2.5}$ ).

The  $\text{Ar}^{37}$  activities vs. depth in the Apollo 16 drill string increased with depth and reached a broad maximum in the neighborhood of  $50 \text{ g cm}^{-2}$  before decreasing. The neutron-production rate for the moon has been calculated from this  $\text{Ar}^{37}$  depth curve by Kornblum *et al.* The  $\text{Ar}^{39}$  activities in Apollo 17 soil were higher than in Apollo 16 soil, probably owing to the higher Fe and Ti contents. The  $\text{H}^3$  activities in Apollo 16 and 17 soil were quite similar and indicate that the 4 August 1972 flare produced very little  $\text{H}^3$  compared to the amount produced by solar flares during the previous 50 yr.

Fleischer, R. L., Hart, H. R., Carter, Jr. M., Comostock, G. M., Renshaw, A., and Woods, R. T.: 'Lunar Surface Cosmic Ray Experiment S-152, Apollo 16', (Final Report) NASA-CR-134019.

This investigation was directed at determining the energy spectra and abundances of low energy heavy cosmic rays (0.03 E or = 150 MeV/nucleon). The cosmic rays were detected using plastic and glass particle track detectors. Particles emitted during the 17 April 1972 solar flare dominated the spectra for energies below about 70 MeV/nucleon. Two conclusions emerge from the low energy data: (1) The differential energy spectra for solar particles vary rapidly for energies as low as 0.05 MeV/nucleon for iron-group nuclei. (2) The abundance ratio of heavy elements changes with energy at low energies; heavy elements are enhanced relative to higher elements increasingly as the energy decreases. Galactic particle fluxes recorded within the spacecraft are in agreement with those predicted taking into account solar modulation and spacecraft shielding. The composition of the nuclei at energies above 70 MeV/nucleon imply that these particles originate outside the solar system and hence are galactic cosmic rays.

Fleischer, R. L., Hart, H. R., and Giard, W., R.: 'Particle Track Record of Apollo 15 Shocked Crystalline Rocks', *Proceedings of the Fourth Lunar Science Conference, Geochim. Cosmochim. Acta* 3, Suppl. 4, 3207-2317.

Cosmic ray track densities in two mare basalts 15058 and 15555 are multivalued at each depth from the surface, and numerous indications of shock are present, suggesting that shock has lowered track densities in some crystals but not in others. From the minimum track densities, the maximum time since the last shock event is derived for each rock. In separate observations 15017, a black glass, has a surface age of  $\sim 14000$  yr derived from impact pits, but because of low track retentivity a solar flare record of only 1 yr.

Flory, D. A., Oró, J., Wikstrom, S. A., Beaman, D. A., and Lovett, A.: 'Organogenic Compounds in Apollo 16 Lunar Samples', *Proceedings of the Fourth Lunar Science Conference, Geochim. Cosmochim. Acta* 2, Suppl. 4, 2229-2240.

The volatile organogenic compounds  $N_2$ , CO,  $CO_2$ ,  $H_2O$ , and  $C_1 - C_3$  hydrocarbons simultaneously released upon stepped pyrolysis of Apollo 16 lunar samples have been analyzed by gas chromatography-mass spectrometry. Aliquots of the same samples were also etched with DCl and the amounts of deuterated to nondeuterated hydrocarbons determined. Three samples of fines and four rocks were analyzed. Total volatiles released from the fines are as follows (in ppm):  $N_2$  (241-350), CO (307-410),  $CO_2$  (33-210),  $CH_4$  (2-32),  $H_2O$  (31-420), and total C (146-257). Total volatiles released from the rocks are as follows (in ppm):  $N_2$  (7-31), CO (6-57),  $CO_2$  (32-302),  $H_2O$  (31-330), and total C (16-105). Temperature release of  $N_2$ , CO, and  $H_2O$  varied for different samples indicating more than one source for these compounds. Much of the water was released at temperatures below  $500^\circ C$  indicating terrestrial atmospheric contamination, but several samples release significant amounts of water above  $800^\circ C$  which can in part be due to an indigenous lunar source. Similar  $CO_2$  release patterns were obtained for all samples indicating a common source. The deuterated to nondeuterated ratios of the hydrocarbons decrease progressing from  $C_1$  to  $C_3$  indicating that hydrolysis of reactive carbon species produces primarily methane. The  $C_2$  and  $C_3$  hydrocarbons, therefore, may be from non-solar sources. The very low  $CD_4/CH_4$  ratio of 0.1 observed in rock 60017 indicates the methane is present as such and could represent true indigenous lunar methane. Hydrocarbons released by acid treatment of crushed rocks were considerably less than by volatilization, which could be due to uniform distribution throughout the bulk of the rock or to synthesis during volatilization.

Forester, D. W.: 'Mössbauer Search for Ferric Oxide Phases in Lunar Materials and Simulated Lunar Materials', *Proceedings of the Fourth Lunar Science Conference, Geochim. Cosmochim. Acta* 3, Suppl. 4, 2697-2707.

Mössbauer studies were carried out on lunar fines and on simulated lunar glasses containing 'magnetite-like' precipitates with the primary objective of determining how much, if any, ferric oxide is present in the lunar soils. Although unambiguous evidence of lunar  $Fe^{3+}$  phases was not obtained, an upper limit was estimated from different portions of the Mössbauer spectra to be between 0.1 and 0.4 wt. % (as  $Fe_3O_4$ ). A  $< 62 \mu m$  fraction of 15021,118 showed  $\sim 0.5$  wt. % ferromagnetic iron at 300K in as-returned condition. After heating to  $650^\circ C$  in an evacuated, sealed quartz tube for  $\sim 1400$  hr, the same sample exhibited  $\sim 1$  wt. % ferromagnetic iron at room temperature. An accompanying decrease in 'excess' absorption area near zero velocity was noted. Thus, the result of the vacuum heat treatment was to convert fine grained iron to larger particles, apparently without the oxidation effects commonly reported. The Ni content of this 'consolidated' iron was estimated to be  $\sim 2$  wt. %. A conversion electron backscatter experiment was carried out on a  $> 147 \mu m$  fraction of 15021,118. A strongly enhanced 'excess area' near zero velocity was observed in this mode, tending to corroborate the evidence of Housley *et al.* that the occurrence of 'excess area' is surface associated.

Fox, S. W., Harada, K., and Hare, P. E.: 'Accumulated Analyses of Amino Acid Precursors in Returned Lunar Samples', *Proceedings of the Fourth Lunar Science Conference, Geochim. Cosmochim. Acta* 2, Suppl. 4, 2241-2248.



Six amino acids (glycine, alanine, aspartic acid, glutamic acid, serine, and threonine) obtained by hydrolysis of extracts have been quantitatively determined in ten collections of fines from five Apollo missions. Although the amounts found, 7–45 ng/g, are small, the lunar amino acid/carbon ratios are comparable to those of the carbonaceous chondrites, Murchison and Murray, as analyzed by the same procedures. Since both the ratios of amino acid to carbon, and the four or five most common types of cosmogenous amino acid found, are comparable for the two extraterrestrial sources despite different cosmophysical histories of the Moon and meteorites, common cosmochemical processes are suggested.

Fruchter, J. S., Stoesser, J. W., Lindstrom, M. M., and Goles, G. G.: 'Apollo 15 Clastic Materials and their Relationship to Local Geologic Features', *Proceedings of the Fourth Lunar Science Conference, Geochim. Cosmochim. Acta* 2, Suppl. 4, 1227–1237.

Ninety sub-samples of Apollo 15 materials have been analyzed by instrumental neutron activation analysis techniques for as many as 21 elements. Soil and soil breccia compositions show considerable variation from station to station although at any given station the soils and soil breccias were compositionally very similar to one another. Mixing model calculations show that the station-to-station variations can be related to important local geologic features. These features include the Apennine Front, Hadley Rille and the ray from the craters Aristillus or Autolycus. Compositional similarities between soils and soil breccias at the Apollo 15 site indicate that the breccias and soils are related in some fundamental way, although the exact nature of this relationship is not yet fully understood.

Ganapathy, R., Morgan, J. W., Krähenbühl, U., and Anders, E.: 'Ancient Meteoritic Components in Lunar Highland Rocks: Clues from Trace Elements in Apollo 15 and 16 Samples', *Proceedings of the Fourth Lunar Science Conference, Geochim. Cosmochim. Acta* 2, Suppl. 4, 1239–1261.

Thirty-three Apollo 15 samples, 3 Luna 20 samples and 2 samples of breccia 14306 were analyzed by neutron activation for Ag, Au, Bi, Br, Cd, Co, Cs, Ge, In, Ir, Ni, Rb, Re, Sb, Se, Te, Tl, U, and Zn.

The siderophile elements Ir, Re, Au, Ni, and Ge are enriched  $10^2$ – $10^3$  fold over indigenous levels in most of the 120 highland samples analyzed thus far. The enrichment is due to an ancient meteoritic component, dating from the era of basin formation. Five varieties can be distinguished on the basis of Ir/Au, Re/Ir and Ge/Au ratios, corrected for a small indigenous contribution:

	Ir/Au	Ge/Au	Sites
LN	0.25–0.55	0.25–0.60	12, 14, 15, 16
R	0.25–0.40	0.27–0.80	16
DN	0.32–1.10	0.07–0.17	14, 15, 16, 20
A	0.85–1.6	0.25–0.60	15, 16
NR	0.52–0.72	0.7 –0.8	16

The Re/Ir ratio is 1.5–2.0 in the R group, 1.0–1.5 in all other groups. KREEP-rich norites are found only in the LN and DN groups, whereas anorthositic rocks are found in all five groups. It appears that the LN group is associated with the Imbrium Basin, while the R and NR groups are derived from one or more smaller impacts, possibly Nectaris.

These data show that 4 of 5 basin-forming planetesimals were deficient in refractories (Ir, Re) relative to normal siderophiles (Au, Ni). Their composition thus was complementary to that of the Moon as a whole, and hence they cannot have served as the principal building blocks of the Moon.

A number of individual Apollo 15 samples are discussed in some detail: six mare basalts; breccias 15455, 15418, and 15459; and green glass 15426.

Gehrke, C. W., Zumwalt, R. W., Kuo, K. C., Ponnampuruma, C., Cheng, C. N., and Shimoyama, A.: 'Extractable Organic Compounds in Apollo 15 and 16 Lunar Fines', *Proceedings of the Fourth Lunar Science Conference, Geochim. Cosmochim. Acta* 2, Suppl. 4, 2249–2259.

The results of a search for extractable organic substances, in particular amino acids, in Apollo 15 and 16 fines, using highly sensitive gas-liquid chromatographic and automatic classical ion exchange methods, are presented. Recovery data from experiments in which known amounts of free amino acids were added to lunar fines, are also reported.

Gibson, E. K., Hubbard, N. J., Wiesmann, H., Bansal, B. M., and Moore, G. W.: 'How to Lose Rb, K, and Change the K/Rb Ratio: An Experimental Study', *Proceedings of the Fourth Lunar Science Conference, Geochim. Cosmochim. Acta 2*, Suppl. 4, 1263–1273.

Thermal volatilization studies on Apollo 16 soils and crystalline rocks have been carried out to measure the depletion of K, Rb, and Na and changes in K/Rb ratios during heating under vacuum. Rubidium can be lost from both soils and rocks at temperatures as low as 1000°C. Because of the greater volatility of Rb as compared to K, the K/Rb ratio can be changed from normal values of 330–360 for the Apollo 16 samples to values as high as 1100 by thermal volatilization.

Rapid heating experiments on soil samples were carried out to approximate agglutinate formation conditions in order to measure changes in alkali element abundances. Equal changes in K/Rb ratios can be produced with longer heating at lower temperatures or heating at higher temperatures for shorter times.

The problem of where the lunar alkali elements have gone during cratering and agglutinate formation has been examined. Among the possibilities examined are: (1) redeposition, (2) cold-trapping, (3) ionization loss, and (4) escape from the lunar gravitation field.

Gibson, E. K. and Moore, C. B.: 'Variable Carbon Contents of Lunar Soil 74220', *Earth Planetary Sci. Letters 20*, 404–408.

Total carbon, sulfur and inorganic gas release studies have been carried out on an additional split of orange soil 74220. The total carbon content was found to be  $4 \pm 3$  ppm C for this sample as compared to an earlier reported value of  $100 \pm 10$  ppm C. Gas release studies on the two splits of 74220 indicates that the carbon may be present as a surface condensate on the sample showing the higher carbon content. The 'surface condensate' evolves CO<sub>2</sub> upon heating to temperatures below 400°C.

Gibson, E. K. and Moore, G. W.: 'Carbon and Sulfur Distributions and Abundances in Lunar Fines', *Proceedings of the Fourth Lunar Science Conference, Geochim. Cosmochim. Acta 2*, Suppl. 4, 1577–1586.

Total sulfur abundances have been determined for 20 Apollo 14, 15, and 16 soil samples and one Apollo 14 breccia. Sulfur concentrations range from 474 to 844 µgS/g. Volatilization experiments on selected samples have been carried out using step-wise heating. Sample residues have been analyzed for their total carbon and sulfur abundances to establish the material balance in lunar fines for these two elements. Volatilization experiments have established that between 31 to 54 µgC/g remains in soils which have been heated at 1100°C for 24 hr under vacuum. The residual carbon is believed to be indigenous lunar carbon whereas all forms of carbon lost from samples below 1100°C is extralunar carbon. Total carbon and sulfur abundances taken from the literature have been used to show the depletion of volatile elements with increasing grade for the Apollo 14 breccias.

Goldstein, J. I. and Axon, H. J.: 'Composition, Structure, and Thermal History of Metallic Particles from 3 Apollo 16 Soils, 65701, 68501, and 63501', *Proceedings of the Fourth Lunar Science Conference, Geochim. Cosmochim. Acta 1*, Suppl. 4, 751–775.

A metallographic and electron probe study of the metal in 284 of the most magnetic particles in 3 Apollo 16 soils, 65701 on Stone Mountain, 68501 on a bright ray from South Ray Crater and 63501 at Station 13 on the continuous ejecta blanket of North Ray Crater was carried out. Most of the metal particles were of large size, > 100 µm, and had been liberated by shock processes from the rocks in which the present metallic structures were formed.

Many of the metallographic structures and metal-silicate associations are very similar to those reported for metal particles at the Apollo 14 site. The Apollo 16 site however contains a much larger proportion of two phase  $\alpha(\text{Fe}) + \text{phosphide}$  structures and a new subpopulation of metal particles which have been fragmented from large melted metal-phosphide spherules or globules. Final equilibration temperatures in the range 450–550°C were determined for most of the  $\alpha(\text{Fe}) + \text{phosphide}$  particles while for the  $\alpha - \gamma$  structures, equilibrium temperatures ranging from 550 to 715°C were observed.

Most of the metal particles (> 75%) from the 3 Apollo 16 highland soils, the Luna 20 highland soil and at Fra Mauro, Apollo 14, are of 'meteoritic' Ni – Co content. Smaller amounts of 'meteoritic' metal are found at the other landing sites. We attribute the origin of these metallic particles to be fragments of meteorites which have bombarded the early crust of the Moon. Some of the metal of meteoritic Ni – Co content may have developed in the original crustal rocks which form the highlands, but no direct evidence for this process is yet available.

Gorenstein, P., Golub, L., and Bjorkholm, P.: 'Detection of Radon Emission at the Edges of Lunar Maria with the Apollo Alpha-Particle Spectrometer', *Science* **183**, 411–413.

The distribution of radioactive Po-210, a decay product of Ra-222, shows enhanced concentrations at the edges of lunar maria. Enhancements are seen at the edges of Mare Fecunditatis, Mare Crisium, Mare Smythii, Mare Tranquillitatis, Mare Nubium, Mare Cognitum, and Oceanus Procellarum. The observation is indicative of the transient emission of radon gas from the perimeters of lunar maria.

Goresy, A. El., Ramdohr, P., and Medenbach, O.: 'Lunar Samples from Descartes Site: Opaque Mineralogy and Geochemistry', *Proceedings of the Fourth Lunar Science Conference, Geochim. Cosmochim. Acta* **1**, Suppl. 4, 733–750.

A cataclastic anorthosite (67075,45), a polymict breccia of type I (67455,8) and highly metamorphosed breccias of type III (65015,81, 65015,82, 66095,78 and 66095,89) were studied in reflected light and with the electron microprobe. Two genetically different Ti-chromites were encountered in sample 67075,45: (1) a primary Ti-chromite barren of ilmenite lamellae or metal grains and (2) a Ti-chromite formed by subsolidus reduction and reequilibration of former Cr-ulvöspinel to chromite + ilmenite + metal. Compositional variation during crystallization of the first spinel type is different from variations observed in mare type basalts. Continuous increase of the TiO<sub>2</sub> content is accompanied by a coupled decrease in both Al<sub>2</sub>O<sub>3</sub> and MgO contents. Metals in the metamorphosed breccias contain from 3 to 6 wt. % Ni and show a small compositional variation. Many of the metal grains contain inclusions and idiomorphic crystals of schreibersite. Cohenite was discovered in a composite metal-phosphide-troilite grain in sample 66095,78. The metals are probably of meteoritic origin and are perhaps in part debris of planetesimals that bombarded the Descartes site 3.9 AE ago. Rusty Rock samples 66095,78 and 66095,98 are enriched in the volatile elements Zn, Cl and Pb. Goethite occurs in two distinct assemblages: (1) with metallic FeNi as narrow reaction rim, (2) with sphalerite, two Cl, Fe, and Zn rich phases probably a sulphate and a phosphate, and a Pb rich phase. Troilite in sample 67455,8 shows also similar sphalerite-goethite reaction rims, however the degree of alteration is much less than 66095. The narrow width of the sphalerite and goethite reaction rims as well as the dominant shock features present support the idea that the unusual enrichment in volatile elements Zn, Pb, and Cl in 66095 and 67455 took place during or shortly after an impact event involving a water-rich body such as a carbonaceous chondrite or a comet.

Graf, H., Shirck, J., Sun, S., and Walker, R.: 'Fission Track Astrology of three Apollo 14 Gas-Rich Breccias', *Proceedings of the Fourth Lunar Science Conference, Geochim. Cosmochim. Acta* **2**, Suppl. 4, 2145–2155.

The three Apollo 14 breccias 14301, 14313, and 14318 all show fission xenon due to the decay of Pu<sup>244</sup>. To investigate possible *in situ* production of the fission gas, we analyzed the U-distribution in these three breccias. The major amount of the U lies in glass clasts and in matrix material and ≤ 25% occurs in distinct high-U minerals. The U-distribution of each breccia is discussed in detail. Whit-

lockite grains in breccias 14301 and 14318 found with the U-mapping were etched and analyzed for fission tracks. The excess track densities are much smaller than indicated by the Xe-excess. Because of a preirradiation history documented by very high track densities in feldspar grains, however, it is impossible to attribute the excess tracks to the decay of  $\text{Pu}^{244}$ . A modified track method has been developed for measuring average U-concentrations in samples containing a heterogeneous distribution of U in the form of small high-U minerals. The method is briefly discussed and results for the rocks 14301, 14313, 14318, 68815, 15595, and the soil 64421 are given.

Haggerty, S. E.: 'Armalcolite and Genetically Associated Opaque Minerals in the Lunar Samples', *Proceedings of the Fourth Lunar Science Conference, Geochim. Cosmochim. Acta* **1**, Suppl. 4, 777-797.

A comprehensive electron microprobe study of armalcolite in samples from five Apollo sites (11-16), together with analytical data previously reported from Apollo 17 and Luna 20 show that three distinct compositional types of armalcolite are present in the lunar samples. These types are classified as armalcolite, Cr-Zr-Ca-armalcolite and Zr-armalcolite. The Zr-free armalcolites are typical of high-Ti mare basalts whereas the Zr-rich armalcolites are typical of non-mare high alumina basalts. The latter armalcolites are in complex oxide intergrowths (baddeleyite, zirconolite, rutile, ilmenite, and chromite) and are in contrast to the Zr-free armalcolites which are commonly only associated with ilmenite. Subsolidus decomposition of armalcolite to an iron and Mg-rich rutile + ilmenite-geikielite<sub>ss</sub>, and the solid state formation of armalcolite from magnesian-ilmenite + niobian-rutile are described for the first time in the lunar samples.

Halliwell, R. S.: 'Analytical and Radio-Histo-Chemical Experiments of Plants and Tissue Culture Cells Treated with Lunar and Terrestrial Materials' (Final Report), NASA-CR-134036.

The nature and mechanisms of the apparent simulation of growth originally observed in plants growing in contact with lunar soil during the Apollo project quarantine are examined. Preliminary experiments employing neutron activated lunar soil indicate uptake of a few elements by plants. It was found that while the preliminary neutron activation technique allowed demonstration of uptake of minerals it presented numerous disadvantages for use in critical experiments directed at elucidating possible mechanisms of stimulation.

Haskin, L. A., Helmke, P. A., Blanchard, D. P., Jacobs, J. W., and Telander, K.: 'Major and Trace Element Abundances in Samples from the Lunar Highlands', *Proceedings of the Fourth Lunar Science Conference, Geochim. Cosmochim. Acta* **2**, Suppl. 4, 1275-1296.

Analyses for major elements, REE, Co, Cr, Cs, Ga, Hf, Ni, Rb, Sc, and Zn have been done on samples of Apollo 16 rocks 60025, 60335, 64455, 65015, 67075, and 67629 and on < 1 mm fines 60601, 61221, 61241, 64501, 65701, 67601, and 69941. FeO, Na<sub>2</sub>O, REE, Co, Cr, Hf, and Sc have been determined in four 4-5 mg chips from 65015 and 20 individual, 2.5-9.5 mg fragments from 65702. It appears that trace element characteristics of small fragments are similar to those of larger rocks. No simple mixing relationship was found among KREEP basalts, VHA basalts, anorthosites, fines, and meteorites. Balances could not be simultaneously achieved for Al<sub>2</sub>O<sub>3</sub> and LIL elements, using analyzed samples as end members for mixing models. Most samples analyzed have negative Eu anomalies, in contrast to the positive anomalies expected for plagioclase cumulates. Most samples may be derived from LIL-rich liquids that flowed into highland valleys. Samples from Apollo 16, station 11 may be derived from older, cumulus anorthosite.

Heiken, G. H., Bulter, P., Simonds, C. H., Phinney, W. C., Warner, J., Schmitt, H. H., Bogard, D. D., and Pearce, W. G.: 'Preliminary Data on Boulders at Station 6, Apollo 17 Landing Site', NASA-TM-X-58116.

A cluster of boulders at Station 6 (Apollo 17 landing site) consists of breccias derived from the North Massif. Three preliminary lithologic units were established, on the basis of photogeologic interpretations; all lithologies identified photogeologically were sampled. Breccia clasts and matrices studied petrographically and chemically fall into two groups by modal mineralogy: (1) low-K Fra Mauro or high basalt composition, consisting of 50–60% modal feldspar, approximately 45% orthopyroxene and 1–7% Fe-Ti oxide; (2) clasts consisting of highland basalt composition, consisting of 70% feldspar, 30% orthopyroxene and olivine and a trace of Fe-Ti oxide.

Herpers, U., Herr, W., Kulus, H., Michel, R., Thiel, K., and Woelfle, R.: 'Manganese-53 Profile, Particle Track Studies and the Rhenium-187 Isotopic Anomaly of Breccia 14305', *Proceedings of the Fourth Lunar Science Conference, Geochim. Cosmochim. Acta 2*, Suppl. 4, 2157–2169.

Microbreccia 14305 has been studied especially for records of cosmic ray bombardment by three different methods: analysing the longlived reaction product  $^{53}\text{Mn}$ , particle tracks, and neutron produced  $^{187}\text{Re}$ . Neutron activation was applied to determine the  $^{53}\text{Mn}$  content in  $\sim 200$  mg samples of defined depths. The activity profile shows distinct maxima on the top and the bottom side. This effect is explained by at least one movement of the rock in the past, so that this object is likely to be a 'tumbling stone'. The upper side has not yet reached  $^{53}\text{Mn}$  saturation activity suggesting a maximum irradiation age of  $\sim 14$  m.y. for the top side-up position. The comparison of the  $^{53}\text{Mn}$  gradient with that of rock 10017 leads to a total exposure age of  $> 20$  m.y. Cosmic ray track densities in olivines, feldspars and pyroxenes show only relatively small variations indicating strong thermal and/or shock annealing during the formation of the breccia 14305. Minimum track densities at different depths give a shallow depth profile comparable to that of  $^{53}\text{Mn}$ . Using theoretical production rates of cosmic ray tracks in lunar material, an upper limit for the irradiation age of  $\sim 23$  m.y. is obtained. The U-distribution of breccia 14305 has been studied by the fission track method at a spatial resolution of U-bearing minerals of  $< 1 \mu$ . The highest U-contents ( $> 100$  ppm U) are observed in apatite. Further, neutron activation experiments proved the existence of an isotopic anomaly in Re in the rocks 14305, 14321 and in the soils 14163 and 14259. The enrichment of  $^{187}\text{Re}$  is in the range of 1.4 to 28% and obviously due to epithermal  $n$ -capture in U ( $^{186}\text{W}(n, \gamma)^{187}\text{W}^{\beta-} \rightarrow ^{187}\text{Re}$ ). The  $n$ -capture rates per atom  $^{186}\text{W}$  were found to be between  $3 \times 10^{-5}$  and  $14 \times 10^{-5}$  which is higher than expected by theory. Correlation with the other  $n$ -induced isotopic anomalies as observed in  $^{157}\text{Gd}$ ,  $^{149}\text{Sm}$ ,  $^{80}\text{Kr}$ , and  $^{131}\text{Xe}$  are discussed in view of an increased epithermal intensity in the lunar neutron spectrum.

Hintenberger, H., and Weber, H. W.: 'Trapped Rare Gases in Lunar Fines and Breccias', *Proceedings of the Fourth Lunar Science Conference, Geochim. Cosmochim. Acta 2*, Suppl. 4, 2003–2019.

Rare gas concentrations and isotopic abundances have been measured in bulk material of the fines and breccias 74241, 74220, 68501, 67461, 65701, 60601, 15471, and 14163. From the samples 74241, 74220, 68501, 15471, and 14163 also grain size fractions have been investigated. From the grain size dependency of the concentrations, the surface correlated components (solar wind components and trapped  $(^{40}\text{Ar})_{\text{SC}}$ ) and the volume correlated components (cosmogenic  $^3\text{He}$ ,  $^{21}\text{Ne}$ ,  $^{38}\text{Ar}$  as well as radiogenic  $^{40}\text{Ar}$ ) have been determined.

In general, the grain size dependency of the concentration  $C(y, d)$  of a trapped rare gas nuclide  $y$  can be described by the formula  $C(y, d) = S_y(d/d_0)^{-n_y}$  ( $d$  = grain diameter). The constants  $S_y$  and  $n_y$  are listed in tables.

The ratios  $(^4\text{He}/^{20}\text{Ne})_{\text{tr}}$  and, especially, the ratios  $(^{20}\text{Ne}/^{36}\text{Ar})_{\text{tr}}$  are correlated to the  $\text{TiO}_2$ -content of the samples. No such correlation exists for the  $(^{36}\text{Ar}/^{84}\text{Kr})_{\text{tr}}$  ratios. This reflects the fact that the differences in the abundance patterns of the trapped rare gases in different soils are mainly caused by diffusion losses, which lead to a higher depletion in the light rare gases in ilmenite-poor samples than in ilmenite-rich ones. Trapped rare gases in samples from the Apollo 15 and especially from the Apollo 14 missions show, however, in many cases more complicated features.

The ratios  $(^{40}\text{Ar}/^{36}\text{Ar})_{\text{SC}}$  for the surface correlated argon vary between 0.42 for 12070 and 7.6 for 74241.

In the orange soil 74220 and in the near-by collected reference sample (gray soil 74241), the abundance patterns of the trapped rare gases are equal although the absolute concentrations in the orange

soil are lower by factors of about 10 than in the gray soil. The isotopic ratios ( $^{40}\text{Ar}/^{36}\text{Ar}$ )<sub>sc</sub> for surface correlated argon in these samples attain high values of up to 5.0 (orange soil) and 7.6 (gray soil). The radiogenic components ( $^{40}\text{Ar}$ )<sub>rad</sub> amount to  $(2.6 \pm 0.3) \times 10^{-5} \text{ cm}^3 \text{ STP/g}$  and  $(1.2 \pm 0.9) \times 10^{-6} \text{ cm}^3 \text{ STP/g}$ . The gas retention ages calculated therefrom are  $(3.5 \pm 0.3) \times 10^9$  and  $(0.3 \pm 0.2) \times 10^9$  yr, respectively. The reference soil 74241 must, accordingly, have been degassed about 300 m.y. ago.

Holmes, H. F., Fuller, E. L., and Gammage, R. B.: 'Interaction of Gases with Lunar Materials: Apollo 12, 14, and 16 Samples', *Proceedings of the Fourth Lunar Science Conference, Geochim. Cosmochim. Acta* 3, Suppl. 4, 2413–2423.

Surface properties of lunar fines samples from the Apollo 12, 14, and 16 missions have been investigated by studying the adsorption of nitrogen, argon, oxygen, carbon monoxide (all at 77K), and water vapor (at 20 or 22°C) on the samples. Initially the samples were all nonporous and had a uniformly low specific surface area (0.3 to 0.6 m<sup>2</sup> g<sup>-1</sup>). Water interacts strongly with the surface of lunar fines, chemisorbing at low pressures followed by a massive adsorption at high pressures. Nitrogen adsorption measurements after the interaction with water showed the surface properties had undergone a severe alteration as a result of the attack by water vapor. This alteration consisted of a marked increase in the specific surface area and the creation of a pore system. The results are interpreted on the basis of a penetration of water into the damage tracks.

Hoyt, H. P., Walker, R. M., and Zimmerman, D. W.: 'Solar Flare Proton Spectrum Averaged over the Last  $5 \times 10^3$  yr', *Proceedings of the Fourth Lunar Science Conference, Geochim. Cosmochim. Acta* 3, Suppl. 4, 2489–2502.

Thermoluminescence (TL) measurements in the top centimeter of lunar rocks show a strong depth dependence that we have previously shown to be semi-quantitatively consistent with that expected from solar flare irradiation. In this paper we derive from the TL data the solar flare differential energy spectrum and integral proton flux above 10 MeV averaged over the last several thousand years. The dose-rate depth profile is obtained using a new TL equilibrium technique which is independent of the TL decay kinetics. The dose-rate depth profile produced by solar flare protons with a differential energy spectrum of the form  $dJ/dE = KE^{-\gamma}$  is calculated for arbitrary  $\gamma$ . The best fit to the TL data in rock 14310 is obtained for  $\gamma = 2.3 \pm 0.2$  and an omnidirectional ( $4\pi$ ) integral flux above 10 MeV of 40–80 prot cm<sup>-2</sup> s<sup>-1</sup>. The TL half-life is determined to be  $2 \times 10^3$  yr. These results are compared to those for  $^{22}\text{Na}$  ( $T_{1/2} = 2.6$  yr) and  $^{26}\text{Al}$  ( $T_{1/2} = 7.4 \times 10^5$  yr) obtained by Wahlen *et al.* and Rancitelli *et al.* and we conclude that the spectral shape and flux of protons in the interval 25–100 MeV is the same within experimental errors when averaged over these three very different time periods. Our integral flux values do not agree with those obtained from measurements of  $^{14}\text{C}$  ( $T_{1/2} = 5.7 \times 10^3$  yr) by Begemann *et al.* and Boeckl. One possible explanation is that the assumed cross section for production of  $^{14}\text{C}$  is inaccurate but a more interesting alternative suggested by Begemann *et al.* is that the  $^{14}\text{C}$  is surface correlated and represents direct implantation of  $^{14}\text{C}$  from the Sun.

Hübner, W., Heymann, D., and Kirsten, T.: 'Inert Gas Stratigraphy of Apollo 15 Drill Core Sections 15001 and 15003', *Proceedings of the Fourth Lunar Science Conference, Geochim. Cosmochim. Acta* 2, Suppl. 4, 2021–2036.

We have studied the rare gases in eight samples each from sections 15001 (207–238 cm depth) and 15003 (125–161 cm depth) with respect to layering of the core, turnover on a centimeter scale, and the cosmic-ray proton irradiation history.  $^4\text{He}$  contents range from 3.18 to  $8.49 \times 10^{-2} \text{ cm}^3 \text{ STP/g}$  comparable to surface fines. The elemental ratios show narrow ranges:  $^4\text{He}/^{20}\text{Ne} = 50\text{--}60$ ;  $^{20}\text{Ne}/^{36}\text{Ar} = 5.6\text{--}6.4$ ;  $^{36}\text{Ar}/^{84}\text{Kr} = 1520\text{--}1670$ ; and  $^{84}\text{Kr}/^{132}\text{Xe} = 5.2\text{--}7.0$ . Mean grain size is a major factor governing the absolute gas contents. Abundant trapped gas is present in all the samples, which shows that the regolith materials had nearly always been exposed to solar wind prior to their deposition. ( $^4\text{He}/^3\text{He}$ )<sub>T</sub> and ( $^{40}\text{Ar}/^{36}\text{Ar}$ )<sub>T</sub> vary significantly on a centimeter scale, which implies that mixing rates at ancient surfaces nearly always decreased rapidly with depth.

With one exception,  $(^4\text{He}/^3\text{He})_T$  ratios fall into two groups: one  $\sim 3000$ ; the other  $\sim 2700$ , but both values occur in each section. This could mean that the *average* long-term geomagnetic index  $K_p$  has undergone secular variations in the past.

The  $(^{40}\text{Ar}/^{36}\text{Ar})_T$  ratio suggests that substantial layers of ejecta from impacts in the Apennine Front may be present at depths of  $\sim 150$ ,  $\sim 220$ , and  $\sim 240$  cm.

The  $^{21}\text{Ne}_c$  contents show that the materials in our sections were irradiated by galactic and/or solar cosmic rays prior to their deposition. If the core was quickly deposited some 450 m.y. ago, as argued by Russ, Burnett, and Wasserburg, then the  $^{21}\text{Ne}_c$  excess is more than one-half the amounts now present in the samples. When and where this pre-irradiation took place cannot be resolved. If the core was slowly accreted for 400 m.y. and had been subsequently undisturbed for 500 m.y., then the  $^{21}\text{Ne}_c$  systematics can be explained by the deposition of unirradiated or mildly pre-irradiated materials, with most of the  $^{21}\text{Ne}_c$ -excess having been acquired during the 400 m.y. accretionary stage.

Huneke, J. C., Jessberger, E. K., Podosek, F. A., and Wasserburg, G. J.: ' $^{40}\text{Ar}/^{39}\text{Ar}$  Measurements in Apollo 16 and 17 Samples and the Chronology of Metamorphic and Volcanic Activity in the Taurus-Littrow Region', *Proceedings of the Fourth Lunar Science Conference, Geochim. Cosmochim. Acta 2*, Suppl. 4, 1725–1756.

Argon analyses are reported for neutron irradiated whole samples and mineral separates of Apollo 16 crystalline rock 68415, Apollo 17 basaltic rock 75055 and fragment 75083,3,3, breccia 76055, soil 74241 and orange glass from soil 74220, giving gas retention and exposure ages of these samples as well as information on the systematic variations of all Ar isotopes necessary to evaluate these ages.

An age of  $3.97 \pm 0.04$  AE is determined for the metamorphosed breccia 76055 which probably dates the time of extensive metamorphism in the impact forming the Serenitatis basin. The Moon was evidently bombarded by *many* large bodies about 3.95 AE ago forming most of the major mare basins and smaller multi-ring basins over a period of less than  $10^8$  yr.

A well-defined age of  $3.78 \pm 0.04$  AE obtained on a plagioclase separate of basalt 75055 and a less precise age of  $3.70 \pm 0.09$  for the basaltic fragment 75083,3,3 are evidence of flooding by basalt lava in the Taurus-Littrow region 3.7–3.8 AE ago. These ages are similar to the ages of some Mare Tranquillitatis basalts and do not extend the 3.1–3.9 AE range of lunar magmatic activity previously determined.

The isotopic variations in Ar released from 74220 were complex, but separable into two distinctly different arrays at intermediate and high temperatures. A gas retention age of  $3.54 \pm 0.05$  AE was determined over the intermediate release containing 47% of the total  $^{39}\text{Ar}$ . The correspondence of this age with the period of lunar magmatism is suggestive evidence for a volcanic origin of the orange glass and possibly a significant fraction of the glass particles observed at other sites.

The apparent age of 68415 is not well determined by the whole sample Ar release. A maximum apparent age of 3.86 AE in the intermediate release is similar to a precise Rb-Sr age of 3.84 AE. The apparent age plateau at 4.09 AE in the intermediate release from the plagioclase is atypically higher than the Rb-Sr age. Anomalous Ar isotopic variations are observed in the Ar release from both 68415 plagioclase and the high temperature release from the 74220 glass. Both have high Cl contents, and in both apparent ages are higher than anticipated from other criteria, suggesting inherited  $^{40}\text{Ar}$ . The possibility of a complex multistage origin for 68415 must be investigated.

Formation times of 95 m.y. ago for Camelot Crater and 30 m.y. ago for Shorty Crater are inferred from the cosmic-ray exposure ages of the associated samples 75055 and 74220, respectively. The exposure age for the soil fragment 75083,3,3 is 310 m.y., for the breccia 76055 is 140 m.y., and for the soil 74241 is 300 m.y. No well-defined exposure age could be determined for 68415.

Janghorbani, M., Miller, M. D., Ma, M.-S., Chyi, L. L., and Ehmann, W. D.: 'Oxygen and other Elemental Abundance Data for Apollo 14, 15, 16, and 17 Samples', *Proceedings of the Fourth Lunar Science Conference, Geochim. Cosmochim. Acta 2*, Suppl. 4, 1115–1126.

Major, minor, and selected trace element abundance data are presented for four basalts, three breccia components, and four soils from the Apollo 15 site; four crystalline rocks, five breccias, and seven soils from the Apollo 16 site; and the orange soil from the Apollo 17 site. In addition, minor and trace

element abundance data are presented for a group of Apollo 14 crystalline rocks, breccias, and breccia components to supplement the major element data on the same samples which we have published previously (Ehmann *et al.*). The Al/Si ratios we obtain for returned lunar breccia and soil samples are found to be in good agreement with the remote X-ray fluorescence data of Adler *et al.*, for regions near the various landing sites. Iron and Al exhibit a strong inverse correlation among the lunar soil and breccia samples we have analyzed. Only the Apollo 16 soil and breccia samples deviate from a regression with the mare basalts and the Apollo 16 cataclastic anorthosites, or VHA basalts as end members. Preliminary evidence is presented that samples with a high solar wind rare gas content suffer an oxygen depletion due to reaction with solar wind hydrogen.

Jovanovic, S. and Reed, G.: 'Volatile Trace Elements and the Characterization of the Cayley Formation and the Primitive Lunar Crust', *Proceedings of the Fourth Lunar Science Conference, Geochim. Cosmochim. Acta* **2**, Suppl. 4, 1313–1324.

Two types of highland terrain appear to be present at the Apollo 16 landing site. The Plains Formation called Cayley is ubiquitous and blankets even those regions that were presumably a part of the mountainous Descartes Formation. The second type of terrain is that associated with the ejectae from North and South Ray craters. The stratigraphy sampled by the ejectae underlays the Cayley layer as characterized above and may permit a redefinition of Descartes Formation as that which underlays the smooth Plains deposits. These conclusions are based on the concentrations and chemical coherence between elements such as Cl – F – P<sub>2</sub>O<sub>5</sub> and Ru – Os.

The primitive lunar crust may be characterized by the type of feldspathic rocks which are enriched in trace elements, such as Cl, Br, U, Te, Ru, and Os, as found in 'rusty' rock 66095 and in 61016; other feldspathic rocks are depleted and may be of secondary origin.

Finally, the diurnal thermal pulse causes labile Hg to establish a concentration gradient into the regolith to depths of 10–12 cm.

Kaiser, W. A. and Rajan, R. S.: 'The Variation of Cosmogenic Kr and Xe in a Core from Estherville Mesosiderite: Direct Evidence that the Lunar <sup>131</sup>Xe Anomaly Is a Depth Effect', *Earth Planetary Sci. Letters* **20**, 286–294.

Kr and Xe were measured by a stepwise heating technique in three samples of a drill core in the 'Minnesota' fragment of the Estherville mesosiderite. The cosmogenic <sup>78</sup>Kr/<sup>83</sup>Kr decreased from the 'top' sample to the 'bottom' sample ('top' = 0.163 ± 0.005, 'bottom' = 0.151 ± 0.005) while the cosmogenic <sup>131</sup>Xe/<sup>126</sup>Xe ratio increased ('top' = 5.58 ± 0.35, 'bottom' = 6.92 ± 0.17). Cosmic-ray track studies have shown that the 'top' sample was indeed closer to the preatmospheric surface than the 'bottom' sample by ~ 10 cm. This is the first direct evidence, in a sample of known geometry, that the cosmogenic <sup>131</sup>Xe/<sup>126</sup>Xe ratio increases as a function of depth, and as such, confirms the hypothesis that the lunar <sup>131</sup>Xe anomaly is a bona fide depth effect due to resonance neutron capture in <sup>130</sup>Ba.

Kirsten, T., Horn, P., and Kiko, J.: '<sup>39</sup>Ar-<sup>40</sup>Ar Dating and Rare Gas Analysis of Apollo 16 Rocks and Soils'. *Proceedings of the Fourth Lunar Science Conference, Geochim. Cosmochim. Acta* **2**, Suppl. 4, 1757–1784.

We report results of <sup>39</sup>Ar-<sup>40</sup>Ar-dating for sixteen Apollo 16 breccias, breccia clasts, and crystalline rocks with igneous textures of the Descartes Highlands, especially from the Cayley Formation. Plateau ages range from 3.85 to 4.03 b.y. Rock ages do not necessarily reflect the ages of formations since mascon basin ejecta were not always isotopically reset by the respective events. However, the entity of rock ages from one formation yields limits on the age of the formation itself. Along these lines of evidence, we arrive at the following ages:

Cayley Formation ~ 3.85 b.y.; Fra Mauro Formation 3.85–3.9 b.y.; Taurus-Littrow Highlands 3.9–4.05 b.y.

<sup>38</sup>Ar – Ca-exposure ages indicate that North Ray Crater was excavated ~ 30 m.y. ago.

Nine Apollo 16 bulk soils as well as grain size fractions and etched sieve fractions of two soils were



analyzed for rare gases. Compared to mare soils, highland soils are depleted in He and Ne due to the lower retentivity of their dominant mineralogical constituents. The surface correlation of trapped gases is better preserved than in mare soils. With the possible exception of the  $^4\text{He}/^3\text{He}$  ratio, the isotopic composition of the solar wind has not undergone significant secular variations within the last 4 b.y.

Mixing of the matured highland regolith sampled around South Ray Crater with immature North Ray Crater ejecta is reflected in the trapped gas content and the cosmic ray exposure ages (55–290 m.y.). Total gas retention ages indicate the archaic nature of Apollo 16 highland soils.

The concentration of orphan  $^{40}\text{Ar}$  relative to  $^{36}\text{Ar}$  varies within the same range as for mare soils, indicating that the time scale for secular changes of the  $^{40}\text{Ar}$  concentration in the lunar atmosphere is in the order of some million rather than some billion years.

Kornblum, J. J., Fireman, E. L., Levine, M., and Aronson, A.: 'Neutrons in the Moon', *Proceedings of the Fourth Lunar Science Conference, Geochim. Cosmochim. Acta* 2, Suppl. 4, 2171–2182.

Neutron fluxes for energies between 15 MeV and thermal at depths of 0 to 300 g cm<sup>-2</sup> in the Moon are calculated by the discrete ordinate method with the ANISN code. A total neutron-production rate for the Moon of  $26 \pm 4$  neutrons cm<sup>-2</sup> s<sup>-1</sup> is determined from the Ar<sup>37</sup> activity measurements in the Apollo 16 drill string, which are found to have a depth dependence in accord with a neutron source function that decreases exponentially with an attenuation length of 155 g cm<sup>-2</sup>.

Kothari, B. K. and Goel, P. S.: 'Nitrogen in Lunar Samples', *Proceedings of the Fourth Lunar Science Conference, Geochim. Cosmochim. Acta* 2, Suppl. 4, 1587–1596.

Total nitrogen has been measured in a number of lunar samples by neutron activation analysis. Experiments show that in our technique any contamination from the atmosphere or laboratory is essentially absent. The lunar fines contain excess nitrogen of about 80 ppm as compared to the crystalline rocks. Most of the nitrogen in fines is from solar wind ion implantation. Soil samples that might have been exposed on the lunar surface for different intervals of time contain nitrogen at about the same level of concentration. This suggests a kind of steady state behavior for the retention of solar wind implanted nitrogen.

Krähenbühl, U., Ganapathy, R., Morgan, J. W., and Anders, E.: 'Volatile Elements in Apollo 16 Samples: Implications for Highland Volcanism and Accretion History of the Moon', *Proceedings of the Fourth Lunar Science Conference, Geochim. Cosmochim. Acta* 2, Suppl. 4, 1325–1348.

Forty-two Apollo 16 samples (13 rocks, 9 soils, 20 soil separates) were analyzed by neutron activation analysis for Ag, Au, Bi, Br, Cd, Cs, Ge, Ir, Ni, Rb, Re, Sb, Te, Tl, U, and Zn. Anorthositic rocks from both Apollo 15 and 16 often show highly anomalous abundances of volatiles, deviating by factors of 10<sup>-2</sup> to 10<sup>4</sup> from the Tl/Cs, Tl/U ratios of lunar basalts, norites, and rhyolites. The highest abundances of 6 volatiles (Cd, Ge, Sb, Se, Tl, and Zn) were found in goethite-bearing rock 66095. Apparently volcanic processes took place in the lunar highlands, involving the release of volatiles including water. Such processes must have been widespread, judging from the fact that all highland soils have systematically higher Tl/U and Pb/U ratios than average rocks.

A model composition of the Moon and Earth was estimated from alkali, U, and Fe contents, on the assumption that each planet accreted from a Ca, Al-rich early condensate and 'chondritic' material that had undergone an Fe/Si fractionation and partial remelting. According to this calculation the Moon contains more early condensate than does the Earth (0.42  $M_J$  vs. 0.06  $M_{\oplus}$ , less troilite (0.025  $M_J$  vs 0.05  $M_{\oplus}$ ), and less metal (0.022  $M_J$  vs 0.23  $M_{\oplus}$ ).

Thallium and lead occur in nearly their cosmic ratio on the Moon, Earth, and eucrites. Apparently both metals were acquired mainly from material of low condensation temperature, containing essentially its full complement of Pb and Tl. If this material contained Tl and H<sub>2</sub>O in terrestrial ratio, the Moon's Tl content can be used to set an upper limit of  $\leq 1.5 \times 10^8$  g cm<sup>-2</sup> to its initial water content.

No significant chemical differences have been detected between Descartes and Cayley material.

The cataclastic anorthosites contain no ancient meteoritic component and hence probably represent deep ejecta from the Nectaris basin. The lower dark unit at North Ray crater, typified by a rock of unusually high Re/Au, Ir/Au ratios (67915), may represent shallow ejecta from Nectaris. The upper dark unit probably consists of shallow ejecta from the Orientale, Imbrium, Crisium, and Humorum basins.

Lambert, G., Grjebine, T., Bristeau, P., and Le Roulley, J. C.: 'Excess of Polonium 210 at the Surface of Apollo 15 Fines', *Proceedings of the Fourth Lunar Science Conference, Geochim. Cosmochim. Acta* 2, Suppl. 4, 2183–2188.

Lunar simulation experiments have shown that about a 2 meters depth of regolith contributes to a possible radon 222 outgassing. During the night this Radon is trapped by the cold surface of the Moon and gives rise to a superficial layer of lead and polonium 210 that apparently coats the surface of some of the fines grains.

Laul, J. C. and Schmitt, R. A.: 'Chemical Composition of Apollo 15, 16, and 17 Samples', *Proceedings of the Fourth Lunar Science Conference, Geochim. Cosmochim. Acta* 2, Suppl. 4, 1349–1367.

The abundances of the bulk elements, TiO<sub>2</sub>, Al<sub>2</sub>O<sub>3</sub>, FeO, MgO, CaO, Na<sub>2</sub>O, K<sub>2</sub>O, MnO, and Cr<sub>2</sub>O<sub>3</sub> and the trace elements Sc, V, Co, Zr, Hf, Th, U, Ba, Ta, and nine REE, La, Ce, Nd, Sm, Eu, Tb, Dy, Yb, and Lu, and the siderophile elements Ni, Ir, and Au elements have been determined by sequential instrumental neutron activation analysis (INAA) in 53 lunar soils and rocks. Two basalts 15643 and 15388 show positive Eu anomalies; these probably represent mesostasis-poor Ap 15 mare basalts. REE patterns of Apollo 15 basalts suggest six lava flows at the Palus Putredinis site. Apollo 15 soils contain 5 to 18 % norite-KREEP contribution. Luna 20 metaigneous rocks are feldspathic and are similar to Apollo 16 metaigneous rocks. Luna 20 soil is derived by ≈ 33 % Luna 20 metaigneous rocks and ≈ 65 % anorthositic gabbroic breccias like 15418. Apollo 16 anorthosites, all low K-group, show the same positive Eu enrichment similar to low K-group anorthosites from other sites. Anorthosite 60015 (97 % pl) is identical to 15415 anorthosite. Likewise, anorthosite 60025 is identical to 69955. The dark clast (glass) 60015,54 seems to be splashed molten breccia rock ejecta by meteoritic impact onto a latively pure anorthositic rock. Breccia 67031 is compositionally identical to breccia 60017 and both probably represent North Ray Crater material which is more feldspathic, lower in REE and other trace elements, including the siderophile elements compared to breccias ejected from the South Ray Crater. Cobalt is a diagnostic indicator between the North and South Ray materials and is enriched in the latter. Breccia 68516 is similar to the recrystallized 68415 rock and both lack Eu anomalies. Apollo 16 breccias are not compacted soils. The Apollo 16 highland soils are anorthositic gabbroic and are rather uniform in bulk and REE compositions. All Apollo 16 soils show negative Eu anomalies (avg. Sm/Eu = 5.1). About 5 % norite-KREEP component seems plausible for the Apollo 16 soils. Four Apollo 17 soils from Stations 5 and 9 in the valley and Station 8 on the Sculptured Hills are very similar and nearly match the Apollo 11 soil in bulk and trace elemental composition, including the siderophiles, and in their similar REE patterns. The absolute REE abundances in Apollo 17 soils are lower by a factor of ≈ 2 relative to the Apollo 11 soil. Compositional data of the 72501 soil (Station 2 on the South Massif avalanche) indicate that the South Massif may be composed of predominantly anorthositic gabbroic material. Anorthositic gabbro 78155 is similar to 10085,11,146. The FeO/MnO correlation, observed previously for maria, is also found for highland samples; this correlation suggests a homogeneous accretion of the Moon.

Leich, D. A., Tombrello, T. A., and Burnett, D. S.: 'The Depth Distribution of Hydrogen and Fluorine in Lunar Samples', *Proceedings of the Fourth Lunar Science Conference, Geochim. Cosmochim. Acta* 2, Suppl. 4, 1597–1612.

The resonant nuclear reaction <sup>1</sup>H(<sup>19</sup>F, αγ)<sup>16</sup>O is used to measure the depth distribution of hydrogen in a glass-coated sample and two feldspar-rich samples from rock 64455, and in a chip from breccia 68815 containing an exposed feldspar-rich region. Results are interpreted in terms of terrestrial H<sub>2</sub>O

surface contamination and a deeper (below 1000 Å) distribution of lunar hydrogen, probably derived from solar proton implantation. Small amounts of hydrogen below the surface of interior rock samples are suggestive of indigenous lunar hydrogen, or hydrogen inherited from preirradiated parent material. Results are also presented for an experiment to test the penetration of H<sub>2</sub>O into laboratory glass samples which have been irradiated with <sup>16</sup>O to simulate the radiation damaged surfaces of lunar glasses. Fluorine distributions are also measured on the 64455 and 68815 samples using a proton beam to induce the same nuclear reaction.

Lipschutz, M. E.: 'Vanadium Isotopic Composition and Concentrations of Ferromagnesian Elements in Returned Lunar Samples' (Final Report), NASA-CR-132045.

The effects are sought of an energetic charged particle irradiation of solar system material which is postulated as having taken place early in its history. A similar irradiation took place much more recently in the history of lunar samples and meteorites and this process is studied by means of a variety of monitors including highly sensitive noble gas nuclides, radionuclides, and tracks. Such monitors cannot be used to study the postulated early irradiation since it could have taken place under conditions such that these monitors were not retained or were subsequently lost. Accordingly, it is necessary that a nongaseous element be used to search for the effects of this irradiation, and one of the most sensitive of these is the vanadium isotopic composition. A comparative study is made of the <sup>50</sup>V/<sup>51</sup>V ratios in 15 meteoritic, 5 terrestrial, and 11 lunar samples.

Lipschutz, M. E., Balsiger, H., Rey, P., Pelly, I. Z., and Mendia, M. D.: 'Vanadium Isotopic Composition and Ferromagnesian Element Contents of Three Apollo 15 Samples', *Proceedings of the Fourth Lunar Science Conference, Geochim. Cosmochim. Acta* 2, Suppl. 4, 1369-1378.

The isotopic ratios of vanadium from three Apollo 15 samples and a standard rock are the same, within the limits of error, as those determined previously in lunar and terrestrial material. The maximum difference possible between the mean isotopic ratios in terrestrial and meteoritic material remains 1%. The concentrations of Cr, Fe, Mg, Ti, and vanadium and the weight ratios of the first four elements relative to vanadium in lunar samples indicate compositional differences between fines 15401 (Apennine Front) and 15601 (Hadley Rille). The concentrations of Cr and Fe parallel that of vanadium in lunar basalts and fines.

Malysheva, T. V. and Kurash, V. V.: 'Mössbauer Spectroscopy of Lunar Samples', *Geochem. Intern.* 10, 87-91.

Two regolith samples returned by Luna-16 were studied by Mössbauer spectroscopy. Pyroxene, olivine, ilmenite, and metallic iron were identified; troilite and magnetite were not detected.

Mao, H. K., Virgo, D., and Bell, P. M.: 'Analytical and Experimental Study of Iron and Titanium in Orange Glass from Apollo 17 Sample 74220', *Proceedings of the Fourth Lunar Science Conference, Geochim. Cosmochim. Acta* 1, Suppl. 4, 397-412.

Apollo 17 soil sample 74220 consists mainly of minute glass spheres, mostly fractured, similar in orange color and in composition to orange glasses separated from soil samples from the other Apollo missions. Comparison of optical absorption of iron and titanium and <sup>57</sup>Fe Mössbauer resonance of iron of orange glass grains with glasses prepared synthetically under controlled oxygen fugacity implies that the orange glasses are significantly reduced relative to terrestrial rocks but oxidized relative to most lunar rocks.

Mark, R. K., Cliff, R. A., Lee-Hu, C., and Wetherill, G. W.: 'Rb-Sr Studies of Lunar Breccias and Soils', *Proceedings of the Fourth Lunar Science Conference, Geochim. Cosmochim. Acta* 2, Suppl. 4, 1785-1795.

Rb-Sr systematics and K concentrations are reported for two Apollo 14 breccias and several Apollo 15, 16, and 17 soils. Basalt clast 14321, 184–55 yields an internal isochron  $4.01 \pm 0.12$  b.y.,  $0.69957 \pm 0.00013$ ; KREEP-rich microbreccia clast 14321, 184-53 gives  $4.05 \pm 0.06$  b.y.,  $0.70104 \pm 0.00033$ . The difference in initial ratio indicates that complete equilibration did not occur during final assembly of 14321. KREEP-rich clast 17 from breccia sample 14066,21 yields an isochron of  $4.06 \pm 0.14$  b.y.,  $0.70033 \pm 0.00034$ . The clast has a whole rock model age of  $5.10 \pm 0.12$  b.y., and thus has been an open system since the differentiation of KREEP. Plagioclase clasts from microbreccia fragments in Apollo 16 soil (61222,3) are distinctly too radiogenic to have been in equilibrium with the whole rock fragments 4 b.y. ago.

Marti, K., Lightner, B. D., and Osborn, T. W.: 'Krypton and Xenon in Some Lunar Samples and the Age of North Ray Crater', *Proceedings of the Fourth Lunar Science Conference, Geochim. Cosmochim. Acta* 2, Suppl. 4, 2037–2048.

Cosmic-ray exposure ages are obtained by the  $^{81}\text{Kr}$ - $^{83}\text{Kr}$  method for three Apollo 16 rocks from Station 11, including three samples from a large boulder. All ages are consistent with an average value of  $48.9 \pm 1.7$  m.y. which is considered to be the age of North Ray Crater. Fission xenon observed in Apollo 14 samples is discussed specifically in relation to a report of neutron produced  $^{236}\text{U}$ . It is shown that the spallation ratio  $^{78}\text{Kr}/^{83}\text{Kr}$  can be used as an irradiation hardness sensor or shielding parameter if the relative abundances of the major target elements, Sr, and Zr, are known. Neutron produced  $^{131}\text{Xe}_n$  is calculated, by taking into account the possible presence of parentless fission xenon in Apollo 14 samples.

McKay, G. A., Kridelbaugh, S. J., and Weill, D. F.: 'The Occurrence and Origin of Schreibersite-Kamacite Intergrowths in Microbreccia 66055', *Proceedings of the Lunar Science Conference, Geochim. Cosmochim. Acta* 1, Suppl. 4, 811–818.

Spherical schreibersite-bearing particles of kamacite commonly occur in the once-molten matrix of two lithic clast types in microbreccia 66055. The Ni and Co contents of these particles fall within meteoritic limits, but the phosphorus content of many particles exceeds meteoritic values. The distribution of Ni between kamacite and schreibersite suggests that the particles last equilibrated at about  $550^\circ\text{C}$ . Experiments indicate that kamacite-schreibersite particles similar in morphology and texture to those found in 66055 can be formed by reduction of Fe and P from a melt similar in composition to that of KREEP.

Moore, C. B., Lewis, C. F., and Gibson, E. K.: 'Total Carbon Contents of Apollo 15 and 16 Lunar Samples', *Proceedings of the Fourth Lunar Science Conference, Geochim. Cosmochim. Acta* 2, Suppl. 4, 1613–1623.

The total carbon contents in Apollo 15 fines range from 29 to  $170 \mu\text{g g}^{-1}$ . Fines from Apollo 16 range from 65 to  $280 \mu\text{g g}^{-1}$ . These samples are similar to those from Apollo 11, 12, and 14, with dark colored fines generally containing more carbon than lighter fines. Sample 61221 (light colored fines) is anomalously high with  $100 \mu\text{g g}^{-1}$  total carbon. Correlations between total carbon content and sample collection station for each mission are evident.

Basalts from Apollo 15 have less than  $27 \mu\text{g g}^{-1}$  total carbon. Anorthositic rocks from Apollo 15 and 16 have less than  $20 \mu\text{g g}^{-1}$  total carbon. Breccias show complex and variable carbon distributions.

Morgan, J. W., Krähenbühl, U., Ganapathy, R., Anders, E., and Marvin, U. B.: 'Trace Element Abundances and Petrology of Separates from Apollo 15 Soils', *Proceedings of the Fourth Lunar Science Conference, Geochim. Cosmochim. Acta* 2, Suppl. 4, 1379–1398.

Nine petrographically distinct separates from Apollo 15 coarse soils were characterized by electron microprobe and analyzed by neutron activation analysis for Ag, Au, Bi, Br, Cd, Cs, Ge, In, Ir, Rb, Re, Sb, Se, Te, Tl, U, and Zn. Like some alkali-poor anorthosites from Apollo 16, 15102 anorthosite

is low in meteoritic siderophiles but enriched in Tl, perhaps by volcanic processes. Norites from 15102 and troctolites from 15302 are lower in KREEP than are Apollo 12 or 14 norites. A possible progenitor of KREEP-rich norite breccias has been found: a mesostasis-rich basalt from 15272 high in KREEP-related elements, but very low in the siderophiles Ir, Re, Au, Sb, and Ge, and hence lacking the ancient meteoritic component that occurs in all lunar norites. At least 2 varieties of ancient meteoritic component are present in the soil separates from this site, consistent with the complex impact history of the Pre-Imbrian surface.

Morrison, G. H., Nadkarni, R. A., Jaworski, J., Botto, R. I., and Roth, J. R.: 'Element Abundances of Apollo 16 Samples', *Proceedings of the Fourth Lunar Science Conference, Geochim. Cosmochim. Acta* 2, Suppl. 4, 1399–1405.

Results are presented for the multielement analysis of samples of lunar soil (60501 and 64501), igneous rock (60315), and the light portion of breccia 60017. A mixing model for soil compositions has been proposed consisting of linear combinations of the KREEP basalt 60315 and the anorthositic gabbroic sample 60017. A comparison of trace elements in lunar soils from different missions indicates the marked depletion of the LIL elements in the Apollo 16 samples.

Müller, O.: 'Chemically Bound Nitrogen Contents of Apollo 16 and Apollo 15 Lunar Fines', *Proceedings of the Fourth Lunar Science Conference, Geochim. Cosmochim. Acta* 2, Suppl. 4, 1625–1634.

Chemically bound nitrogen contents have been determined in Apollo 16 and 15 lunar bulk fines and grain size fractions using the Kjeldahl method. The results show, as in our previous work, that the main amount of nitrogen is present in a bound state. Nitrogen analyses on grain size fractions of fines have revealed that nitrogen is concentrated on grain surfaces and is derived most likely from the solar wind. Correlation of nitrogen with trapped noble gases provides further evidence for solar wind origin of nitrogen in lunar fines. Nitrogen can be used as a reference element in terms of solar elemental abundances because it is chemically active and, therefore, is better retained in fine-grained material than the lighter solar wind noble gases. Carbon to nitrogen atomic ratios of Apollo 14, 15, and 16 bulk fines are remarkably constant ranging from 1.35 to 1.75, and are interpreted as lower limits for the abundance ratio of these elements in the Sun.

Nakamura, N., Masuda, A., Tanaka, T., Kurasawa, H.: 'Chemical Compositions and Rare-Earth Features of Four Apollo 16 Samples', *Proceedings of the Fourth Lunar Science Conference, Geochim. Cosmochim. Acta* 2, Suppl. 4, 1407–1414.

Four Apollo 16 rocks were analyzed for RE, Ba, Si, Al, Ca, Mg, Fe, Mn, Ti, Cr, Na, K, and P. The anorthosite 60025 shows a positive Yb anomaly. The absolute RE abundances in this sample are higher than in the anorthosite 15415 by factors of 2 and 3. The RE patterns of the samples studied are very similar to each other except Eu, but 67915 (partially melted breccia) has a pattern slightly upwards concave. The igneous rock (66095) appears to have a positive Ce anomaly of about 9%.

There are smooth changes of abundances of almost all elements investigated with the abundance change of  $P_2O_5$ . The relationship between RE and Si/Al weight ratio for the Apollo 16 samples suggests that the two component mixing model is not necessarily appropriate to account for the chemical features of these materials.

Nguyen, L.-D., Simon, M. de Saint, Puil, G., and Yokoyama, Y.: 'Rare Earth Elements in Luna 20 Soils and their Implications for Cosmochemistry', *Proceedings of the Fourth Lunar Science Conference, Geochim. Cosmochim. Acta* 2, Suppl. 4, 1415–1426.

Ten rare earth elements (REE) are determined in Luna 20 fines by a new improved isotopedilution method using high sensitive and accurate mass-spectrometer combining a new chemical separation procedure, a new identification method of different REE and accurate spike calibration. The method allows determination of the REE contained in samples of less than 1 mg with a sufficient accuracy.

The Eu depletion was found also in Luna 20 soils, a highland sample. This result seems to indicate that the Moon as a whole is depleted in Eu and that it is necessary to suppose another mechanism, in addition to partial melting or fractional crystallization, to explain this phenomenon; the possibility of vaporization of Eu from oxides during a Hayashi phase is examined.

Niebuhr, H. H., Zeira, S., and Hafner, S. S.: 'Ferric Iron in Plagioclase Crystals from Anorthosite 15415', *Proceedings of the Fourth Lunar Science Conference, Geochim. Cosmochim. Acta* **1**, Suppl. 4, 971-982.

Single crystals of anorthite from anorthosite 15415 were oriented with X-ray diffraction and studied with electron spin resonance at X and K band frequencies. The crystals were partially twinned after pericline (volume ratio 1:10) and albite (volume ratio 1:50) laws. X-ray diffraction photographs using the Laue method at various distances showed a mosaic structure with angular displacement of the domains of approximately one degree.

The ESR spectra can be grouped into two distinct sets of lines: One group includes a large number of lines in the vicinity of  $g = 2$  and is due mainly to  $Mn^{2+}$  ions. The other group includes lines in the region of 600-2000 G which are identified as  $Fe^{3+}$  signals. The magnitudes and directions of the resonance fields for two  $Fe^{3+}$  positions have been determined.

The intensity of the  $Fe^{3+}$  electron spin resonance in one of the anorthite crystals has been compared quantitatively with the  $Cr^{3+}$  signal intensity in a corundum crystal which was doped with a known amount of  $Cr_2O_3$ . It is found that approximately one percent of the iron in anorthite from anorthosite 15415 is in the ferric state.

Nunes, P. D., Tatsumoto, M., Knight, R. J., Unruh, D. M., and Doe, B. R.: 'U - Th - Pb Systematics of Some Apollo 16 Lunar Samples', *Proceedings of the Fourth Lunar Science Conference, Geochim. Cosmochim. Acta* **2**, Suppl. 4, 1797-1822.

U, Th, and Pb concentrations and lead isotopic compositions of Apollo 16 samples are interpreted as follows: (1) An early period of lunar differentiation of either global or regional scale occurred about 4.47 b.y. ago. (2) The Imbrian impact event affected many Apollo 16 samples about 3.99 b.y. ago. (3) Some Apollo 16 metaclastic rocks and breccias contain a large amount of KREEP-like material. (4) Lead produced in the early history of the Moon has been concentrated in lunar highland soils yielding high  $^{207}Pb/^{206}Pb$  ratios corresponding to apparent ages of  $> 4.8$  b.y. (5) South Ray Crater soils reflect the approximately 2-b.y.-old event previously proposed for the Apollo 12 and 14 samples.

Philpotts, J. A., Schuhmann, S., Kouns, C. W., Lum, R. K. L., Bickel, A. L., and Schnetzler, C. C.: 'Apollo 16 Returned Lunar Samples: Lithophile Trace-Element Abundances', *Proceedings of the Fourth Lunar Science Conference, Geochim. Cosmochim. Acta* **2**, Suppl. 4, 1427-1436.

Lithium, K, Rb, Sr, Ba, rare-earth, Zr, and Hf abundances have been determined by mass-spectrometric isotope-dilution for Apollo 16 soils, anorthosite 61016, and 'basalt' 68415 whole-rock and separated pyroxene and plagioclase. Our sample of 61016 is similar to some other lunar anorthosites in lithophile trace-element concentrations but at a slightly lower level. It was probably accumulated from a little differentiated basalt. Basalt 68415 might be a homogeneous mixture of KREEP and anorthositic material: it appears to have crystallized under conditions as reducing as those holding for mare-basalts. The soil fines cover only a limited compositional range. No obvious chemical differences were noted between the Descartes and Cayley formations. Most of the compositional variation of the soils can be accounted for in terms of the addition of plagioclase. The existence of very high alumina basalt as an independent magma-type appears debatable in view of its KREEP-like lithophile trace-element relative concentrations and the observed lunar radioactivity distribution.

Ragan, D. P.: 'Apollo 14 Rare Gases.  $Pu^{244}$  Xenon', Ph.D. Thesis, Washington Univ., St. Louis Univ. Microfilms, Order No. 73-5057.

The first results of rare gas measurements on the recently constructed mass spectrometer facility are reported. Four stepwise temperature extractions were made on Apollo 14 samples 14306-light, 14306-dark, 14301 and 14311. Neon, argon, krypton, and xenon data are reported. Analysis of xenon in 14301 shows a large enrichment of the heavy isotopes due to the decay of now extinct  $\text{Pu}^{244}$ . The separation of the fission gas from the spallation gas in the different temperature fractions allowed a measurement of the fission xenon yield spectrum. Computations on the spallation spectrum in the rocks were made. Evidence for more than one component in a rock was observed in 14301 and 14311. The spectrometer used to measure the gases is described in detail. Two features, original with this spectrometer, are the automatic data acquisition system and the peak jumping (switching) hardware. These two technical improvements are also discussed in full.

Reedy, R. C., Arnold, J. R., and Trombka, J. I.: 'Expected Gamma-Ray Emission Spectra from the Lunar Surface as a Function of Chemical Composition', NASA-TM-X-70453.

The gamma rays emitted from the Moon or any similar body carry information on the chemical composition of the surface layer. The elements most easily measured are K, U, Th and major elements such as O, Si, Mg, and Fe. The expected fluxes of gamma ray lines were calculated for four lunar compositions and one chondritic chemistry from a consideration of the important emission mechanisms: natural radioactivity, inelastic scatter, neutron capture, and induced radioactivity. The models used for cosmic ray interactions were those of Reedy and Arnold and Lingenfelter. The areal resolution of the experiment was calculated to be around 70 to 140 km under the conditions of the Apollo 15 and 16 experiments. Finally, a method was described for recovering the chemical information from the observed scintillation spectra obtained in these experiments.

Rho, J. H., Bauman, A. J., and Cohen, E. A.: 'Fluorometric Search for Porphyrins in Apollo 15 Exhaust-Contaminated Surface Fines and Deep Drill Cores and Apollo 16 Surface Fines', *Proceedings of the Fourth Lunar Science Conference, Geochim. Cosmochim. Acta* 2, Suppl. 4, 2261-2265.

Portions of Apollo 15 surface fines (15013,1) from an area contaminated by landing vehicle exhaust were Soxhlet-extracted with benzene: methanol 3:2 v/v both in air and in argon. Only the argon extract contained a compound (about 1 ppb) which fluoresced at 660 and 725 nm with maximal excitation at 425 nm, absorbed at 425 nm and partitioned into benzene from 6 N HCl. Its emission spectrum was porphyrin-like but with a maximum shifted about 50 nm toward the red relative to that of porphyrins. Similarly argon-extracted cores 15002 (160-200 cm down) and 15001 (200-240 cm down), each 3 g, yielded extracts free of porphyrins, as was also the case for an Apollo 16 surface fines sample 65500,10 (5 g) collected at Station 5.

Rhodes, J. M. and Hubbard, N. J.: 'Chemistry, Classification, and Petrogenesis of Apollo 15 Mare Basalts', *Proceedings of the Fourth Lunar Science Conference, Geochim. Cosmochim. Acta* 2, Suppl. 4, 1127-1148.

Two, chemically defined mare basalt groups have been sampled at the Apollo 15 landing site. This paper examines the chemical, petrographic and spatial characteristics of these groups. One group is olivine normative, the other quartz normative. The olivine normative basalts are characterized by higher FeO and  $\text{TiO}_2$  and lower  $\text{SiO}_2$  than the quartz normative basalts, and by lower abundances of several large ion lithophile elements. The within-group chemical variation is attributed to moderate amounts (< 15%) of near-surface crystal fractionation, dominated by olivine in the olivine normative basalts and by pigeonite in the quartz normative basalts. The latter are thought to have been derived by olivine fractionation from a more primitive magma.

The between-group chemical characteristics cannot be explained by near-surface crystal fractionation. It is a primary feature, related either to varying degrees of partial melting in the lunar mantle, or to derivation from different depths in a mantle that is inhomogeneous with respect to trace and minor elements.

Rose, H. J., Cuttitta, F., Berman, S., Carron, M. K., Christian, R. P., Dwornik, E. J., Greenland, L. P., and Ligon, D. T.: 'Compositional Data for Twenty-Two Apollo 16 Samples', *Proceedings of the Fourth Lunar Science Conference, Geochim. Cosmochim. Acta* 2, Suppl. 4, 1149–1158.

Major, minor, and trace element analyses are presented for ten soils and twelve rocks. Both the rocks and soils are enriched in CaO and Al<sub>2</sub>O<sub>3</sub> in comparison with previous Apollo missions.

The soils at stations other than at North Ray Crater are relatively homogeneous in major element composition. However, Co and Ni vary by four-fold in concentration, although the Co/Ni ratio remains constant. There is a positive correlation between Ni and Zr.

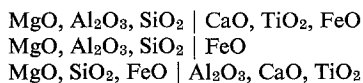
In the rocks, the major variations of the trace elements appear to be controlled by the pyroxene/plagioclase ratio with the breccias richer in plagioclase than the crystalline samples.

Salisbury, J. W., Hunt, G. R., and Logan, L. M.: 'Infrared Spectra of Apollo 16 Fines', *Proceedings of the Fourth Lunar Science Conference, Geochim. Cosmochim. Acta* 3, Suppl. 4, 3191–3196.

Mid-infrared spectra of Apollo soil samples are interpreted in terms of their mineralogy, and hence the average mineralogy of local parent material. Soil samples apparently derived from Cayley material vary in mineralogical composition from anorthositic to ultramafic, in part because of sampling bias. Two soil samples from Stone Mountain that may be derived from Descartes material are not strikingly different from typical Cayley material. A comparison of Apollo 11 and Apollo 16 soil spectra indicates that cross-contamination effects have not disguised compositional differences.

Saxena, S. K. and Walter, L. S.: 'A Statistical-Chemical and Thermodynamic Approach to the Study of Lunar Mineralogy', *Geochim. Cosmochim. Acta* 38, 79–95.

Principal components analysis is used to study the chemical compositions of pyroxenes of five Apollo 12 specimens. Important correlations recognized in the variation of oxide weight per cent are:



where the oxides on one side of the bar are correlated positively with each other and negatively with the oxides on the other side. Several other similarly distinct relationships with significantly less variance could be noted. These correlations indicating substitutional relationships can be interpreted as representative of stable and metastable trends of crystallization by using crystal-chemical and thermodynamic information. The per cent variance of pyroxene groups with characteristic trends in each specimen can be evaluated and interpreted in terms of history of crystallization. Distribution of Fe and Mg in certain pairs of olivine and pyroxene, which are found in contact in the rock and which may have crystallized simultaneously, is useful in recognizing the tendency towards chemical equilibrium in Fe–Mg distribution during a limited interval in the liquidus or subsolidus stages.

Simkin, T., Noonan, A. F., Switzer, G. S., Mason, B., Nelen, J. A., Melson, W. G., and Thompson, G.: 'Composition of Apollo 16 Fines 60051, 60052, 64811, 64812, 67711, 67712, 68821, and 68822', *Proceedings of the Fourth Lunar Science Conference, Geochim. Cosmochim. Acta* 1, Suppl. 4, 279–289.

Examination of the 1–2 mm fines from 4 Apollo 16 stations (4, 8, 10, and 11) revealed the following: (1) There is a preponderance of impact breccia and a rarity of primary igneous rocks; (2) Anorthite-rich breccias and recrystallized breccias predominate at all stations; (3) North Ray Crater sample 67712 is distinctive in its abundance of anorthositic fragments and paucity of glassy and more mafic materials, presumably because this sample was scraped from a buried boulder; (4) LM sample 60051 contains more single plagioclase crystals and anorthositic fragments than the remaining two (68822 and 64812); and (5) Samples believed to be from South Ray Crater ejecta (Cayley Plains) (68822, Station 8) and from probable Descartes Formation (64812, Station 4) are not significantly different



from one another from the standpoint of bulk chemistry or lithology, but can be distinguished by glass compositions.

All sample sites show the following features: (1) There is evidence of a metamorphic sequence, ranging from glassy microbreccias with heterogeneous mafic mineral compositions to coarsely crystalline granulites with homogeneous plagioclase, olivine, and pyroxene compositions; (2) Quenched, probably impact-derived glasses are the dominant igneous-like rocks; (3) The compositional spread of breccia matrices is easily matched by a simple mixing model of typical anorthite ( $An_{95}$ ) with typical olivine ( $Fo_{74}$ ) and orthopyroxene ( $En_{72}Fs_{24}Wo_4$ ); most matrices contain about 10 percent mafic minerals; (4) Most modal and normative data can be classified into dominant anorthite (70–75%) with subordinant olivine, orthopyroxene, and clinopyroxene in that order of abundance; and (5) 185 analyses of glasses reveal a dominance of bulk soil compositions, although KREEP-like and mare basalt types also occur.

Simoneit, B. R., Christiansen, P. C., and Burlingame, A. L.: 'Volatile Element Chemistry of Selected Lunar, Meteoritic, and Terrestrial Samples', *Proceedings of the Fourth Lunar Science Conference, Geochim. Cosmochim. Acta* 2, Suppl. 4, 1635–1650.

Using vacuum pyrolysis and high resolution mass spectrometry we have investigated the gas release patterns of representative lunar samples, meteorites, terrestrial samples and synthetic samples doped with various sources of carbon and nitrogen. The pyrolytic gas evolution patterns were intercorrelated, allowing an assessment of the possible sources of the volatilizable material in the lunar samples to be made.

Lightly surface adsorbed species and more strongly chemisorbed species are released from ambient – 300°C and 300–500°C, respectively. The low temperature volatiles (< 500°C) derived from various chondrites correlate well with the gas evolution patterns of volatile-rich samples as for example 74220 and 61221. Solar wind entrapped species and molecules derived from reactions probably in the grain surfaces are evolved from about 500–700°C, respectively. Solar wind implanted C, N, and S species are generated from 750–1150°C, probably by reaction with the mineral matrix during the annealing process. Possible indigenous and/or refractory carbide, nitride and sulfide C, N and S are released in the region 1200°C to fusion.

Smith, J. W., Kaplan, I. R., and Petrowski, C.: 'Carbon, Nitrogen, Sulfur, Helium, Hydrogen, and Metallic Iron in Apollo 15 Drill Stem Fines', *Proceedings of the Fourth Lunar Science Conference, Geochim. Cosmochim. Acta* 2, Suppl. 4, 1651–1656.

Analysis for C, S, N, H<sub>2</sub>, and He was undertaken by vacuum pyrolysis and for metallic Fe by acid hydrolysis. The data show a maximum of all components analysed at the surface and a minimum in the deepest sample (with the exception of sulfur). C, N, and S all showed greatest enrichment of the heavy isotope (C<sup>13</sup>, N<sup>15</sup>, and S<sup>34</sup> in the surface sample and least in the deepest sample. The effects are interpreted as resulting from maximum solar irradiation in the surface sample and least in the bottom sample, however, the interpretation may well be more complicated if the samples had undergone heating.

Srinivasan, B.: 'Variations in the Isotopic Composition of Trapped Rare Gases in Lunar Sample 14318', *Proceedings of the Fourth Lunar Science Conference, Geochim. Cosmochim. Acta* 2, Suppl.4, 2049–2064.

Rare gases were extracted from lunar sample 14318 by stepwise heating, and analyzed mass spectrometrically. Neon, argon, and krypton are a mixture of spallation and trapped components. The isotopic compositions of the trapped rare gases are found to vary with extraction temperature. These variations can be discussed in terms of mass-dependent fractionation. The isotopic compositions of the trapped rare gases for the whole sample (as determined from the sum of the temperature fractions) show enrichment in the heavier isotopes, relative to the isotopic pattern of trapped gases in lunar fines. The calculated values for the enrichments are: 5.1% per mass unit across neon, 2.1% per mass unit across

argon, and 0.9% per mass unit across krypton. The inverse correlation with atomic weight lends support to the hypothesis of mass-dependent fractionation having occurred at some point in the history of rare gases now trapped in 14318. 'Surface' exposure ages based on spallogenic  $^{21}\text{Ne}$  and  $^{126}\text{Xe}$  are  $39 \pm 6$  m.y. and  $56 \pm 9$  m.y., respectively.

Stettler, A., Eberhardt, P., Geiss, J., Grögler, N., and Maurer, P.: 'Ar $^{39}$ -Ar $^{40}$  Ages and Ar $^{37}$ -Ar $^{38}$  Exposure Ages of Lunar Rocks', *Proceedings of the Fourth Lunar Science Conference, Geochim. Cosmochim. Acta* 2, Suppl. 4, 1865-1888.

We have applied the Ar $^{39}$ -Ar $^{40}$  technique of K-Ar dating to 15 lunar rocks. The mare basalts 10071 (feldspar); 12051; 15076; and 70035 gave high temperature plateau ages of 3.51; 3.16; 3.35, and 3.74 AE respectively. Mare basalt 12018 is highly degassed and the shape of the release curve suggests a low temperature plateau at 0.65 AE. The two glass-rich basalts 12008 and 12009 show similar, complex release curves with an age minimum at intermediate temperatures. However, the total Ar $^{39}$ -Ar $^{40}$  age of these two rocks is in agreement with the age commonly observed for Apollo 12 basalts.

Several Apollo 14 and 15 rocks have ages compatible with the proposed 3.95 AE cataclysm. These include the Apollo 15 anorthosites 15415 and 15418. It still remains an open question whether these rocks were formed by an igneous process at this time or whether they are thoroughly outgassed remnants of the proposed original anorthositic crust of the Moon.

A mare basalt-like clast from the polymict breccia 15459 collected at the Apennine Front gives an age of 3.33 AE, similar to the age of the Apollo 15 mare basalts. Thus breccia 15459 was formed a long time after the Imbrian impact.

Surkov, Yu. A., Fedoseyev, G. A., Sobornov, O. P., and Tarasov, L. S.: 'Radioactivity of Lunar Soil Supplied by the Automated Station 'Luna-20'', *Proceedings of the Fourth Lunar Science Conference, Geochim. Cosmochim. Acta* 2, Suppl. 4, 1437-1444.

The data on the radioactivity of lunar soil supplied by 'Luna-20' from the continental region near the crater Apollonius-C were obtained by the low-background gamma-spectrometry method. On the basis of the data obtained in this experiment and the results achieved by other authors a conclusion about some peculiarities of regolith formation in the above region of the Moon is drawn. Proceeding from the natural radioelement content in lunar samples and comparing it with data on the radioactivity of basic and ultrabasic terrestrial rocks, some suggestions are made about the similarity between the primary matter of the Earth and that of the Moon.

Tarasov, L. S., Nasarov, M. A., Shevaleevsky, I. D., Makarov, E. S., and Ivanov, V. I.: 'Mineralogy of Anorthositic Rocks from the Region of the Crater Apollonius C (Luna-20)', *Proceedings of the Fourth Lunar Science Conference, Geochim. Cosmochim. Acta* 1, Suppl. 4, 333-349.

Mineralogy of rocks returned by the automatic station Luna-20 has been studied. Highland rocks of the anorthositic series and basaltic rocks of maria type have been distinguished and are distinctly different.

Orthorhombic pyroxene predominates in anorthosites but is lacking in basalts. Monoclinic pyroxenes in anorthositic rocks are represented by high-calcium varieties similar to diopsides, and in basaltic pyroxenes by the autite-pigeonite series. Olivines are characterized by higher magnesia content in highland rocks. Plagioclases in anorthosites are anorthites and in basalts bytownites. In basaltic rocks potassic, high-silica glasses have been established and in anorthosites - glasses of plagioclase composition.

A specific feature of highland rocks is the presence of magnesian varieties of ilmenite and picroilmenite. The lack of intermediate compositions between picroilmenites and magnesian ilmenites may bear witness either of the isomorphic miscibility gap in this region or of the lack of necessary physico-chemical conditions for the formation of such intermediate compositions. The composition of spinels varies over wide ranges, but in highland rocks the more chromous and magnesian varieties are prevalent. Also pink magnesian spinel which had not been observed in maria rocks is present. In

highland rocks there occurs magnesian-chromous armalcolite represented by beautiful idiomorphic laths. The accessory minerals metallic iron, troilite, and phosphates have been noted in anorthosites and basalts. In one thin section of troctolitic rock an unusual phase corresponding in composition to aluminum carbide was established.

Taylor, G. R. and Wooley, B. C.: 'Evaluations of Lunar Samples for the Presence of Viable Organisms', *Proceedings of the Fourth Lunar Science Conference, Geochim. Cosmochim. Acta 2*, Suppl. 4, 2267–2274.

Samples from the six successful Apollo lunar exploration missions were examined for the presence of biological formed elements and were used to inoculate a variety of culture media designed to promote growth of a broad spectrum of microorganisms. No evidence of viable organisms was obtained from any of these analyses. Following incubation of the lunar material–culture medium complexes, microbial growth dynamics studies were conducted with known test species to evaluate the possible presence of toxic factors. Only extracts of culture media which had been in contact with a mixture of lunar material from both Apollo 11 core tubes proved to be toxic to all species tested. Attempts to reproduce this toxic effect with individual Apollo 11 core samples obtained at other parts of the core stem and analyzed under somewhat different conditions were unsuccessful. In all, 48 different lunar samples were examined. These samples were collected at the lunar surface, in trenches, and in core samples to a depth of 297 cm.

Taylor, H. C. J. and Carter, J. L.: 'Silicate Mineral Chemistry of Apollo Soils 15411, 15501, 66081, and 69941', *Proceedings of the Fourth Lunar Science Conference, Geochim. Cosmochim. Acta 1*, Suppl. x, 291–307.

The utilization of small amounts of material in the mineralogical and chemical characterization of lunar soil samples appears to be very successful in formulating major geological deductions. Such knowledge should be valuable in the planning of future extraterrestrial scientific missions. Mineral analyses of pyroxenes from the less than 1 mm size fraction of Apollo 15 soil samples 15411,46 and 15501,53 and plagioclase feldspars, pyroxenes, and olivines from the less than 1 mm size fraction of Apollo 16 soil samples 66081,5 and 69941,13 can be used to distinguish mare, KREEP, and ANT (anorthosite-norite-troctolite) or highland 'basalt' components in these soils.

Comparison of mineral chemistry in soils 15411 and 15501 from the Apennine Front/Hadley Rille area allow characterization of the 15411 soil, collected at Spur Crater on the Hadley Delta front, as consisting primarily of gabbroic-anorthosite components, whereas the 15501 soil collected near Hadley Rille consists primarily of mare-type basaltic components. Contamination of the 15501 mare-type basalt soil with minor amounts of the gabbroic-anorthosite components may indicate the effect of downslope mass wasting of materials from the Apennine Front onto the mare surface.

Apollo 16 soil 66081 from the Descartes area shows only ANT components, whereas soil 69941 from South Ray Crater has a major ANT component together with a possible minor KREEP and ultramafic component. The possible ultramafic component consists of olivine as forsteritic as  $Fo_{94.5}$  and by Mg-orthopyroxene with enstatite values as high as  $En_{87.3}$ .

Taylor, H. P. and Epstein, S.: ' $O^{18}/O^{16}$  and  $Si^{30}/Si^{28}$  Studies of Some Apollo 15, 16, and 17 Samples', *Proceedings of the Fourth Lunar Science Conference, Geochim. Cosmochim. Acta 2*, Suppl. 4, 1657–1679.

The whole-rock  $\delta O^{18}$  values from 8 sample sites on the near side of the Moon vary only from about +5.4 to +6.8, a remarkably small variation compared to that observed in meteorites and the Earth. However, the whole-rock surface soil samples from *all* of these lunar localities are slightly enriched in  $O^{18}$  and  $Si^{30}$ . This is due to very large  $O^{18}$  and  $Si^{30}$  enrichments that are observed on the outermost 2 to 4% of material (the 'amorphous' coatings) on the surfaces of the grains and glassy agglutinates that make up the lunar fines. These isotopic effects, which are brought about by fractional vaporization or fractional vapor condensation as a result of particle bombardment of the soils exposed at the

lunar surface, are observed experimentally by partial-fluorination 'stripping' experiments. The  $\delta O^{18}$  'stripping' patterns for the Apollo 16 soil samples are generally somewhat different from those previously observed at other lunar sites. This is attributed to larger amounts of adsorbed water on the outermost grain-surfaces in the Apollo 16 fines. Several experiments were conducted which indicate that the  $\delta O^{18}$  value of this adsorbed water is about  $-20$  to  $-10$  per mil, or very similar ordinary terrestrial meteoric waters. These data correlate well with the common occurrence of goethite in trace amounts in the Apollo 16 rocks. The Apollo 17 orange soil sample is unique among all lunar soils studied so far, in that it shows no surface  $O^{18}$  or  $Si^{30}$  enrichment whatsoever. Thus the orange soil cannot have been exposed at the lunar surface for any significant length of time. Other experiments were made which show that the  $O^{18}$  and  $Si^{30}$  enrichment patterns on the grain surfaces are still preserved even after heating at  $630^{\circ}C$  for 5 hr, at which temperature other indications of a lunar surface exposure history have been largely obliterated (i.e., loss of solar wind  $H_2$ , He, etc.). Thus, such  $O^{18}$  and  $Si^{30}$  enrichment patterns may represent one of the few pieces of evidence that may allow us to 'see through' a lunar heating or metamorphic event and thus decipher whether or not a particular breccia sample ever resided on the lunar surface as part of the regolith. There are also indications that the exact shapes of these isotopic patterns may be sensitive to such heating events and to other aspects of the petrologic history of lunar soils and soil-breccias.

Taylor, L. A., Mao, H. K., and Bell, P. M.: 'Rust' in the Apollo 16 Rocks', *Proceedings of the Fourth Lunar Science Conference, Geochim. Cosmochim. Acta* **1**, Suppl. 4, 829-839.

Apollo 16 samples of all four rock types and from all stations contain evidence for hydration and oxidation - i.e., the presence of hydrated iron oxide, probably goethite. Rock 66095 contains native FeNi grains with a characteristic intergrowth of schreibersite and, to lesser extents, of cohenite. Troilite also contains sphalerite ( $28 \pm 2$  mole % FeS). The goethite contains 1.5-4.6 wt. % chlorine and occurs mainly on the edges of FeNi metal, causing a rust color in the cracks and space around the native metal grains, which also contain abundant chlorine. This observation suggests the presence of lawrencite ( $FeCl_2$ ), a phase that deliquesces and oxidizes very rapidly upon exposure to water or to a moist atmosphere. Certain generalizations can be made concerning the rusted rocks: (1) the rust is restricted to Highland rocks; (2) the native metal compositions are different in various rocks, negating a common meteoritic source for the chlorine that produced the oxidation; (3) the only common factor among the rusted rocks appears to be the presence of chlorine; (4) if the rusting process occurred on the Moon, the two most probable sources for the chlorine and water that produced the oxyhydration are impact processes or fumarolic activity; (5) the oxyhydration of the lawrencite continues by contact of the samples with terrestrial water vapor.

Taylor, L. A., Williams, K. L., and Sardi, O.: 'Selected Apollo 17 Soils: Mineralogy and Geochemistry of Opaque and Non-Opaque Phases', *Earth Planetary Sci. Letters* **21**, 6-12.

Soil samples 74220 ('orange soil'), 74241 and 75081 were sized and the compositions of the opaque and silicate phases were determined. The ilmenites, particularly in 74241, contain up to 7.8 wt. % MgO and display higher birefractance than low-Mg ilmenites. They commonly contain exsolution-like chromite and rutile and occasionally are in association with native Fe in an assemblage probably resulting from reduction. The chromian ulvöspines are similar to Apollo 11 spinels in that they contain near-equal amounts of chromite and ulvöspinel molecules. No primary chromites were observed. Most native Fe has Ni and Co contents of  $< 1$  wt. %; some 74220 contained 5-6% Ni and  $< 1$  % Co in association with schreibersite. All armalcolites examined are optically and chemically similar and the common mantling by Mg ilmenite leads us to conclude they are the ortho-armalcolite of S. E. Haggerty. We have collected optical (reflectivity and birefractance) and microhardness data for the ilmenites, ulvöspinel and armalcolites. These are the first microhardness determinations for the last two minerals.

Taylor, S. R., Gorton, M. P., Muir, P., Nance, W., Rudowski, R., and Ware, N.: 'Lunar Highlands Composition: Apennine Front', *Proceedings of the Fourth Lunar Science Conference, Geochim. Cosmochim. Acta* **2**, Suppl. 4, 1445-1459.

Analytical data for 42 elements for 26 Apollo 15 rocks, soils, breccia clasts, mineral separates, and emerald green glass are given. Mare basalt 15016 has a flat REE pattern, a small Eu anomaly and a high content of Cr, Ni, Co, Sc, and V, consistent with a high degree of partial melting and a small degree of fractionation.

The emerald green glass has REE 3–5 times chondrites, a flat REE pattern, a small Eu depletion, and other element concentrations consistent with a high degree of partial melting from a source region similar to that of Apollo 12 basalts.

The LM soil (Station 8) has a KREEP component probably derived from a ray from Aristillus or Autolycus. The highland soils are variable, often resembling individual breccia samples. Nickel in the Apennine front soils is not higher than in the mare soils suggesting that deeper layers of the highlands were not as exposed to the early intense bombardment as higher levels (e.g., the Apollo 16 site at Descartes).

This early bombardment of the highlands, culminating in the mare basin forming collisions has resulted in destruction and mixing of any primary crust. Only a statistical approach, such as employed by the Apollo soil survey, can establish the frequency of the pre-impact rock compositions. The composition of most of the Apollo 15 breccias can be represented as mixtures of low K Fra Mauro basalt and highland basalt (anorthositic gabbro). These two end members form respectively the black and white clasts of the 'black and white' breccia 15455.

The involatile elements (REE, Ba, Th, U, Zr, Hf, Nb, etc.) show strong positive correlations, interpreted as due to mixing. These relationships, which are also shown at the Descartes site, enable highland compositions for many elements to be established from the orbiter XRF and gamma-ray data. The resulting average highland composition is a mixture of 69% highland basalt (anorthositic gabbro) and 31% low K Fra Mauro basalt.

The composition of the emerald green glass may limit the elemental abundances in the source region to 2–3 times the chondritic abundances. The uniform values observed for K-Zr and K-Ba ratios in highland and mare samples place constraints on heterogeneous accretion models which invoke volatility differences.

Taylor, S. R., Gorton, M. P., Muir, P., Nance, W. B., Rudowski, R., and Ware, N.: 'Composition of the Descartes Region, Lunar Highlands', *Geochim. Cosmochim. Acta* 37, 2665–2683.

Analytical data for 40 elements are reported for Apollo 16 soils 60601, 61181, 61501, 64801, 67701 68501, 65701 and breccias 60015, 60017, 60018, 60315, 61016, 61175, 65015 and 66055. The soils are uniform except for the North Ray Crater rim sample which is richer in  $Al_2O_3$ .

The breccia components show great diversity in composition. Low-K Fra Mauro basalt, Highland basalt (anorthositic gabbro) and plagioclase are important constituents. Medium-K Fra Mauro basalt is an important constituent of breccias 65015 and 60315.

The breccias contain many meteorite fragments and high nickel contents, evidence of the early highland bombardment.

Most of the refractory elements (REE, Th, U, Zr, Hf, Nb, Ba) show strong positive correlations, interpreted as resulting from mixing. The REE patterns of the breccias show extreme variation relative to chondrites. There is a good inverse correlation between REE and the europium anomaly ( $Eu/Eu^*$ ). The La/Yb ratio is constant at 3.1 except in plagioclase. Eu depletion or enrichment is interpreted as due to addition or removal of plagioclase.

The Cayley and Descartes formations cannot be distinguished chemically and the differences in surface expression are not due to chemical distinctions. They are interpreted as structural differences, related to early highland cratering and mare basin formation.

The complex soil and breccia compositions are related to mixing of four components. These are Low-K Fra Mauro basalt, Highland basalt (anorthositic gabbro) and subordinate plagioclase and Medium-K Fra Mauro basalt. These compositions have been used in a computer program (PET-MIX III) to provide fits for the analytical data in terms of the end-members.

An average highland composition is proposed, based on the Apollo 15 and 16 orbital data for Si, Al, Mg and Th. Abundances for most other elements are derived from the interelement relationships and correlations, and checked by the mixing program.

The resulting composition consists of 69% Highland basalt (anorthositic gabbro) and 31% Low-K Fra Mauro basalt. There is no significant Eu anomaly. The abundances are:  $SiO_2$ : 45.2%;  $TiO_2$ :

0.68%; Al<sub>2</sub>O<sub>3</sub>: 24.9%; FeO: 6.3%; MgO: 8.5%; CaO: 13.8%; Na<sub>2</sub>O: 0.4%; K<sub>2</sub>O: 0.11%; Cr<sub>2</sub>O<sub>3</sub>: 0.11%; Ba: 144 ppm; Th: 1.8 ppm; U: 0.46 ppm; Pb: 1.6 ppm; Zr: 156 ppm; Hf: 3.2 ppm; Nb: 10.8 ppm; Y: 32 ppm; ΣREE: 85 ppm.

Trombka, J. I., Arnold, J. R., Reedy, R. C., Peterson, L. E., and Metzger, A. E.: 'Some Correlations between Measurements by the Apollo Gamma-Ray Spectrometer and Other Lunar Observations', *Proceedings of the Fourth Lunar Science Conference, Geochim. Cosmochim. Acta* 3, Suppl. 4, 2847–2853.

Observations by the Apollo 15 and 16 gamma-ray spectrometers are compared with those of a number of other experiments, both compositional and non-compositional. A general correspondence with topography is seen. The Van de Graaff area is a unique farside region with respect to observations by the laser altimeter, the subsatellite magnetometer, and the gamma-ray spectrometer, X-ray and alpha particle orbital measurements show a broad general agreement with gamma-ray data, though results from additional elements in the gamma-ray spectrum are needed to extend the comparison with X-ray data. A comparison of Th concentrations with those found at various landing sites shows generally good agreement, with the orbital values tending to be somewhat higher.

Tsay, F.-D., Manatt, S. L., Live, D. H., and Chan, S. I.: 'Metallic Fe Phases in Apollo 16 Fines: Their Origin and Characteristics as Revealed by Electron Spin Resonance Studies', *Proceedings of the Fourth Lunar Science Conference, Geochim. Cosmochim. Acta* 3, Suppl. 4, 2751–2761.

The intense electron spin resonance (ESR) signals ( $g = 2.08 \pm 0.03$ ) detected in the Apollo 16 fines from three sites (61141,4, Station 1; 64501,22, South Ray Crater; 67601,20, North Ray Crater) are found to be essentially similar in  $g$ -value, in lineshape asymmetry and in temperature dependence to those previously observed for the Apollo 11–15 fines. On the basis of these similarities, it is concluded that these ESR signals like those detected in the Apollo 11–15 fines are principally ferromagnetic in nature arising from metallic Fe phases having the body-centered cubic structure, and not from hematite, magnetite, or any other ferric oxides. It is shown that a quantitative correlation exists between the ESR linewidth observed for the Apollo 11–16 fines and their average Ni contents in the metallic Fe phases as determined by other means. For the three Apollo 16 fines investigated, the ESR linewidths are found to be essentially identical. This together with a high Ni content in the metallic Fe phases of these samples as determined from ESR linewidth correlation indicates a common source of meteoritic origin for the metallic Fe phases of these samples. Significant variations are observed in the metallic Fe content as well as in the total Ni content for these samples, in particular, between the fines from South Ray Crater and that from North Ray Crater. These variations appear to correlate with the surface exposure ages of the samples. It is also shown that the first-order crystalline anisotropy energy,  $2K_1/M_s$ , determined from ESR linewidth measurements is essentially equivalent to the remanence coercive force,  $H_{RC}$ , obtained in static magnetic susceptibility measurements for the lunar fines.

Turkevich, A. L.: 'The Average Chemical Composition of the Lunar Surface', *Proceedings of the Fourth Lunar Science Conference, Geochim. Cosmochim. Acta* 2, Suppl. 4, 1159–1168.

The available analytical data from twelve locations on the Moon are used to estimate the average amounts of the principal chemical elements (O, Na, Mg, Al, Si, Ca, Ti, and Fe) in the mare, the terra, and the average lunar surface regolith. These chemical elements comprise about 99% of the atoms on the lunar surface. The relatively small variability in the amounts of these elements at different mare (or terra) sites, and the evidence from the orbital measurements of Apollo 15 and 16, suggest that the lunar surface is much more homogeneous than the surface of the Earth. The average chemical composition of the lunar surface may now be known as well as, if not better than, that of the solid of the Earth's surface.

Turner, G., Cadogan, P. H., and Yonge, C. J.: 'Argon Selenochronology', *Proceedings of the Fourth Lunar Science Conference, Geochim. Cosmochim. Acta* 2, Suppl, 1889–1914.

The K-Ar ages of samples from Apollos 15, 16, and 17 and Luna 20 have been determined by the Ar<sup>40</sup>-Ar<sup>39</sup> method. The age of an Apollo 17 basalt confirms evidence from Apollo 11 samples that extrusion of mare basalts began as early as 3.8 aeons ago. Ages of highland samples cluster in the interval 3.88 to 4.05 aeons and are taken to indicate that at least three and probably six of the major lunar basins formed in this period. The implications of this observation are discussed. Cosmic ray exposure ages have been determined using the Ar<sup>38</sup>-Ar<sup>37</sup> method and used to date North Ray (46 m.y.) and Camelot (90 m.y.) craters.

Vinogradov, A. P.: 'Preliminary Data on the Lunar Soil Brought Back by the Luna-20 Automatic Station', NASA-TT-F-15128.

A comparison of the lunar material of Luna-20 with material derived from other lunar probes is reported. Differences and some contradictions found among the varying chemical compositions of lunar materials from the different lunar probes are discussed. It is concluded that the lunar anorthosites as well as the terrestrial anorthosites should become the object of further long term research to determine their origin and age.

Vinogradov, A. P. and Zadorozhny, I. K.: 'Rare Gases in Regolith and Fragments of Rocks Supplied by the Automatic Station 'Luna-20'', *Proceedings of the Fourth Lunar Science Conference, Geochim. Cosmochim. Acta* 2, Suppl. 4, 2065–2077.

The content and isotopic composition of rare gases in regolith samples and 24 rock fragments isolated from regolith fractions have been investigated by the mass-spectrometric method.

The He and Ne concentrations in regolith samples selected from the upper and the lower zone of the core differ by not more than 20% and are within the ranges of experimental errors. The He and Ne concentrations measured in the regolith are approximately half and that of argon slightly higher than their concentrations in the regolith from Mare Fecunditatis. The concentrations of rare gases in individual fragments (sizes which varied in the range of 0.2–1.7 mm) are 2–3 orders of magnitude lower than their concentration in the fine regolith fraction (< 0.083 mm).

The isotopic ratios of gases in fragments vary over ranges: <sup>4</sup>He/<sup>He</sup>3 from 2860 to 320, <sup>40</sup>Ar/<sup>36</sup>Ar from 24 to 1.6, <sup>20</sup>Ne/<sup>22</sup>Ne from 12 to 6. The observed variations may be explained by the presence of radiogenic argon and of cosmogenic gases, in addition to the main solar wind gas component. The <sup>40</sup>Ar/<sup>36</sup>Ar ratio = 1.6–1.8 for the fine fraction of 'Luna-20' regolith is somewhat higher than its ratio in regolith of 'Luna-16'. The <sup>4</sup>He/<sup>20</sup>Ne ratio vary within the range 23–57, and the <sup>20</sup>Ne/<sup>36</sup>Ar ratio vary from 4.5 to 0.8.

Radiation ages calculated according to the content of cosmogenic <sup>21</sup>Ne and <sup>38</sup>Ar isotopes are within the range of 100 to 400 m.y. for most fragments. The ages obtained are slightly lower than the radiation ages of rocks from Mare Fecunditatis.

A few particles show very high radiation ages, about 900 m.y. Probably these observed anomalies may be explained by the effect of solar flare proton irradiation.

Walton, J. R., Lakatos, S., and Heymann, D.: 'Distribution of Inert Gases in Fines from the Cayley-Descartes Region', *Proceedings of the Fourth Lunar Science Conference, Geochim. Cosmochim. Acta* 2, Suppl. 4, 2079–2095.

Nec<sup>21</sup> exposure ages of bulk fines are distinctly younger at the rim of North Ray Crater (about 55 m.y. or younger) than elsewhere at the Apollo 16 site. The most likely explanation is that the age of North Ray Crater is certainly less than 60 m.y. and probably less than 30 m.y. An alternative, but less likely explanation is that these are the ages of South Ray Crater, with North Ray Crater being older than about 75 m.y. The older, mature 'country fines' have apparent ages greater than 300 m.y. Fines at all stations are mixtures of "country fines", North Ray and South Ray ejecta. At Station 13

they are predominantly North Ray ejecta. South Ray ejecta are most abundantly seen at Stations 8 and 9.

Fines from highland regions are poorer in trapped helium and neon than fines from mare regions. This is almost certainly due to differences in chemistry and mineralogy. Fines richer in  $\text{TiO}_2$  contain more trapped He and Ne than those poor in titania.

Fines from the trench at Station 1 (61221) and from Station 11 show unusually large  $(\text{He}^4/\text{He}^3)_T$  ratios of 2880 or greater. This means either that these fines have undergone uncommonly large He losses or that the geomagnetic index  $K_p$  has undergone long-term secular variations. The  $(\text{Ar}^{40}/\text{Ar}^{36})_T$  ratio of about 1.0 in fines which seem to have been deposited on the surface only 30–60 m.y. ago implies that the average concentration of neutral  $\text{Ar}^{40}$  in the lunar atmosphere during this period was not very different from the average value during the last 4000 m.y. If this entity decreased between 4000 and 3300 m.y. ago, it must have gone through a minimum value and then increased again. We propose that the neutral  $\text{Ar}^{40}$  in the lunar atmosphere comes mainly from the interior of the Moon since about 3000 m.y. ago.

Fines 61221 from the trench at Station 1 have unique inert gas contents with certain elemental and isotopic ratios unlike those of any other fines in the area. We suggest that this high-albedo material is perhaps the best representative for materials of the Cayley Formation at the Apollo 16 site.

Wänke, H., Baddenhausen, H., Dreibus, G., Jagoutz, E., Kruse, H., Palme, H., Spettel, B., and Teschke, F.: 'Multielement Analyses of Apollo 15, 16, and 17 Samples and the Bulk Composition of the Moon', *Proceedings of the Fourth Lunar Science, Geochim. Cosmochim. Acta* 2, Suppl. 4, 1461–1481.

The concentration of all major and many minor and trace elements was determined in 21 lunar samples from Apollo 15, 16, and 17. Altogether we report on 54 elements including oxygen which was determined directly by neutron activation as were most of the other elements. Many of the major and minor elements were measured with a standard accuracy between 1 and 5%. For a number of trace elements like Ga, As, Hf, and W we report here on the first results on anorthositic rocks. The three Apollo 17 soils analyzed including the orange soil 74220 were found to have great similarity in their composition to the Apollo 11 samples. The concentrations of F, Cu, Zn, and Ga are about 3 to 10 times higher than found in any lunar sample so far. The orange soil 74220 is very similar to the soil sample 74241 collected nearby except for a 3 times lower F content.

Mainly using the data of this work and those from our previous reports element correlations were studied in great detail. It was found that among the LIL elements the ratio K/La remains rather constant over a concentration range of about 3 orders of magnitude. This ratio is of great importance as one of these elements belongs to the group of highly refractory elements and the other to the more volatile elements. Evidence is presented that the observed K/La-ratio of about 70 is valid for the whole Moon or at least for that part of the Moon which underwent magmatic differentiation.

All refractory LIL elements are always found in proportions close to the solar (Cl) abundance ratios. These elements were found to be highly enriched in the Allende inclusions in the same abundance ratios. Therefore it is suggested that this group of elements is derived from high temperature condensates. All alkali elements except Na are found in constant abundance ratios. These ratios come close to that in Cl chondrites, except Cs which is about a factor of 4 lower. Taking into account both the refractory elements and the alkali elements with their varying volatility we suggest a two component model of the Moon: component (a) the high temperature condensates (HTC) and component (b) the chondritic component (ChC).

The K/La-ratios were found to be different for the Moon (70), basaltic achondrites (140) and Earth (450). Taking our data on Ca, Al-rich Allende inclusions as representative for HTC we calculated the contribution of the HTC to the composition of the Moon, the basaltic achondrites and the Earth as 69%, 48%, and 22%. For a number of elements the lunar abundances are tabulated.

Weeks, R. A.: 'Ferromagnetic Phases of Lunar Fines and Breccias: Electron Magnetic Resonance Spectra of Apollo 16 Samples', *Proceedings of the Fourth Lunar Science Conference, Geochim. Cosmochim. Acta* 3, Suppl. 4, 2763–2781.



Electron magnetic resonance measurements have been made at 9 GHz and at temperatures from 1.2 to 400K and 35 GHz (300K) on samples of fines and breccias from Apollo 11–16. Unsorted Apollo 16 fines (< 1 mm) have  $\Delta H$  (average) = 580 G and specific intensities that have the same range as fines from the other Apollo collections. The temperature dependence of  $\Delta H$   $d\Delta H/dT \sim 1.8$  from 1.2 to 400K for most Apollo 11–16 samples, but for some  $d\Delta H/dT > 1.8$  at the lowest temperatures. A magnetic transition or compensation point between 160 and 130K is deduced from the temperature dependence of  $\Delta H$ . The magnetic properties of the ‘characteristic’ resonance are not in accord with those of iron particles. On the bases of the properties of the ‘characteristic’ resonance as a function of temperature and Apollo site, laboratory heat treatments on synthetic materials and lunar crystalline rocks and a comparison with the ‘characteristic’ resonance of the resonance spectra of breccia specimens for which iron particle sizes have been determined from other measurements, it is suggested that some fraction (~ 20%) of the ‘characteristic’ resonance is due to sub-micron particles of ferric oxide phases. Possible source for ferric oxide phases in fines are (1) oxidation of fines by cometary impacts, (2) oxides derived from ancient volcanic activity, and (3) remnants of carbonaceous chondrites which have impacted the Moon.

Williams, K. and Taylor, L. A.: ‘Optical Properties and Chemical Compositions of Apollo 17 Armalcolites’, *Geology* 2, 5–8.

Armalcolite present in Apollo 17 samples 74242 and 75082 displays textures which Haggerty used as criteria for distinguishing two distinct varieties – ortho-armalcolite and para-armalcolite. Reflectivity measurements and microprobe analyses were performed on numerous grains of both ‘varieties’ of armalcolite present in these specimens. No major differences in optical properties and no consistent compositional variations were found in these armalcolites. Therefore, the need for distinguishing two ‘varieties’ of armalcolite, whose only major difference appears to be their paragenesis, is unnecessary and unjustified.

Wlotzka, F., Spettel, B., and Wänke, H.: ‘On the Composition of Metal from Apollo 16 Fines and the Meteoritic Component’, *Proceedings of the Fourth Lunar Science Conference, Geochim. Cosmochim. Acta* 2, Suppl. 4, 1483–1491.

In a metal sample separated from fines 60601 As, W, Ir, and Au were determined by INAA, and Ni and Co by electron microprobe in individual particles. Nickel and Co contents are within the meteoritic range. Compared to a solar abundance the Ir/Au ratio is a factor of 2 lower, which is caused by an excess of Au. Together with the Au the elements As and perhaps Pd and Re are enriched. The same anomalies are found in the microbreccia 14305 and the bulk fines 60601, 61161 and 65701. Three explanations are discussed:

(1) Presence of an ancient meteorite component with high Au, As and Pd to Ni ratios. This view is supported by the fact that the Ir/Au and Ir/Ni ratios are lower in the metal samples than in the bulk fines. This could mean that the ancient component shows up purer in the metal than in the bulk soil, because the siderophile elements of the younger micrometeorite component did not yet equilibrate completely with the metal.

(2) Conservation of a primary difference in Ir/Au ratios of different parts of the Moon, connected with the higher condensation temperature of Ir. This explanation is ruled out, because it should also separate Ir from Ni, which is not observed.

(3) Addition of an indigeneous Au-rich component, This is considered unlikely because of the constancy of the low Ir/Au and high Au/Ni ratios found, which would require the addition of the Au-rich and the meteoritic components in a constant ratio.

Wrigley, R. C.: ‘Radionuclides at Descartes in the Central Highlands’, *Proceedings of the Fourth Lunar Science Conference, Geochim. Cosmochim. Acta* 2, Suppl. 4, 2203–2208.

Thorium, uranium, potassium,  $^{26}\text{Al}$ , and  $^{22}\text{Na}$  were measured in six soil samples, 60051, 61161, 64801, 65701, 68841, and 69961, and two rock samples, 61016 and 67455, collected from the Apollo 16 site

in the central highlands. Although the soil samples spanned what was thought to be two major lunar formations, Cayley and Descartes, no difference could be discerned in the primordial radionuclide concentrations of the two. It is possible the Descartes Formation was not sampled. Both rock samples have very low concentrations of primordial radionuclides. Sample 67455 represents the white portion of the white breccia boulders on the rim of North Ray Crater, which appear to represent a deep white layer in the crater. Thus, based on concentrations of primordial radionuclides, significantly different units exist in vertical section at the site. Variations in  $^{26}\text{Al}$  soil concentrations are not due to chemical variations; they are probably due to average sampling depth differences or possibly to very local regolith mixing.

Wszolek, P. C. and Burlingame, A. L.: 'Carbon Chemistry of the Apollo 15 and 16 Deep Drill Cores', *Proceedings of the Fourth Lunar Science Conference, Geochim. Cosmochim. Acta* **2**, Suppl. 4, 1681–1692.

The carbon chemistry of the Apollo 15 and 16 deep drill cores is a function of the surface exposure plus the chemical and mineralogical composition of the individual samples. The depth profiles of carbide and methane yields in the Apollo 15 core show a general decline with depth and correlate with the solar wind noble gas content, percentage agglutinates, track densities, and metallic iron. All horizons examined were exposed for a considerable time on the lunar surface.

The Apollo 16 core samples show that chemical and mineralogical composition plays an important role in determining the nature of carbide-like material present in the fines. The higher aluminum and calcium contents and lower iron contents of highlands material result in carbide-like material yielding less  $\text{CD}_4$  and more  $\text{C}_2\text{D}_2$  (deuteroacetylene) upon DF acid dissolution. Aluminum and/or calcium carbides may be synthesized by solar wind implantation of carbon into these soils. Depth profiles for carbide, methane,  $^{20}\text{Ne}$ , and  $^{36}\text{Ar}$  show irregular patterns. The bottom of the core exhibits several unusual features including a larger  $\text{CH}_4$  yield than expected for its low exposure time and an unusual low temperature  $\text{SO}_2$  pyrolysis release.

Wszolek, P. C., Simoneit, B. R., and Burlingame, A. L.: 'Studies of Magnetic Fines and Volatile-Rich Soils: Possible Meteoritic and Volcanic Contributions to Lunar Carbon and Light Element Chemistry', *Proceedings of the Fourth Lunar Science Conference, Geochim. Cosmochim. Acta* **2**, Suppl. 4, 1693–1706.

Iron-rich composite grains isolated from Plum Crater soil sample 61500 are enriched in carbon, carbide, methane,  $^{36}\text{Ar}$  and sulfide; they appear to have formed at moderate temperatures from mature regolith fines. A very strongly magnetic fraction, mostly metal particles, is also enriched in carbide and may represent a small contribution of meteoritic origin. The nonmagnetic fraction from 61500, enriched in feldspar, produces a substantial proportion of deuteroacetylene,  $\text{C}_2\text{D}_2$ , upon DF acid dissolution suggesting the presence of material behaving like calcium and/or aluminum carbide.

Volatiles released during pyrolysis of subsurface soil 61221 were analyzed by high resolution mass spectrometry and strongly resemble those evolved by Murray and Murchison carbonaceous chondrites. Under certain favorable conditions a large variety of relatively complex meteoritic carbon compounds can be preserved in significant amounts. Orange soil 74220 and black soil 74001 release  $\text{CO}_2$ ,  $\text{SO}_2$ ,  $\text{H}_2\text{O}$ , and  $\text{CO}$  at low pyrolysis temperatures suggesting either a chondritic or volcanic source for these volatiles.

## 7. Lunar Exosphere

Bhandari, N., Goswami, J. N., Lal, D., and Tamhane, A. S.: 'Long-Term Fluxes of Heavy Cosmic-Ray Nuclei Based on Observations in Meteorites and Lunar Samples', *Astrophys. J.* **185**, 975–983.

Results of observations of fossil tracks due to very heavy (VH) and very very heavy (VVH) cosmic-ray nuclei ( $Z > 20$  and  $Z \geq 30$ , respectively) in a variety of extraterrestrial samples – lunar and meteoritic are presented. These samples represent irradiation by solar as well as galactic cosmic rays during the

past  $10^3$ – $10^8$  yr, with effective shielding depths of  $10^{-3}$ – $10$  cm of typical stony material, corresponding to the kinetic-energy interval (6–1500) MeV per nucleon. Based on these data, we have deduced the average kinetic energy spectrum of VH and VVH nuclei in the ancient cosmic radiation.

Our observations indicate that (i) at energies less than 10 MeV per nucleon, the VH and VVH nuclei are entirely of solar origin and (ii) the relative abundance of  $(Z \geq 30)/(Z > 20)$  nuclei is almost constant in the kinetic-energy interval (50– $10^3$ ) MeV per nucleon, but that at lower energies, less than 30 MeV per nucleon, the heavier nuclei progressively become more abundant. The ratio of abundance  $(Z \geq 30)/(Z > 20)$ , increases by more than a factor of 5 in going down from 50 to 6 MeV per nucleon. (Effects of shielding geometry and erosion during irradiation have been considered; their effects are found to be unimportant for the conclusions drawn here.) Taking into account typical erosion rates, the exponents in the power-law kinetic-energy spectra of solar VH and VVH nuclei are determined to be  $-3$  and  $-5$ , respectively.

Chou, C.-L., Baedecker, P. A., and Wasson, J. T.: 'Atmophilic Elements in Lunar Soils', *Proceedings of the Fourth Lunar Science Conference, Geochim. Cosmochim. Acta* 2, Suppl. 4, 1523–1533.

Ten volatile elements are more abundant in soil 14163 than in 14259 by factors of 1.4 or greater, too high to be explained by the 15% higher KREEP content of 14163. The enrichments suggest that these elements are easily volatilized by energetic events generated by solar particles or micrometeorites and as a result move from site to site through the lunar atmosphere. The elements Zn, C, and Cd are correlated with excess  $\text{Ar}^{40}$  in Apollo 15 soils. Since concentrations also increase in the direction of the Apennine Front, the correlation chiefly indicates that the Front regolith is enriched in these elements relative to the Apollo 15 regolith away from the Front. The absence of known lunar rock types showing Zn and Cd concentrations as high as those in the Apollo 15 Front regolith or the Apollo 14 or 16 highlands regoliths and the relatively uniform concentrations of both elements in these soils despite differences in major element composition suggest that large amounts of these elements were released as volatiles during early lunar magmatic activity.

Gorenstein, P., Golub, L., and Bjorkholm, P. J.: 'Spatial Features and Temporal Variability in the Emission of Radon from the Moon: An Interpretation of Results from the Alpha Particle Spectrometer', *Proceedings of the Fourth Lunar Science Conference, Geochim. Cosmochim. Acta* 3, Suppl. 4, 2803–2809.

Observations of  $^{222}\text{Rn}$  and  $^{210}\text{Po}$  on the lunar surface with the orbiting Apollo Alpha Particle Spectrometer reveal a number of features in their spatial distribution and indicate the existence of time variations in lunar radon emission. Localized  $^{222}\text{Rn}$  or  $^{210}\text{Po}$  around the craters Aristarchus and Grimaldi and the edges of virtually all maria indicating time varying radon emission suggest a correlation between alpha 'hot spots' and sites of transient events as seen from the Earth. In a gross sense, the slower variations of  $^{222}\text{Rn}$  seem to correlate with the distribution of gamma activity.

The distribution of radon gas in the lunar atmosphere is characterized by an enhancement near the terminator. On the dark side of the Moon radon apparently does not migrate freely; it is stored in the regolith or condensed out upon the surface.

Hodges, R. R.: 'Helium and Hydrogen in the Lunar Atmosphere', *J. Geophys. Res.* 78, 8055–8064.

Solar wind ions impinge on the surface of the Moon, become neutralized, and are subsequently released to become part of the neutral lunar atmosphere. Of the gas species supplied by the solar wind, only helium and hydrogen are light enough to be lost from the Moon by Jeans' thermal escape mechanism. To study the behavior of helium and hydrogen, a Monte Carlo technique has been used, in which random ballistic trajectories of individual molecules are traced over a spherical Moon. In the computation, a particle is 'created' on the sunlit surface, and the locations of its subsequent encounters with the surface are recorded until it escapes. Global distributions of helium and hydrogen concentrations have been computed, based on the hypothesis that the release of neutral gases from the lunar surface is confined to daytime and correlated with the solar wind influx. The resulting

helium model is in good agreement with the measurements from the Apollo 17 lunar surface mass spectrometer. In view of the absence of atomic hydrogen in the lunar atmosphere and the need for a loss mechanism for the solar wind influx of protons, a molecular hydrogen atmosphere model is proposed in which predicted amounts of H<sub>2</sub> are below presently established upper bounds.

Hodges, R. R., Hoffman, J. H., Johnson, F. S., and Evans, D. E.: 'Composition and Dynamics of Lunar Atmosphere', *Proceedings of the Fourth Lunar Science Conference, Geochim. Cosmochim. Acta* 3, Suppl. 4, 2855–2864.

The model of lunar atmosphere is updated to take into account new information on the dynamics and amounts of H<sub>2</sub>, <sup>4</sup>He, <sup>20</sup>Ne, <sup>36</sup>Ar, and <sup>40</sup>Ar. Helium and neon appear to be in close balance with the solar wind, although <sup>36</sup>Ar is depleted in the atmosphere, suggesting that surface materials are not saturated with argon. Atmospheric carbon compounds, which should result from the solar wind influx of carbon, remain undetected, as do nitrogen compounds. However, evidence of a volcanic gas release is presented, which suggests the transient presence of these elements.

Hoffman, J. H., Hodges, R. R., Johnson, F. S., and Evans, D. E.: 'Lunar Atmospheric Composition Results from Apollo 17', *Proceedings of the Fourth Lunar Science Conference, Geochim. Cosmochim. Acta* 3, Suppl. 4, 2865–2875.

The Apollo 17 mass spectrometer has confirmed the existence of helium, neon, argon, and possibly molecular hydrogen in the lunar atmosphere. Helium and neon concentrations are in agreement with model predictions based on the solar wind as a source and their being non-condensable gases. <sup>40</sup>Ar and <sup>36</sup>Ar both exhibit a pre-dawn enhancement which indicates they are condensable gases on the nightside and are re-released into the atmosphere at the sunrise terminator. Hydrogen probably exists in the lunar atmosphere in the molecular rather than atomic state, having been released from the surface in the molecular form. Total night-time gas concentration of known species in the lunar atmosphere is  $2 \times 10^3$  mol cm<sup>-3</sup>.

Jordan, J. L., Heymann, D., and Lakatos, S.: 'Inert Gas Patterns in the Regolith at the Apollo 15 Landing Site', *Geochim. Cosmochim. Acta* 38, 65–78.

He, Ne, Ar, Kr and Xe were measured mass-spectrometrically in eight bulk fines and one sample of 2–4 mm fines (15603) from stations LM-ALSEP, 2, 6, 6<sup>a</sup>, 7<sup>a</sup>, and 9. We have also measured these gases in size fractions of samples 15091 and 15601. These samples come from three morphologically distinct selenographic settings: the Apennine Front, the Mare and Hadley Rille. Measured gas contents in these samples are comparable to those from previous Apollo missions. He<sup>4</sup> and the other trapped gases are inversely proportional to grain diameter in the size fractions of 15091 and 15601. More than 90% of the trapped gas in 15601 is surface correlated; hence is probably directly implanted solar wind. Size fractions of 15091 contain large volume correlated amounts of He<sup>4</sup>, Ne<sup>20</sup> and Ar<sup>36</sup>. He<sup>4</sup>/Ne<sup>20</sup> ranges from about 20 to 60; Ne<sup>20</sup>/Ar<sup>36</sup> from 5 to 8; Ar<sup>36</sup>/Kr<sup>84</sup> from 2400 to 3200; and Kr<sup>84</sup>/Xe<sup>132</sup> from 3.2 to 7.3. The lowest He<sup>4</sup>/Ne<sup>20</sup> ratios occur in samples rich in green glass spherules which have He<sup>4</sup>/Ne<sup>20</sup> ≤ 10. He<sup>4</sup>/He<sup>3</sup> ranges from about 2100 to 2700; Ne<sup>20</sup>/Ne<sup>22</sup> from 12.7 to 13.2; Ne<sup>21</sup>/Ne<sup>22</sup> from 0.035 to 0.041; and Ar<sup>36</sup>/Ar<sup>38</sup> from 5.26 to 5.45. The measured Ar<sup>40</sup>/Ar<sup>36</sup> ratios range from 0.757 to 3.56; when corrected for radiogenic Ar<sup>40</sup>, the range becomes 0.6 to 3.4. The largest corrected Ar<sup>40</sup>/Ar<sup>36</sup> ratios occur in samples from the Apennine Front, the smallest occur in the Mare. This could be due to slope effects between the front as opposed to the mare terrain. An alternative possibility is that the Front fines acquired their atmospheric Ar<sup>40</sup> at a time when the concentration of neutral Ar<sup>40</sup> in the lunar atmosphere was relatively large.

Ne<sup>21</sup> radiations ages were calculated for all samples. There is evidence in the landing area for debris from craters with ages less than  $100 \times 10^6$  yr, but these craters cannot be firmly identified from the data.

Lindeman, R., Freeman, J. W., and Vondrak, R. R.: 'Ions from the Lunar Atmosphere', *Proceedings of the Fourth Lunar Science Conference, Geochim. Cosmochim. Acta* 3, Suppl. 4, 2889–2896.

The ionization of neutral atoms in the lunar atmosphere produces an ionosphere around the Moon. These ions are accelerated by the interplanetary electric field and local surface fields to energies of 10 to 500 eV. The Suprathermal Ion Detector Experiment has been observing these ions from the lunar atmosphere. The observations have been divided into four categories based on the acceleration mechanism.

Manka, R. H.: 'Lunar Atmosphere and Ionosphere', Ph.D. Thesis, Rice University, Houston, Tex., Univ. Microfilms, Order No. 72–26417.

To determine the interaction of lunar ions with electric and magnetic fields in the solar wind, the following characteristics of the lunar atmosphere and ionosphere are calculated: (1) The production of ions by photo- and charge-exchange ionization of lunar atmosphere; (2) the trajectory of these ions under acceleration of interplanetary electric and magnetic fields; (3) the energy and flux of ions which impact the Moon; (4) the trapping efficiency for lunar ions which impact the lunar surface; and (5) the implied density in the neutral lunar atmosphere of certain species such as Ar-40. The effects of surface electric and magnetic fields upon ion acceleration are also considered. Applications of these calculations are made to data from lunar surface experiments and lunar sample analyses.

Plieninger, T., Krätschmer, W., and Gentner, W.: 'Indications for Time Variations in the Galactic Cosmic Ray Composition Derived from Track Studies on Lunar Samples', *Proceedings of the Fourth Lunar Science Conference, Geochim. Cosmochim. Acta* 3, Suppl. 4, 2337–2346.

In order to improve the charge assignments to etchable VH cosmic ray ion tracks, pyroxene crystals from Apollo 11 lunar rock sample 10047,13 were irradiated with  $9.6 \text{ MeV n}^{-1}$  Fe ions at the Linac of the University of Manchester (England). Using the track-in-track technique, the lengths of artificial Fe and pre-existing galactic cosmic ray tracks within the same crystals were compared. By this, a direct comparison was possible without referring to etchable ranges, which were found to be difficult to develop completely by etching. Under the chosen etching conditions, the length distributions of artificial Fe and cosmic ray tracks coincide at a peak centered at about  $16\text{--}18 \mu\text{m}$ . A more detailed evaluation of track lengths shows that annealing effects have shortened the mean length of galactic Fe tracks by about  $0.5 \mu\text{m}$ . Additional peaks at  $6 \mu\text{m}$  and  $12 \mu\text{m}$  were ascribed to Ca and Cr cosmic ray ions. A primary ratio  $(V + Cr + Mn)/Fe = 0.7 \pm 0.2$  for the energy range  $300\text{--}600 \text{ MeV n}^{-1}$  can be derived under the assumption of a maximum shielding depth of 5 cm. Length distributions measured in pyroxene crystals from the lunar regolith (sample 10084) show ratios ranging between 0.4 and 0.7. A comparison with recent data about the present day galactic cosmic ray composition indicates that the ratios obtained in rock and soil samples cannot be explained by the variation of the composition with energy. Therefore a variation with time of the VH cosmic ray composition is proposed.

Price, P. B., Chan, J. H., Hutcheon, I. D., Macdougall, D., Rajan, R. S., Shirk, E. K., and Sullivan, J. D.: 'Low-Energy Heavy Ions in the Solar System', *Proceedings of the Fourth Lunar Science Conference, Geochim. Cosmochim. Acta* 3, Suppl. 2347–2361.

In the previously inaccessible energy interval between  $\sim 10 \text{ keV/nucleon}$  and  $\sim 20 \text{ MeV/nucleon}$ , we report measurements of the energy spectra of various ions from He to the elements heavier than Fe during various solar conditions ranging from nearly quiet times to periods of intense flares. Though the fluxes vary in absolute magnitude by many powers of ten, there is at all times an enrichment of heavy ions that monotonically increases with atomic number and decreases with energy. At sufficiently high energy ( $\sim 20 \text{ MeV/nucleon}$  for intense flares, lower for weak flares) the composition approaches that in the photosphere. The enrichment of heavy ions results in very high track densities observed in the outer few microns of small grains within lunar soils and breccias and within gas-rich meteorites. It also should give rise to anomalously high ratios of heavy to light rare

gases in such grains and these effects should be detectable by mass spectrometry if the outer 1 to 2 microns containing solar wind gas could be removed. At various epochs extending back some 4 G.y., the steepest profiles of solar flare track densities in lunar and meteoritic grains are similar to the Surveyor glass profile, suggesting that the distribution of energy in solar flares has not changed with time. The intensity of radiation damage in micron-size grains studied by transmission electron microscopy varies widely from site to site but not with depth at a given site. In the Apollo 15, 16, and 17 cores that sampled depths down to  $\sim 250$  cm, the radiation damage level does not vary significantly with depth.

Stauber, M. C., Padawer, G. M., Brandt, W., D'Agostino, M. D., Kamykowski, E., and Young, D. A.: 'Nuclear Microprobe Analysis of Solar Proton Implantation Profiles in Lunar Rock Surfaces', *Proceedings of the Fourth Lunar Science Conference, Geochim. Cosmochim. Acta* **2**, Suppl. 4, 2189-2201.

The lunar surface is viewed as a target for charged particles of solar and galactic origin. The particles are implanted in the exposed rock surface layers with concentrations proportional to the particle fluence, and with depth profiles determined by the energy and angular distribution of the impinging particles. Concurrently, the particles cause erosion by sputtering of lunar material from the rock surfaces in ways that are correlated with their implantation characteristics. The lithium nuclear microprobe technique, developed in our laboratories, is applied to the determining of implantation concentrations of protons in lunar rocks. The method employs probing beams of lithium nuclei from an accelerator to penetrate lunar surface layers and to measure the depth profiles of implanted protons by means of a resonant nuclear reaction. Initial experiments with lithium ion beams as a probe in the energy range from 2.86 to 4.00 MeV have been conducted. Results from these experiments show the presence of hydrogen in each of the assayed samples. The measured hydrogen depth concentration profile in each case is found to consist of two components: A surface peak followed at greater depths by a relatively constant low-level plateau. It is surmised that the surface hydrogen peak is due to contamination by terrestrial hydrogen, since we have also observed it in specially treated laboratory test samples. We report in detail on the data analysis by presenting a theory that extracts from such measurements, in a self-consistent manner, the flux and its energy distribution of a species of ancient and modern solar particles. A modeling of solar particle implantation profiles in lunar rocks traces the evolution of these profiles under the combined influence of diffusion of atomic particles implanted in the rock, and rock surface erosion. It is shown that such diffusion may have a significant effect on the shape of the implantation profiles in certain rock materials. It is further demonstrated that where diffusion effects are not significant, the shape of the implanted ion density profile is determined primarily by the energy distribution of the impinging solar ion flux and is comparatively insensitive to the specific angular distribution of the flux.

Wallis, M. K.: 'Perturbation of the Solar Wind by the Lunar Atmosphere', *J. Geophys. Res.* **79**, 275-279.

The effects of atmospheric ions on the solar wind flow past the Moon may be represented by source terms in a steady flow. The sources appropriate to ions of large Larmor radius are found to differ qualitatively from those given earlier. The transverse force is the major perturbing effect and gives limits on the lunar atmospheric density at some 5 times higher than those previously derived.

Yokoyama, Y., Sato, J., Reyss, J. L., and Guichard, F.: 'Variation of Solar Cosmic-Ray Flux Deduced from  $^{22}\text{Na}$ - $^{26}\text{Al}$  Data in Lunar Samples', *Proceedings of the Fourth Lunar Science Conference, Geochim. Cosmochim. Acta* **2**, Suppl. 4, 2209-2227.

All available data of measurements made on the pair  $^{22}\text{Na}$ - $^{26}\text{Al}$  in lunar samples returned from Apollo 11 to 17 missions were compiled, normalized for chemical compositions, and compared with theoretically calculated production rates. The following conclusions were deduced: (1) The Solar proton flux for the production of  $^{22}\text{Na}$  varied from mission to mission;  $4\pi$  integral fluxes were  $97 \pm 11$ ,

$75 \pm 5$ ,  $94 \pm 13$ ,  $64 \pm 9$ ,  $63 \pm 8$ , and  $275 \pm 40$  protons  $\text{cm}^{-2} \text{s}^{-1}$  for Apollo 11, 12, 14, 15, 16, and 17 respectively with a mean rigidity of 100 MV. A large enhancement for the last mission is due to the big solar flare of August 1972. (2) The mean flux for the past million years, deduced from the production of  $^{26}\text{Al}$ , was  $70 \pm 14$  protons  $\text{cm}^{-2} \text{s}^{-1}$  with a mean rigidity of 150 MV which corresponds to a flux of  $110 \pm 22$  protons  $\text{cm}^{-2} \text{s}^{-1}$  with a mean rigidity of 100 MV.

## 8. Lunar Coordinates and Mapping of the Moon

Jones, R. L.: 'Estimates of the Moon's Geometry Using Lunar Orbiter Imagery and Apollo Laser Altimeter Data', NASA-TR-R-407.

Selenographic coordinates for about 6000 lunar points identified on the Lunar Orbiter photographs are tabulated and have been combined with those lunar radii derived from the Apollo 15 laser altimeter data. These coordinates were used to derive that triaxial ellipsoid which best fits the Moon's irregular surface. Fits were obtained for different constraints on both the axial orientations and the displacement of the center of the ellipsoid. The semiaxes for the unconstrained ellipsoid were  $a = 1737.6$  km,  $b = 1735.6$  km, and  $c = 1735.0$  km which correspond to a mean radius of about 1736.1 km. These axes were found to be nearly parallel to the Moon's principal axes of inertia, and the origin was displaced about 2.0 km from the Moon's center of gravity in a direction away from the Earth and to the south of the lunar equator.

## 9. Morphology of the Lunar Surface

Hodges, C. A., Muehlberger, W. R., and Ulrich, G. E.: 'Geologic Setting of Apollo 16', *Proceedings of the Fourth Lunar Science Conference, Geochim. Cosmochim. Acta* **1**, Suppl. 3, 1-25.

Materials of the Cayley Plains and Descartes Mountains at the Apollo 16 site apparently are not of volcanic origin, as suggested prior to the mission, but may instead be products of basin-forming impacts.

The plains are highly cratered, with North Ray, South Ray, and Baby Ray craters the youngest and most prominent examples. Numerous older craters up to a kilometer in diameter have scattered materials over the plains from depths as great as 200 m. No outcrops were sampled by the crew; the feldspathic breccias, which constitute most of the returned specimens, were obtained from the regolith and, more importantly, from North Ray and South Ray ejecta which probably represent much of the local vertical section of the Cayley Formation. A preliminary model of South Ray ejecta distribution predicts that the average thickness, where sampled, is probably not over 6 cm, and in most areas, it is likely less than 1 cm except for individual blocks.

The Moonwide occurrence of Cayley-like plains and the apparent impact origin of the returned samples suggest a possible relation of such plains deposits to multi-ring impact basins. The apparent contemporaneity of all the Imbrian light plains units, including those around and genetically related to the Orientale basin, suggests further that at least the top layer of these deposits may be a product of the Orientale impact. It seems probable that the total thickness of plains materials at Apollo 16 comprises a sequence of deposits from multi-ring basins, including Nectaris and Imbrium as well as Orientale.

At Stone Mountain, prime sampling target for Descartes materials, difficulties in finding suitable 'borehole' craters may have prevented adequate sampling of the mountain-forming (bedrock) materials there; however, North Ray Crater may have intersected correlative materials from Smoky Mountain. If the rocks of the Descartes Mountains also are breccias, then an impact origin for these likewise must be sought; the mountainous morphology seems to require a mechanism of formation different from that of the plains. Proximity of the materials to the Nectaris Basin suggests a possible source of such breccias, but gradation with ridged, probably Imbrium ejecta to the west of the crater Descartes suggests derivation from the Imbrium Basin, at least for Stone Mountain materials.

Thus the Descartes Highlands as well as the deeper plains units may consist of ejecta from Nectaris and/or Imbrium, covered by ballistic ejecta from Orientale. According to this interpretation, the term

Cayley Formation at this site should be restricted to the uppermost (sub-regolith) plains unit, defined by physical properties and carter density; it is possibly derived in part from the Orientale Basin.

Kaula, W. M., Schubert, G., Lingenfelter, R. E., Sjogren, W. L., and Wollenhaupt, W. R.: 'Lunar Topography from Apollo 15 and 16 Laser Altimetry', *Proceedings of the Fourth Lunar Science Conference, Geochim. Cosmochim. Acta* 3, Suppl. 4, 2811-2819.

In the orbital plane of Apollo 15 the mean lunar radius is 1737.3 km, the mean altitude of terrae above maria is about 3 km, and the center-of-figure is displaced from the center-of-mass by about 2 km away from longitude 25° E.

The Apollo 16 laser altimeter obtained a total of about  $7\frac{1}{2}$  revolutions of partially overlapping data. The principal difference in results from Apollo 16 is the absence of any great farside basin similar to the 1400-km wide feature found by Apollo 15, 1200 km to the south. This absence of a farside depression in the Apollo 16 orbital plane largely accounts for a greater mean radius: 1738.1 km; a greater mean altitude of terrae above maria: about 4 km; and a greater offset of centers: about 3 km, also away from 25° E.

In the Apollo 16, as well as Apollo 15, data the farside terrae are much 'rougher' than the nearside terrae. Mare surfaces are generally smooth to within  $\pm 150$  m, and have slopes of 1:500 to 1:2000 persisting over distances as great as 500 km.

Mattingly, T. K. and El-Baz, F.: 'Orbital Observations of the Lunar Highlands on Apollo 16 and their Interpretation', *Proceedings of the Fourth Lunar Science Conference, Geochim. Cosmochim. Acta* 1, Suppl. 4, 49-56.

From orbital altitudes, the lunar highlands display the same surface characteristics on both the far and near sides. Rugged terra and plains forming materials all appear as if dusted with a uniform mantle. No stratigraphy or evidence of layering are seen in highland craters, with the possible exception of South Ray Crater in the Descartes landing site area.

Among the discussed small scale features of the lunar highlands are: fine lineaments, that appear to be real rather than artifacts of lighting, on both horizontal and inclined surfaces; ridge-like scarps that cut across highland topography; and benches that are believed to be high lava marks rather than talus accumulates.

Phillips, R. J., Adams, G. F., Brown, W. E., Eggleton, R. E., Jackson, P., Jordan, R., Peeples, W. J., Porcello, L. J., Ryu, J., Schaber, G., Sill, W. R., Thompson, T. W., Ward, S. H., and Zelenka, J. S.: 'The Apollo 17 Lunar Sounder', *Proceedings of the Fourth Lunar Science Conference, Geochim. Cosmochim. Acta* 3, Suppl. 4, 2821-2831.

The Apollo Lunar Sounder Experiment, a coherent radar operated from lunar orbit during the Apollo 17 mission, has scientific objectives of mapping lunar subsurface structure, surface profiling, surface imaging, and galactic noise measurement. Representative results from each of the four disciplines are presented. Subsurface reflections have been interpreted in both optically and digitally processed data. Images and profiles yield detailed selenomorphological information. The preliminary galactic noise results are consistent with earlier measurements by other workers.

Schultz, P. H.: 'A Preliminary Morphologic Study of the Lunar Surface', Ph.D. Thesis, Texas Univ., Austin, University Microfilms, Order No. 73-7640.

Lunar Orbiter photographs reveal a wide variety of surface features that are classified, illustrated, and interpreted. The shapes in plan of lunar craters describe typical geometries and indicate a variety of processes that influence craters in different size ranges. Floor, wall, and rim features reflect different origins and modifications, and these features are arranged and discussed separately in selected size ranges for crater diameters from approximately 0.1 km to greater than 100 km. A reference for comparisons between the lunar surface and other planetary bodies is also included.



## 10. Origin and Stratigraphy of Lunar Formations

Arkani-Hamed, J.: 'On the Formation of the Lunar Mascons', *Proceedings of the Fourth Lunar Science Conference, Geochim. Cosmochim. Acta* 3, Suppl. 4, 26–2684.

A new mascon hypothesis is proposed which accounts for: (1) the existence of lunar mascons for more than 3 b.y., (2) the evidence for extensive volcanic activity from 3.7 to 3.2 b.y. ago, (3) the existence of negative gravity anomaly rings, (4) insufficient mare material in Mare Orientale, and (5) the lack of mascons associated with craters smaller than 200 km diam. Moreover, it provides a simple mechanism for mass transfer into the basins. The hypothesis is based on the perturbations introduced into a spherically symmetric thermal evolution model of the Moon by a giant impact.

Bryan, W. B.: 'Wrinkle-Ridges as Deformed Surface Crust on Ponded Mare Lava', *Proceedings of the Fourth Lunar Science Conference, Geochim. Cosmochim. Acta* 1, Suppl. 4, 93–106.

Wrinkle-ridges in Mare Imbrium developed as low swells concurrently with the inpouring of the most recent lava flows, as shown by ponding and deflection of the flows. Deformation completed after consolidation of the lava deformed the flows by sharp wrinkling along the crest of the swells. Monoclinical down-faulting of the mare basin is also indicated. An early, dark mare fill is downwarped toward the center of Mare Serenitatis, and tensional deformation associated with the downwarp extends into adjacent highlands. Later compressional deformation produced a wrinkle ridge along the east margin of Serenitatis which locally is thrust over highland material. A younger light-colored central fill shows both radial and concentric compressional patterns of wrinkle ridges: wrinkle-ridge morphology is controlled in part by pre-existing joint blocks. This pattern, or an alternate pattern of en-echelon concentric ridges, can be explained by isostatic subsidence of the spherical surface shell represented by mare lava fill. This collapse could take the form of central sagging (model 1) or uniform surface collapse along vertical marginal ring faults (model 2). Model 2 collapse is shown to be the most effective source of crustal shortening.

El-Baz, F. and Evans, R. E.: 'Observations of Mare Serenitatis from Lunar Orbit and their Interpretation', *Proceedings of the Fourth Lunar Science Conference, Geochim. Cosmochim. Acta* 1, Suppl. 4, 139–147.

Visual observations of color differences of Serenitatis mare materials from orbit complement photography and other remotely sensed data. The light tan gray inner fill of the Serenitatis Basin is younger than the dark blue gray annulus; the latter continues into and appears to be contemporaneous with the fill of Mare Tranquillitatis. Mare ridges occur in both the inner basin fill and the dark annulus of Serenitatis. Ridges are interpreted as the result of structural deformation and up-doming after the solidification of the basaltic lavas.

On the southeastern rim of the Serenitatis Basin is the darkest blue gray unit within which Apollo 17 landed. Highland massifs surrounding this unit have unstable slopes which are believed to be the result of localized tectonic activity. On the southwest rim of the basin are the dark tan to brown gray mantling materials of the Sulpicius Gallus Formation. Farther west on the rim are dark blue gray patches which resemble the mare material of the Serenitatis dark annulus.

Hédervári, P.: 'Energetics of the Development of Lunar Calderas', *Z. Geophys.* 39, 1007–1021.

It is well-known that surprising and convincing morphological similarity exists between the terrestrial calderas of collapse-origin and many of the lunar ring-mount structures, which suggests that the origin of these features of the Earth and of the Moon might have been the same or at least very similar.

On the base of this morphological likeness the author supposes that many of the ring-like structures on the Moon – especially among the larger features – really can be regarded as calderas of collapse-origin, of gigantic dimensions. However – naturally – there may be crater-like features of impact origin on the Moon as well.

Supposing that some or many lunar ring-structures may have their origin by a collapse-process – similar to the case of certain terrestrial volcanic features, such as Krakatau of Indonesia, Mount Mazama of Oregon, Santorini of Greece, Fernandina of Galápagos-islands, and many others in Japan, in Kamchatka and elsewhere –, the author made some calculations regarding the energetics of the development of the respective ‘lunar calderas’. Thermal, collapse and potential energies were calculated for the case of models of different dimensions and on the basis of certain plausible suppositions.

Houston, W. N., Moriwaki, Y., and Chang, C.-S.: ‘Downslope Movement of Lunar Soil and Rock Caused by Meteoroid Impact’, *Proceedings of the Fourth Lunar Science Conference, Geochim. Cosmochim. Acta* 3, Suppl. 4, 2425–2435.

The relative importance of downslope movement of lunar soil and rock caused by meteoroid-impact-induced vibrations as a mode of lunar soil ‘erosion’ has been assessed. Magnitudes of downslope movements were estimated by superimposing meteoroid-impact-induced dynamic stresses on existing static stresses in slopes of various inclinations. Accelerations in excess of the yield accelerations were double-integrated to obtain an estimate of the movements. It was found that only the very steep lunar slopes have experienced significant downslope movements due to shaking from meteoroid impacts alone and that lunar slope degradation must arise primarily by other mechanisms.

McGetchin, T. R., Settle, M., and Head, J. W.: ‘Radial Thickness Variation in Impact Crater Ejecta: Implications for Lunar Basin Deposits’, *Earth Planetary Sci. Letters* 20, 226–236.

A review of cratering data and available semi-empirical calculations suggests that the variation of ejecta thickness,  $t$ , with increasing range from lunar craters may be approximately modelled by the expression

$$t = 0.14 R^{0.74} (r/R)^{-3.0}$$

where  $r$  is range from the center of the crater and  $R$ , the crater radius, all in meters. This equation has been used to estimate the thickness of ejecta deposits at each of the Apollo sites contributed from the large multi-ringed frontside lunar basins. Predicted average thickness of Imbrium ejecta at Apollo 15 is 812 m; at Apollo 14, 130 m; at Apollo 17, 102 m; and at Apollo 16, 50 m. Since the sequence of formation of these basins is known, the stratigraphic column resulting from superimposed ejecta blankets can be calculated. Results suggest that pre-Nubium crustal material at upland Apollo sites lies at depths greater than 280 (Apollo 14) to 1940 m (Apollo 17). Predicted stratigraphic sections for the Apollo sites are tabulated.

McKay, D. S. and Heiken, G.: ‘The South Ray Crater Age Paradox’, *Proceedings of the Fourth Lunar Science Conference, Geochim. Cosmochim. Acta* 1, Suppl. 4, 41–47.

Relative exposure ages based on agglutinate content are calculated for 26 Apollo 16 surface and core samples. These ages increase from the northern part of the traverse to the southern part and are in general agreement with cosmogenic gas ages and particle track ages. An apparent paradox exists in which presumed ray soil from South Ray Crater is much older than the age of South Ray Crater itself as determined by a variety of methods. The most likely explanation for the paradox is that the presumed South Ray Crater soil is not ejecta from South Ray Crater but is pre-existing regolith upon which blocks and fragments from South Ray Crater are scattered.

Oberbeck, V. R., Hörz, F., Morrison, R. H., and Quaide, W. L.: ‘Emplacement of the Cayley Formation’, NASA-TM-X-62302.

Analysis of the effects of ejection of materials from large lunar craters, photogeologic evidence, remote measurements of surface chemistry and petrology of lunar samples are synthesized. Previous

theories for emplacement of the Cayley are volcanic ash emplacement and emplacement as ejecta from multiringed basins. Calculations show that materials ejected beyond the continuous deposits of large lunar craters produce secondary impact craters that excavate and deposit masses of local material equal to multiples of the crater ejecta deposited at the same place. It is shown that the main influence of a large cratering event on terrain at distances greater than 50 km from large lunar craters is one of cratering and deposition of local material by secondary craters rather than deposition of ejecta from the large crater.

Oberbeck, V. R. and Morrison, R. H.: 'On the Formation of the Lunar Herringbone Pattern', *Proceedings of the Fourth Lunar Science Conference, Geochim. Cosmochim. Acta* **1**, Suppl. 4, 107-123.

The V-shaped ridge components of the lunar herringbone pattern are simulated by simultaneous and nearly simultaneous impact cratering in the laboratory. The results of the simulations, together with a mathematical model developed for the case of simultaneous impacts, indicate that the pattern resulted from simultaneous impact formation of adjacent secondary craters. In addition, preliminary experimental results suggest that many secondaries of the crater Copernicus were produced by fragments that impacted either simultaneously or nearly simultaneously with the uprange fragments impacting first, at angles greater than  $60^\circ$  measured from the normal to the surface.

Orowan, E.: 'Origin of the Surface Features of the Moon', *Proc. Roy. Soc. London A.* **336**, 141-163.

The current theories of the Moon are variants of Galileo's hypothesis, according to which the smooth dark areas were oceans, since 1610 only the fluid of the oceans has been changed, from water to (subsequently solidified) lava. Recent high-resolution photographs, however, are incompatible with the Galilean hypothesis and its modern versions: the smooth dark surfaces, including the floors of the large dark craters, seem to be denuded areas on the once-molten lunar body, from which the 'lunar soil' has been blown away by explosions of comets. The lunar soil seems to be the impact-crushed ancient crust of the Moon, mixed with the debris of meteorites and comets; it is the material of the rugged highlands. The exposed areas of the lunar body are partly glazed with thin coats of lava, and covered with dust darkened at the surface.

The multitudes of small craters are meteorite indentations; the large craters, however, have been created by the explosion of comets, as suggested by Kopal. If the impact is weak, the explosion sweeps the soil, or, in bare marial areas, the comet-debris, to a circular or crescent-shaped wall; a more violent impact also indents the brittle lunar body in a manner than can be reproduced in many details by a steel-ball indentation of a block of glass. A simple calculation combining the Hertz theory of elastic contact with the Griffith biaxial theory of fracture explains the flatness of the crater floor, and the terraced wall; the polygonal shape of the indentation craters and the tangential rays around them are inertia effects due to the near-sonic velocity of crack propagation.

Indentation leaves behind residual stresses which are partially relieved in moonquakes. The delay of the stress release may be analogous to the delayed fracture of glass caused by the reduction of the surface energy by adsorption or chemisorption. The surface-active agents are probably water and other volatiles injected by the comets into the indentation cracks; streams of such volatiles seem to have excavated the sinuous rilles.

The usual calculations of high-velocity impact cannot be applied to the Moon because they are based on an approximation for calculations of armour-plate penetration: under hypervelocity impact, steel can be regarded as a heavy non-viscous liquid because its yield stress is roughly pressure-independent and relatively negligible. The debris of a brittle body, however, obeys Coulomb's law of soil mechanics: its shear strength is approximately proportional to the pressure, instead of being independent of it.

Schaber, G. G.: 'Lava Flows in Mare Imbrium: Geologic Evaluation from Apollo Orbital Photography', *Proceedings of the Fourth Lunar Science Conference, Geochim. Cosmochim. Acta* **1**, Suppl. 4, 73-92.

A study of Apollo photographs indicates that all Eratosthenian age mare deposits in the Imbrium basin consist of extensive lava flows from a single eruptive source region bounded by 18°N–23°N and 28°W–32°W in the south-southwest corner of the basin. It is suggested that three major eruptive periods occurred between  $3.0 \pm 0.4$  b.y. and  $2.5 \pm 0.3$  b.y. Lavas assigned to these three phases extended for 1200, 600 and 400 km, respectively over slopes approaching 1:1000. These materials cover an area of  $2 \times 10^5$  km<sup>2</sup> and have a volume of perhaps  $4 \times 10^4$  km<sup>3</sup>.

The vent source of the youngest lava phase appears to be a 20 km long, structurally controlled fissure at 22°50'N and 31°20'W. The flow heights and lengths are consistent with the lunar gravity and imply extremely high rates of lava extrusion with low viscosity of the basalt melt playing a secondary role. The location of the volcanic source region on the intersection of major ring faults from two large basins suggests a basin structural control.

Schonfeld, E. and Meyer, C.: 'The Old Imbrium Hypothesis', *Proceedings of the Fourth Lunar Science Conference, Geochim. Cosmochim. Acta* **1**, Suppl. 4, 125–138.

We propose that the order of lunar events was such that the Imbrium event predates the formation of the lunar rock type called KREEP. This hypothesis is used to explain the distribution of KREEP in the regions of Imbrium ejecta and the location of KREEP within the Imbrium and Procellarum mare regions. Model ages of KREEP materials have been previously interpreted to mean that their 'formation' age (time of initial extrusion) is about 4.3–4.4 AE. Consequently we suggest that the Imbrium impact was before 4.3–4.4 AE rather than at  $\sim 3.9$  AE as is currently believed. This Old Imbrium Hypothesis is not yet proven but seems to be consistent with a large variety of basic lunar observations.

Taylor, G. J., Drake, M. J., Hallam, M. E., Marvin, U. B., and Wood, J. A.: 'Apollo 16 Stratigraphy: The ANT Hills, the Cayley Plains, and a Pre-Imbrium Regolith', *Proceedings of the Fourth Lunar Science Conference, Geochim. Cosmochim. Acta* **1**, Suppl. 4, 553–568.

We have classified 645 particles in the 1–2 mm size range from five Apollo 16 soil samples. There are five major categories of lithic fragments: anorthositic/noritic/troctolitic (ANT) monomict breccias, light-matrix breccias, poikiloblastic noritic/anorthositic fragments, spinel-troctolites, and feldspathic basalts. ANT breccias are texturally and compositionally similar to those in other samples; pyroxene compositional trends suggest they formed by fractional crystallization. Light-matrix breccias have the oldest ages yet reported for lunar rocks (4.1–4.25 b.y.). They are plagioclase-rich, polymict fragments that contain clasts of mafic silicates, plagioclase, and ANT rock fragments set in a very fine-grained, slightly annealed matrix. They are interpreted as ancient soil breccias. Many pyroxene clasts in light-matrix breccias are compositionally similar to those in ANT rocks. However, a significant number have compositions that are characteristic of lunar extrusive rocks, i.e., subcalcic augites and ferroaugites. Most poikiloblastic fragments and feldspathic basalts contain small quantities of phosphate phases and K-rich interstitial glass, which implies that they are enriched (relative to ANT rocks) in large-ion lithophile elements. Spinel-troctolites consist of euhedral (Mg, Al)-rich spinels set in a fine-grained, usually quenched groundmass of olivine, plagioclase, and mesostasis. The presence of angular clasts of olivine and plagioclase, as well as recognizable rock fragments, suggests that spinel-troctolites are impact-melts of a pre-existing rock or regolith.

Light-matrix breccias are very abundant (41% of the lithic fragments) in the soils from the rim of North Ray Crater, and moderately abundant in two other soils associated with craters. It appears that the Apollo 16 site is underlain by a layer of this type of material. The soil at Station 6 on the slope of Stone Mountain contains the highest proportion of ANT fragments (46%), but a low percentage of poikiloblastic fragments (26%). This implies that the Descartes Mountains are predominantly composed of ANT rock. In contrast, the soil at Station 10 (on the Cayley Plains) is the richest in poikiloblastic fragments (43%) and the most impoverished in ANT particles (26%), perhaps indicating that the Cayley Formation is constituted mainly of poikiloblastic rock. Statistics are not adequate to uniquely assign spinel-troctolites or feldspathic basalts to a single unit. The stratigraphic sequence at the Apollo 16 site appears to be ANT bedrock, overlain by a pre-Imbrian regolith (light-matrix breccias), which in turn is overlain by the Descartes Mountains (ANT breccias). The Cayley Plains material may be predominantly poikiloblastic rocks, which fill in the low areas between the mountains.

Trask, N. J.: 'The Contributions of Ranger Photographs to Understanding the Geology of the Moon', NASA-CR-133090.

Vidicon photographs returned to Earth by Rangers 7, 8, and 9 in 1964 and 1965 were used to study the details of lunar geologic units previously recognized from Earth-based telescopic photographs and to make geologic maps at a variety of scales. The photographs from each mission changed continuously in scale as the spacecraft approached impact. The final frames had resolutions some 1000 times better than the best Earth-based photographs. Lunar stratigraphic units mapped at a scale of 1:1000000 displayed, at these larger scales, differences in properties and, possibly, in ages, but a clear-cut stratigraphic succession of subunits was not apparent. The plains-forming materials in both terra and mare were divisible into units mainly on the basis of the differences in the total number of superposed craters and in the relative number of craters of various morphologic types.

Turner, R.: 'A Model of the Eastern Portion of Schröter's Valley', Univer. of Arizona, *Lunar Planetary Lab.* 10, 81-93.

A relief model of the eastern portion of Schröter's Valley has been completed using Lunar Orbiter, Apollo 15, and Earth-based photography. The main results derived from this study are as follows: (1) the head of the Valley (the 'Cobra head') is not a simple crater, but rather a slightly-widened section of the Valley emanating from a shield, (2) the east side of the 'Cobra head' is a very high peak (2.3 km above the surrounding plains) forming part of a broad shield with an average slope of 12°, and (3) both sides of the Valley display a raised rim in the region measured. These and other observations indicate the Valley was formed by fluid processes, probably lava, and that *the Valley may therefore be a lava drainage channel*, the drained lava presumably underlying the more recent Oceanus Procellarum basalts.

Ulrich, G. E.: 'A Geologic Model for North Ray Crater and Stratigraphic Implications for the Descartes Region', *Proceedings of the Fourth Lunar Science Conference, Geochim. Cosmochim. Acta* 1, Suppl. 4, 27-39.

The topographic setting and the areal distribution of rock types on the rim of North Ray Crater reflect a stratigraphic sequence that can be extrapolated to the rest of the Descartes region. The crater itself is on a low ridge which appears to be a down-faulted block of Smoky Mountain and thus the best sampling locality for materials of the Descartes Highlands. The rounded form of the rim and wall and general lack of blocks in the ejecta reflect the low coherence of most of the target material of this relatively young crater. The rock types collected include friable light-matrix breccias from the upper half of the crater, coherent glass-rich dark-matrix breccias from the lower part of the crater and locally in the upper 50 m, and a few rocks with metaclastic and igneous textures occurring as inclusions within the dark-matrix breccia. The sequence of geologic events interpreted is as follows: (1) Pre-Imbrian terrane underlies the entire site but was not penetrated by the youngest local craters. (2) More than 250 m of crudely stratified feldspathic material was emplaced from a major basin (Imbrium?). These materials segregated into 'dry' light-matrix breccias on top, dark melt-rich breccias below, and locally molten masses that crystallized to igneous textures at depth. Down-faulting of North Ray ridge may have occurred at this time. (3) Subsequently, the upper 50 m of light and dark breccias may have been emplaced as ejecta from a younger basin, possibly Orientale, over much of the site. (4) The relatively recent excavation of this sequence was accomplished by the impact event that created North Ray Crater.

Young, R. A., Brennan, W. J., Wolfe, R. W., and Nichols, D. J.: 'Analysis of Lunar Mare Geology from Apollo Photography', *Proceedings of the Fourth Lunar Science Conference, Geochim. Cosmochim. Acta* 1, Suppl. 4, 57-71.

Apollo orbital photography has provided new information regarding the relationships between, and possible modes of origin of, mare surface features. Development of some mare surface features

occurred simultaneously with widespread mare flooding, but small scale volcanism and tectonism in many cases postdated the latest widespread mare flooding. Many mare ridges had complex origins and developed progressively through time. Processes involved include reactivation of submare fractures, flexuring, faulting, plutonism, and volcanism. Faulting is seldom obvious, but is revealed by elevation differences of adjacent mare surfaces and colinearity of landforms. Volcanism associated with ridge development has tended to obscure features formed earlier in ridge history. This local volcanism is indicated by volcanic cones, presumed endogenic rimless craters, monor flow fronts, and 'squeeze ups', many of which lie along ridge crests or flanks. Lunar rilles have diverse origins: volcanic rilles (lava tubes and lava channels) should be distinguished from tectonic rilles (extension fractures and graben faulting). Convergence of flow lines in lava beneath a hardened crust may develop lava tubes of sinuous form, and collapse of tube roofs under post-mare impact flux may account for sinuous rilles. Ridge and rille development in some cases is related, but ridges and rilles may form sequentially as well as simultaneously.

## 11. Physical Structure of the Lunar Surface

Ahrens, T. J., O'Keefe, J., and Gibbons, R. V.: 'Shock Compression of a Recrystallized Anorthositic Rock from Apollo 15', *Proceedings of the Fourth Lunar Science Conference, Geochim. Cosmochim. Acta* 3, Suppl. 4, 2575-2590.

Hugoniot measurements on 15418, a recrystallized and brecciated gabbroic anorthosite, yield a value of the Hugoniot elastic limit (HEL) varying from  $\sim 45$  to 70 kbar as the final shock pressure is varied from 70 to 280 kbar. Above the HEL and to 150 kbar the pressure-density Hugoniot is closely described by a hydrostatic equation of state constructed from ultrasonic data for single-crystal plagioclase and pyroxene. Above  $\sim 150$  kbar, the Hugoniot states indicate that a series of one or more shock-induced phase changes are occurring in the plagioclase and pyroxene. From Hugoniot data for both the single-crystal minerals and the Frederick diabase, we infer that the shock-induced high-pressure phases in 15418 probably consist of a  $3.71 \text{ g cm}^{-3}$  density, high-pressure structure for plagioclase ( $\text{An}_{93}$ ) and a  $4.70 \text{ g cm}^{-3}$  perovskite-type structure ( $\text{En}_{64}$ ) for pyroxene. Using the Kelly-Truesdell mixture theory we separately calculated the entropy production in each phase, and predict incipient and complete melting in the plagioclase occurs upon release from  $\sim 500$  and  $\sim 600$  kbar. For the pyroxene component, incipient and complete melting occurs upon release from 700 and 850 kbar. The onset of shock-induced vaporization will occur upon release from  $\sim 1300$  kbar and would require the impact of an iron meteoroid traveling at a velocity of  $\sim 8 \text{ km s}^{-1}$ .

Bhandari, N., Goswami, J., and Lal, D.: 'Cosmic Ray Irradiation Patterns of Luna 16 and 20 Soils: Implications to Lunar Surface Dynamic Processes', *Earth Planetary Sci. Letters* 20, 372-380.

Comprehensive fossil track data in mineral grains from several horizons of Luna 16 and 20 cores are presented. The cosmic ray irradiation of Luna 16 soil is distinctly different from Luna 20 soil, the former being more intensely irradiated. Track data for Luna 16/20 samples are compared with those for samples collected from different lunar mare and highland sites. Luna 20 track density distribution patterns are similar to those observed at other lunar sites. However, Luna 16 data are at variance and necessitate a complex irradiation history. Various suggestions made so far for explaining the high irradiation dose of Luna 16 samples appear inadequate. The possibility that the regolith growth at the Luna 16 site is governed by a different mechanism, to some extent controlled by the local topography, is discussed.

Bhandari, N., Goswami, J., and Lal, D.: 'Surface Irradiation and Evolution of the Lunar Regolith', *Proceedings of the Fourth Lunar Science Conference, Geochim. Cosmochim. Acta* 3, Suppl. 4, 2275-2290.

Fossil tracks have been analyzed in Apollo 14, 15, and 16 samples. Principal results of the analyses are summarized below:

(i) Surface exposure ages of lunar rocks, designated as *suntan* ages are generally smaller than 3 m.y. indicating that rocks fragment and fresh surfaces are exposed at rates of the order of 0.3 mm/m.y. Differences in exposure age distribution for Apollo sites 11, 12, 14, 15, and 16 appear significant and probably reflect differences in the survival characteristics of different rocks.

(ii) Most surface rocks (80%) have had a complex fossil track irradiation history so that the exposure geometry and shielding varied in the past 10–100 m.y. Not more than twenty percent of the rocks exhibit a simple one stage exposure history corresponding to accumulation of most of the fossil tracks in a single geometry.

(iii) Fossil track data on Apollo 15, 16 surface samples and the 2.5 m drill stem of Apollo 15 core support our earlier model that generally the lunar regolith is made up of discrete layers of soil ejected in different cratering events. Typical surface irradiation ages of these layers range from 1–50 m.y. The throw-away layers keep their identity except to the extent of mixing up to depths of a few cm/(10–50) m.y. due to micrometeorite impacts. This short range mixing occurs till a layer is buried by blanketing from a fresh layer.

(iv) The formation ages of some major craters at Apollo 15 and 16 sites have been estimated on the basis of the irradiation ages of the ejecta.

Brownlee, D. E., Hörz, F., Vedder, J. F., Gault, D. E., and Hartung, J. B.: 'Some Physical Parameters of Micrometeoroids', *Proceedings of the Fourth Lunar Science Conference, Geochim. Cosmochim. Acta* 3, Suppl. 4, 3197–3212.

Detailed morphological parameters (depth/diameter ratio, circularity index) of microcraters in the 0.2–100  $\mu\text{m}$  diam range were obtained via SEM techniques for three lunar glass surfaces. The depth/diameter ratios are typically 0.5–0.8 with a range of 0.3–1.3. The circularity index varies from 0.4–1.0 with a pronounced maximum at 0.7–0.9. These parameters are compared with microcraters produced in the laboratory via electrostatic particle accelerators. The following conclusions are drawn:

The great majority of observed crater depths are compatible with micrometeoroid densities of 2–4  $\text{g cm}^{-3}$ ; crater depths are incompatible for projectile densities  $< 1 \text{ g cm}^{-3}$  and  $> 7 \text{ g cm}^{-3}$ . The circularity index of microcrater pits indicates rather equidimensional if not spherical projectiles. Needles, platelets and other highly irregular shapes can be excluded. Less than 5% of all craters observed may offer different conclusions. These results differ in part significantly from popular views about physical parameters of micrometeoroids.

Butler, J. C., Greene, G. M., and King, E. A.: 'Grain Size Frequency Distributions and Modal Analyses of Apollo 16 Fines', *Proceedings of the Fourth Lunar Science Conference, Geochim. Cosmochim. Acta* 1, Suppl. 4, 267–278.

Grain size frequency distributions of 19 lunar fines (less than 1 mm) samples from the Apollo 16 site are bimodal with modes in the 1–4 $\phi$  (500–62.5  $\mu\text{m}$ ) and greater than 5 $\phi$  (less than 31.25  $\mu\text{m}$ ) ranges. Differences in grain size frequency distribution parameters can be correlated with site geology. Samples collected at Stone Mountain (Stations 4, 5, and 6) appear to contain mixtures of South Ray Crater ejecta and older regolith. Modal analyses of the 74–53, 53–44 and 37–30  $\mu\text{m}$  fractions of eight of the samples revealed no appreciable differences among the Stone Mountain samples.

Carrier, W. D., Mitchell, J. K., and Mahmood, A.: 'The Relative Density of Lunar Soil', *Proceedings of the Fourth Lunar Science Conference, Geochim. Cosmochim. Acta* 3, Suppl. 4, 2403–2411.

The specific gravity and minimum and maximum bulk densities were determined for three one-gram lunar soil samples containing particles less than 1 mm in diameter: 14163,148, 14259,3 and 15601,82. The specific gravity varied from 2.90 to 2.93 for the Apollo 14 samples to 3.24 for the Apollo 15 sample. The difference is attributed to the higher proportion of agglutinates and breccias and fewer mineral fragments and basalts in the Apollo 14 soils. The minimum bulk densities varied from 0.87 to 1.10  $\text{g cm}^{-3}$ ; and the maximum densities varied from 1.51 to 1.89  $\text{g cm}^{-3}$ . The ranges in values were

due to differences in the specific gravity, re-entrant intra-granular voids, particle shape, surface texture and grain arrangements. The *in situ* lunar soil in the plains areas of the Moon can have a low to medium relative density at the surface, increasing rapidly to a very high relative density at depths greater than 10 to 20 cm. The sub-surface soil may be overconsolidated and the variation of relative density with depth may be a strong indicator of the deposition age.

Carter, J. L.: 'Morphology and Chemistry of Probable VLS (Vapor-Liquid-Solid)-Type of Whisker Structures and Other Features on the Surface of Breccia 15015,36', *Proceedings of the Fourth Lunar Science Conference, Geochim. Cosmochim. Acta* **1**, Suppl. 4, 413-421.

A 62 mm<sup>2</sup> siliceous glass-covered surface of a fragment of breccia 15015 (15015,36) was studied in detail by scanning electron microscope, scanning electron microprobe and energy dispersive techniques. Four types of features were observed: (1) low velocity, hot target-type impacts, (2) out-gassing structures, (3) several types of metallic iron mounds, primarily with a waist of iron sulfide and (4) whisker structures. It is concluded that (1) an irregularly-shaped breccia surface was partially coated with siliceous melt to various depths in an impact-generated hot debris cloud, (2) the siliceous melt coating the breccia was out-gassing while solidifying, (3) there were at least four nucleation events resulting in mounds with average diameters of approximately 45, 19, 10 and 0.2  $\mu\text{m}$ , (4) the whisker structures are of probable VLS (Vapor-Liquid-Solid)-type growth, (5) the sulfur was supplied from an external source such as an impact-generated cloud, (6) the iron was supplied both from an impact-generated cloud and by *in situ* reduction of the liquid siliceous surface, (7) the lack of hypervelocity-type craters suggests that the siliceous glass coated surface was exposed when cold for only a very short time to either micrometeoritic bombardment or to high velocity projectiles in an impact-generated debris cloud, and (8) sample 15015,36 is, thus, from the shielded (probably buried) portion of the rock.

The proposed VLS-type growth on the surface of breccia 15015,36 is the first recognized in nature. It occurs as probable metallic iron stalks with bulbous tips of a mixture of iron and sulfur. The stalks vary from less than 0.015  $\mu\text{m}$  to 0.15  $\mu\text{m}$  in diameter with a length 2 to 10 times bulb diameter. The bulbs vary from less than 0.03  $\mu\text{m}$  to 0.2  $\mu\text{m}$  in diameter. VLS produced metallic iron needles may be the source of some of the hard magnetic component in low-grade breccia. Since probable VLS-type of whisker growth has occurred in an impact situation on the lunar surface, it may have been an important growth mechanism in the early accretionary history of the Earth especially before it acquired an appreciable oxidizing atmosphere.

Carter, J. L. and Padovani, E.: 'Genetic Implications of Some Unusual Particles in Apollo 16 Less than 1 mm Fines 68841,11 and 69941,13', *Proceedings of the Fourth Lunar Science Conference, Geochim. Cosmochim. Acta* **1**, Suppl. 4, 323-332.

The less than 1 mm fines 68841,11 (light-colored ray ejecta) and 69941,13 (dark-colored ray ejecta) from South Ray Crater contain unusual types of metallic particles and silicate spheres with textured surfaces. The metallic particles consist of two types: rounded forms and irregularly-shaped forms. The rounded forms have euhedral crystals of schreibersite (18.6 wt. % Ni) intergrown with metallic iron (4.1 wt. % Ni, 0.8 wt. % Co), FeS and chemically defined bornite ( $\text{Cu}_5\text{FeS}_4$ ). The irregularly-shaped forms have low contents of schreibersite, are intergrown with plagioclase laths and olivine and have well-developed crystals of hydrated iron oxide probably lepidocrocite on their surfaces. It is suggested that this material formed in a hot impact ejecta blanket or in an igneous environment and later was exposed by meteoritic impact.

The silicate spheres have a porous surface consisting of a network of plagioclase laths that formed during quenching of melts of essentially highland basalt composition. Most sphere surfaces are free of angular debris but have attached spherules and hemispheres of the same composition and texture as the host sphere. The original melt could be either impact-produced or volcanic in origin. The volcanic hypothesis is favored because of (1) the apparent relative homogeneity of the original silicate melt, (2) the similar composition of the spheres and the attached spherules and hemispheres, (3) the general lack of surface debris, (4) the apparent lack of shocked debris and (5) the apparent lack of metallic iron of meteoritic composition within the spheres.



Christie, J. M., Griggs, D. T., Heuer, A. H., Nord, G. L., Radcliffe, S. V., Lally, J. S., and Fisher, R. M.: 'Electron Petrography of Apollo 14 and 15 Breccias and Shock-Produced Analogs', *Proceedings of the Fourth Lunar Science Conference, Geochim. Cosmochim. Acta* 1, Suppl. 4, 365–382.

Six lunar breccias were studied in detail by optical and transmission electron microscopy and separated into two classes on the basis of presence or absence of recovery and recrystallization textures: Class A breccias with no recrystallization include samples 14063, 14301, and 15498; Class B breccias with recrystallization include samples 14321, 15455, and 15418. Samples of Apollo 16 soil (65010) experimentally shocked to 50, 100, and 250 kbar pressure were sectioned and studied for comparison with the breccias. It is concluded that the Class A breccias were formed from unconsolidated lunar regolith by deformation due to shock waves of a few tens of kilobars. The Class B breccias could also have been produced from unconsolidated material at higher shock stresses, the annealing being achieved by the heating resulting from the shock deformation. Our observations are consistent with magnetic studies, which indicate that (a) the iron in the Class A breccias is fine grained and that in the Class B rocks is coarse-grained and (b) there is an increase in the fine-grained iron particles (associated with shock vitrification of pyroxene) in the 250 kbar experimental sample.

Chung, D. H.: 'Elastic Wave Velocities in Anorthosite and Anorthositic Gabbros from Apollo 15 and 16 Landing Sites', *Proceedings of the Fourth Lunar Science Conference, Geochim. Cosmochim. Acta* 3, Suppl. 4, 2591–2600.

Laboratory measurements of ultrasonic velocities in lunar samples 15065, 15555, 15415, 60015, and 61016 as well as in synthetic materials corresponding to compositions of anorthositic gabbros are presented as a function of hydrostatic pressure to about 7 kbar. Combining these laboratory data with the observed variations of the seismic velocities with depth in the eastern part of Oceanus Procellarum as reported by Toksöz *et al.*, the author examined the seismic velocity distributions in the Moon with reference to the variations to be expected in a homogeneous medium. The lunar mantle begins about 60 km and the velocity of  $P$  waves in this area is about  $7.7 \text{ km s}^{-1}$ , however, one velocity model suggests a thin layer of  $V_P \sim 9 \text{ km s}^{-1}$  immediately below the crust, which is attributed to a laterally placed garnet layer. Variation of the seismic parameter with depth in the upper crust (about 20 km thick) is much too rapid to be explained by compression of a uniform material and the departure from expectation is so great that no reasonable adjustment of the material parameters can bring agreement; therefore, this author concludes that this result in this region of the Moon is not due to self-compression but to textural gradients. In the lower crust (about 40 km thick), the region is shown to be relatively homogeneous, consisting probably of anorthositic rocks, consistent with interpretation by Toksöz *et al.* Below the 60 km depth, lunar mantle models consisting of predominantly pyroxene with some olivine in an anorthositic matrix are favored with our laboratory measurements. The composition of such combinations would meet the known geophysical constraints imposed by the mean density and moment of inertia as well as the *in situ* seismic velocity distributions. And further, such a composition of lunar mantle is essentially in agreement with geochemical and petrological analyses of Ringwood *et al.* and Green *et al.* as the source of lunar basalts.

Cremers, C. J. and Hsia, H. S.: 'Thermal Conductivity and Diffusivity of Apollo 15 Fines at Low Density', *Proceedings of the Fourth Lunar Science Conference, Geochim. Cosmochim. Acta* 3, Suppl. 4, 2459–2464.

The thermal conductivity of the Apollo 15 fines, sample 15031,38, was measured under vacuum conditions as a function of temperature. Measurements were made for a sample density of  $1300 \text{ kg m}^{-3}$ . The conductivity was found to vary from about  $0.57 \times 10^{-3} \text{ Wm}^{-1} \text{ K}^{-1}$  at 95 K to about  $1.36 \times 10^{-3} \text{ Wm}^{-1} \text{ K}^{-1}$  at 406 K. The data are compared with the correlation using a cubic temperature dependence and also with data from samples gathered during prior Apollo missions. The thermal diffusivity is obtained for the sample by calculation using the given density and measured thermal conductivity along with specific heats from the literature.

Durrani, S. A., Khan, H. A., Malik, S. R., Aframian, A., Fremlin, J. H., and Tarney, J.: 'Charged-Particle Tracks in Apollo 16 Lunar Glasses and Analogous Materials', *Proceedings of the Fourth Lunar Science Conference, Geochim. Cosmochim. Acta* 3, Suppl. 4, 2291–2305.

The main thrust of the paper is to study the effects of temperature and radiation damage on the registration and retention of heavily-charged particle tracks in lunar glasses and analogous materials in an effort to interpret the temperature and radiation history of lunar samples. Fossil-fission and external-particle tracks have been differentiated by a series of annealing experiments. The etch-pit diameter is the primary parameter in these experiments as well as in those involving the registration of artificially accelerated heavy ions of varying residual energies. It is also shown that glass detectors intensely irradiated with  $\sim 3$  MeV protons (to fluences of up to  $\sim 1.4 \times 10^{17} \text{ cm}^{-2}$ ), either before or especially after exposure to heavy ions or fission fragments, are significantly less efficient in the registration of the latter highly-charged particles than are unirradiated detectors. The heavy-ion tracks yield much smaller etch pits if the detectors are subsequently irradiated with protons. These observations have an important bearing on the quantitative analysis of lunar track data. Also reported in the paper are useful track-etching parameters for lunar glasses; uranium-content values; and some age estimates.

Engelhardt, W. von, Arndt, J., and Schneider, H.: 'Apollo 15: Evolution of the Regolith and Origin of Glasses', *Proceedings of the Fourth Lunar Science Conference, Geochim. Cosmochim. Acta* 1, Suppl. 4, 239–249.

Modal compositions of 6 soil and 5 breccia samples from Apollo 15 have been determined and electron microprobe analyses have been made of 89 glass particles from breccias and soils.

The constituents of the Apollo 15 regolith and regolith breccias were derived from mare basalts and Apennine Front material. The regolith samples are different in maturity and content of mare and Apennine material. In a local soil or a particular breccia the proportion of both source materials depends on the effectiveness at the particular site of impact generated lateral transport and bedrock excavation.

The Apennine Front is considered to consist of a debris of plagioclase-rich and noritic rocks of the pre-Imbrian lunar crust, impact melt rocks and impact melt glasses from Imbrian and pre-Imbrian events.

A few of the analyzed glass particles (0.1–1 mm) are interpreted as diaplectic plagioclase glasses, the majority as quenched impact-melted rocks. Five distinct rock families are distinguished as source materials: Two feldspat-rich noritic types of low- and high-alkali contents, two pyroxene-rich mare types of low- and high-Ti-contents and a pyroxene-rich type of probably deep-seated origin (green glasses).

The cooling rates of two Apollo 11 and 15 glass particles have been deduced from heating experiments.

Finkelman, R. B.: 'Analysis of the Ultrafine Fraction of the Apollo 14 Regolith', *Proceedings of the Fourth Lunar Science Conference, Geochim. Cosmochim. Acta* 1, Suppl. 4, 179–189.

Analyses were obtained on more than 2400 randomly selected particles from the sub- $37 \mu\text{m}$  (ultrafine) fraction of ten Apollo 14 regolith samples. The analyses were conducted with an energy dispersive electron microprobe system. The semiquantitative data were used to group the particles into ten categories. The pyroxene/plagioclase and olivine/plagioclase ratios are inconsistent with those ratios in the Apollo 14 breccias and rocks. The data suggest that fragmented basalts similar to Apollo 12 olivine basalts may have made significant contributions to the ultrafine fraction of the Fra Mauro regolith. Among a number of unusual particles encountered are brown, birefringent lath-shaped grains with 60 weight percent  $\text{SiO}_2$  and 34 weight percent  $\text{FeO}$  ( $\text{FeSi}_2\text{O}_5$ ) and a glass with 20–25 weight percent  $\text{CaO}$ , 0–8 weight percent  $\text{MgO}$ , 40–45 weight percent  $\text{Al}_2\text{O}_3$  and approximately 30 weight percent  $\text{SiO}_2$ .

Fleischer, R. L. and Hart, H. R.: 'Investigations of Lunar Materials', (Final Report) NASA-CR-134023.

In the particle track work, a series of dating techniques for learning about the surface history of soil and rock samples was developed. The surface behavior and history of diverse lunar rocks and soils, erosion rates, and deposition rates were studied, along with incident heavy cosmic ray spectrum.

Garlick, G. F. J., Steigmann, G. A., Lamb, W. E., and Geake, J. E.: 'Fluidization of Lunar Dust Layers and Effect on Optical Polarization of the Diffuse Reflectance of Light', *Proceedings of the Fourth Lunar Science Conference, Geochim. Cosmochim. Acta* 3, Suppl. 4, 3175-3180.

Previous studies indicated a large change in the reflectance of lunar dust layers when fluidized so that intergrain cohesion disappeared. Changes have now been measured in the degree of polarization of the diffusely reflected light on fluidization of the dust layer. The typical curves of polarization vs phase angle are enhanced, except at small phase angles; the fractional changes often being greater than the corresponding increase in reflectance. The characteristics vary from sample to sample and show differences in dependence on the wavelength of the reflected light. In the Dollfus type plot of albedo vs polarization, fluidized dust layers give a distribution of points which are displaced from the distribution for static dust layers and lunar surface measurements. Changes in polarization due to surface disturbance may provide a sensitive method of detecting and observing incipient dust storms on the Martian surface.

Hartung, J. B., Hörz, F., Aitken, F. K., Gault, D. E., and Brownlee, D. E.: 'The Development of Microcrater Populations on Lunar Rocks', *Proceedings of the Fourth Lunar Science Conference, Geochim. Cosmochim. Acta* 3, Suppl. 4, 3213-3234.

A Monte Carlo model was developed to simulate microcrater population development on lunar rocks. The model produces craters according to a selected flux and size distribution of impacting particles and destroys them by the superposition of larger, subsequent impacts. Using a model cratering rate corresponding to 2.5 craters with pit diameters larger than 0.05 cm per cm<sup>2</sup> per m.y., which is based on a conservative or low estimate of the meteoroid flux, a production crater size distribution can exist not more than 1 m.y. The half-life of a population of craters with pit diameters of 0.01 cm is about 1 m.y. Longer exposure times permit lunar rock surfaces to approach an equilibrium condition with respect to the cratering process.

The measured areal crater densities for 26 lunar rocks with surfaces judged to be in equilibrium are all less than that predicted by the Monte Carlo model. This difference is attributed to increased spallation associated with larger craters and the presence of unrecognized pitless craters. These effects vary with rock type, thus indicating that different areal crater densities on lunar rock surfaces not clearly in production are due to different mechanical properties of the target rock and are not necessarily related to its exposure time. Determinations of exposure ages exceeding 1 m.y. based on microcrater statistics are subject to serious question.

Heiken, G., Duke, M., McKay, D. S., Clanton, U. S., Fryxell, R., Nagle, J. S., Scott, R., and Sellers, G. A.: 'Preliminary Stratigraphy of the Apollo 15 Drill Core', *Proceedings of the Fourth Lunar Science Conference, Geochim. Cosmochim. Acta* 1, Suppl. 4, 191-213.

The crew of Apollo 15 collected a 242-cm-long core of the regolith developed on the surface of Palus Putredinus (3°39'20" E, 26°26'00" N). This core consists of 42 major textural units, which range from a few millimeters to 13 cm thick.

The regolith at this site was deposited layer by layer, each layer having been reworked, to some degree, by micrometeorite bombardment. The particle composition of six layers for which we had samples varies in a random fashion, thus supporting the heterogeneous, layered model of the regolith.

The ratio of lithic fragments derived from the Apennine Front to that derived from the mare surface is about 1:1. This lithic ratio, in a regolith section 3.75 km from the base of the front, is an indication of the efficiency of lateral transport of soil by impact processes and mass wasting.

Heiken, G. H., McKay, D. S., and Fruland, R. M.: 'Apollo 16 Soils: Grain Size Analyses and Petrography', *Proceedings of the Fourth Lunar Science Conference, Geochim. Cosmochim. Acta* **1**, Suppl. 4, 251-265.

Soils from South Ray Crater, North Ray Crater, and the inter-ray area of Station 10 have a similar provenance, containing breccia fragments of low to medium metamorphic grade and low light/dark lithic fragment ratios; these appear to be characteristic of the Cayley Formation. The primary difference between soils possibly derived from North Ray and South Ray craters is in the agglutinate content. A soil from Stone Mountain (Station 4) is characterized by breccia fragments of medium to high metamorphic grade and a high light/dark lithic fragment ratio; this soil may be derived from the Descartes Formation. Differences between the selenomorphic units, the Descartes and Cayley formations, may be lithologic as well as structural.

The mean grain size varies from 84 to 280  $\mu\text{m}$  and all of the samples are poorly to very poorly sorted. There appears to be a relation between the sorting, grain size, and agglutinate content, with the finer-grained, better sorted soils containing more than 30% agglutinates.

'Shadowed' soils, collected close to large boulders, are similar in all respects to the 'reference' soils collected at least 5 m from the boulders.

Housley, R. M., Cirlin, E. H., and Grant, R. W.: 'Characterization of Fines from the Apollo 16 Site', *Proceedings of the Fourth Lunar Science Conference, Geochim. Cosmochim. Acta* **3**, Suppl. 4, 2729-2735.

We describe the characteristics of Apollo 16 fines samples 61281,8; 65701,13; 66031,6; 67701,26; and 67712,16 observed microscopically during the course of size and magnetic separations. Sample 67712,16 is unique in that almost all grains are rounded and no glass welded aggregates are present. All samples except 67712,16 contained about 0.5 wt. % of metal fragments 45  $\mu\text{m}$  or more in diameter including occasional spheres and large single crystals. Some of this metal showed rust spots.

Mössbauer spectra showed all the samples to be high in olivine compared to samples from other Apollo sites and to vary significantly in modal composition from each other. The fine grained Fe metal content and the excess absorption area near zero velocity in the Mössbauer spectra both vary with particle size and regolith maturity in the way one would predict from our model of Fe metal reduction and agglomeration during glass aggregate formation. The excess area is interpreted as being due to Fe<sup>0</sup> atoms which have been reduced by solar wind bombardment, but have not yet aggregated into small grains as a result of micrometeorite impacts.

Ivanov, A. V., Tarasov, L. S., Rode, O. D., and Florensky, K. P.: 'Comparative Characteristics of Regolith Samples Delivered from the Lunar Mare and Highland Regions by the Automatic Stations Luna-16 and Luna-20', *Proceedings of the Fourth Lunar Science Conference, Geochim. Cosmochim. Acta* **1**, Suppl. 4, 351-364.

The high content of anorthositic rocks and their metamorphosed varieties, as well as related basaltic rocks of non-mare type, that predominate among particles of primary magmatic rocks is an important peculiarity of the highland regolith sample returned by the automatic station, Luna-20, from the region of Apollonium-C crater (3°32' N and 56°33' E).

The significantly higher content of particles of primary magmatic rocks (50-70% of the total number of particles of coarse fractions), in comparison with breccias, sintered and slagged particles, is also typical for the Luna-20 regolith sample. On the contrary, a predominance (up to 70%) of strongly reworked particles, generated as a result of considerable, or total, exogenous transformation on the lunar surface, was observed in the Luna-16 regolith sample delivered from Mare Fecunditatis. This and other characteristics of highland regolith (coarser-grained materials, lower density of surface defects, etc.) indicate a noticeably lower degree of reworking of surface materials in the region of the Luna-20 landing site as compared to the mare region of the Luna-16 landing site.

The observed peculiarities of the Luna-20 regolith sample may have a local character associated with the nearby Apollonium-C crater. However, these peculiarities may also reflect the general character of regolith forming processes in different structural regions of the Moon. The difference in relief

may result in the formation of a thick but relatively slightly transformed regolith layer in lunar high-land depressions but a more highly transformed, more homogeneous one in lunar maria.

Jagodzinski, H. and Korekawa, M.: 'Diffuse X-Ray Scattering by Lunar Minerals', *Proceedings of the Fourth Lunar Science Conference, Geochim. Cosmochim. Acta* 1, Suppl. 4, 933-951.

A short review on diffuse X-ray scattering to be expected by radiation damage is given. In order to separate the various contributions, the diffuse scattering caused by anti-phase domains in lunar bytownites and anorthites is investigated and interpreted in terms of stepped boundaries of the domains. Reflections  $h + k + l = 2n$  are also surrounded by a diffuse halo; but this diffuseness is most probably only partly correlated with strains in the antiphase boundary. It is supposed that the observed differences in the diffuse scattering are caused by another type of defects, which have an important influence on the structure of the domain boundary. The contribution of radiation defects to the diffuse scattering is apparently very low because of the low exposure age of rock 68415. Tridymite single crystals from rock 15076 show a new type of diffuse X-ray scattering, which may be explained by displacements of ordered chains parallel to ( $h00$ ) and the symmetrically equivalent directions in reciprocal space of tridymite.

Jedwab, J.: 'Rare Micron-Size Minerals in Lunar Fines', *Proceedings of the Fourth Lunar Science Conference, Geochim. Cosmochim. Acta* 1, Suppl. 4, 861-874.

A method for selecting and analyzing individual micron-size particles by petrographic microscope, SEM, EMP, and XRD has been used with lunar fines. Small amounts of blue and white rutile, nickel sulfide, transparent iron oxides, silicon carbide, silicate-metal composites, dendritic troilite and molybdenite were found. The occurrence of these minerals is believed to be due to deposition from vapor, impact recrystallization and technological contamination.

Lindsay, J. F.: 'Evolution of Lunar Soil Grain-Size and Shape Parameters', *Proceedings of the Fourth Lunar Science Conference, Geochim. Cosmochim. Acta* 1, Suppl. 4, 215-224.

Despite an age difference of possibly as much as  $0.4 \times 10^9$  yr between substrates at the Apollo 15 and 16 sites the average properties of the soils from the two sites are very similar. The soils have essentially the same graphic mean, graphic standard deviation and graphic skewness. However, the graphic kurtosis of the Apollo 16 soils is slightly but significantly smaller than that of the Apollo 15 soils.

At the Apollo 15 site deeper soil samples are coarser grained, more poorly sorted and more negatively skewed. Kurtosis cannot be interpreted simply in terms of depth below the lunar surface. These trends are consistent with earlier models for an evolutionary sequence. The variations about the mean values for each parameter and the presence of apparently mature soils at depths of up to 2 m in the core suggest that reworking and mixing of the soil is considerable.

At the Apollo 16 site the trend is reversed and grain size and graphic standard deviation both decrease deeper in the soil layer. Simple relationships are not apparent for skewness and kurtosis. The reason for the reversal in trend appears to be the presence of a very-fine-grained well-sorted layer sampled by core segment 60001. Vertical mixing of this soil has produced a sequence of layers that gradually change upward away from the source.

Soil from the bottom of core segment 60001 at the Apollo 16 site is light in color and has unusual grain-size parameters, which suggest that it was sorted during transport in a gaseous medium and may be ray material.

The shape parameters of the Apollo 15 soil particles are determined largely by the glass content and thus the maturity of the soil. The particles with reduced sphericities are concentrated in two narrow zones approximately one standard deviation either side of the mean grain size of the soils.

McKay, D. S., Clanton, U. S., and Ladle, G.: 'Scanning Electron Microscope Study of Apollo 15

Green Glass', *Proceedings of the Fourth Lunar Science Conference, Geochim. Cosmochim. Acta* 1, Suppl. 4, 225-238.

Apollo 15 green glass droplets and related forms show a variety of low velocity impact features which occurred at the time of formation of the droplets. Composite forms, which consist of a crystallized core on which mounds of glass adhere, indicate a sequence of core formation and crystallization, followed by impact of molten droplets. The complicated and time dependent texture and morphology of the green glass forms are best explained by formation in a volcanic lava fountain rather than by meteorite impact.

Meyer, H. O. and McCallister, R. H.: 'Mineralogy and Petrology of Apollo 16: Rock 60215,13', *Proceedings of the Fourth Lunar Science Conference, Geochim. Cosmochim. Acta* 1, Suppl. 4, 661-665.

Rock 60215 is an anorthositic cataclastite with 97% plagioclase, minor orthopyroxene, opaque minerals and lithic clasts. Plagioclase (An<sub>96</sub>) grains vary in size and shape. Twinning, undulose extinction, fragmentation, and shock effects are common as well as recrystallization to cryptocrystalline feldspar. Orthopyroxene grains (62-68% En: CaO < 1 wt. %) are very small and occur interstitially to granulated feldspar. Lithic clasts are mineralogically equivalent to anorthosites and troctolites. The troctolitic clasts are common and often have subophitic texture. Some intersertal glass is also present. Rock 60215 formed from impact brecciation. Its lithic clasts may be derived either from magmatic crystallization or crystallization from an impact melt.

Mitchell, J. K., Carrier, W. D., Costes, N. C., Houston, W. N., and Scott, R. F.: 'Surface Soil Variability and Stratigraphy at the Apollo 16 Site', *Proceedings of the Fourth Lunar Science Conference, Geochim. Cosmochim. Acta* 3, Suppl. 4, 2437-2445.

The results of penetration tests, analyses of footprint and Lunar Roving Vehicle track depths, and core tube sample data have been used to deduce details of near-surface stratigraphy (to depths of several tens of centimeters) and lateral variability in soil conditions. Local variations (meter scale) in penetration resistance and porosity may be large, and soil stratigraphy may be complex. Since average properties are about the same at all sites, these variations probably reflect individual cratering and depositional events. These local variations cannot be anticipated on the basis of surface appearance or behavior.

Mizutani, H. and Newbigging, D. F.: 'Elastic Wave Velocities of Apollo 14, 15, and 16 Rocks', *Proceedings of the Fourth Lunar Science Conference, Geochim. Cosmochim. Acta* 3, Suppl. 4, 2601-2609.

Elastic wave velocities of two Apollo 14 rocks, 14053 and 14321, three Apollo 15 rocks, 15058, 15415, and 15545, and one Apollo 16 rock 60315 have been determined at pressures up to 10 kbar. For sample 14321, the variation of the compressional wave velocities with temperature has been measured over the temperature range from 27 to 200°C. Overall elastic properties of these samples except sample 15415 are very similar to those of Apollo 11, 12, and 14 rocks and are concordant with Toksöz *et al.*'s interpretation that lunar upper crust is of basaltic composition. Temperature derivative of the *P* wave velocity for sample 14321 is a half to one order of magnitude larger than that for single crystalline minerals. This suggests that the seismic velocity in the lunar crust may be affected significantly by the temperature distribution.

Morrison, D. A., McKay, D. S., Fruland, R. M., and Moore, H. J.: 'Microcraters on Apollo 16 and 15 Rocks', *Proceedings of the Fourth Lunar Science Conference, Geochim. Cosmochim. Acta* 3, Suppl. 4, 3235-3253.

Microcrater frequency distributions, determined for 11 Apollo 16 rocks and three Apollo 15 rocks, fall into four categories. Category 1 rocks (68415, 68416, 69935, 62235) are angular, cratered on one side only and have moderate crater densities. Category 2 rocks (60016, 66075, 61175) are sub-rounded, cratered on all sides and have distributions suggestive of the steady state. Category 3 rocks (61015, 62295) are subangular and cratered on only one side but the crater frequency distributions have some of the characteristics of category 2 rocks. Category 4 rocks (15015, 15017, 15076, 60335) are angular, cratered on only one side and have moderated to very low crater densities.

The crater frequency distributions of categories 1 and 4 have properties indicating the possibility of estimating the time they were exposed to micrometeor bombardment. Category 1 rocks appear to have been exposed for 2–3 m.y. These rocks particularly 68415, 68416, and 69935 may be ejecta from South Ray Crater, indicating an age of 2–3 m.y. for South Ray Crater. Category 4 rocks have been exposed for much shorter periods. We estimate exposure times of  $3\text{--}7 \times 10^2$  yr for 15017 (glass surface),  $2 \times 10^4$  yr for 15015 (glass surface), and approximately  $8 \times 10^5$  yr for 60335 and 15076. Total exposure time for category 2 rocks is estimated to be in excess of 20 m.y. If any category 2 rocks are North Ray ejecta then North Ray Crater formed more than 20 m.y. ago.

The crater frequency distributions for glass surfaces 15015 and 15017 show a reduction in the frequency of craters less than  $30 \mu$  in diam. Our data show a relatively flat slope of  $-1.3$  in the range  $10\text{--}30 \mu$  ( $\mu$ m) central pit diameter, approximately  $-2.5$  below  $10 \mu$ m central pit diameter, and approximately  $-2.0$  below  $1.0 \mu$ m central pit diam.

Small particles of varying morphology appear to have deposited continuously on the surfaces of 15015 and 15017 with deposition rates significantly larger than microcratering rates. The abundance of accretionary particles on the surface of 15015 is sufficient to produce a steady-state crater distribution by superposition of particles on craters. This steady-state distribution would be substantially different than the steady-state distribution of craters that result from destruction of craters by other craters.

Spalling is a function of pit diameter. Craters less than  $3 \mu$  show no spall. For larger craters the relation between pit ( $P_a$ ) and spall ( $S_a$ ) diameter is:  $S_a = 2.37 P_a^{1.07}$ .

Data from rock 14301 suggest a cumulative flux equation of the form  $\phi = 10^{-12.26} M^{-1.21} \text{cm}^{-2} \text{yr}^{-1}$  for a micrometeor mass ( $M$ ) of  $10^{-6}$  g and larger. For masses down to  $10^{-10}$  g the exponent on  $M$  is  $-0.5$ , (i.e. the crater diameter range  $10\text{--}30 \mu$ m). Below this exponents increase to  $-1.0$  and then decrease to  $-0.79$ .

Neukum, G., Hörz, F., Morrison, D. A., and Hartung, J. B.: 'Crater Populations on Lunar Rocks', *Proceedings of the Fourth Lunar Science Conference, Geochim. Cosmochim. Acta* 3. Suppl. 4, 3255–3276.

Approximately 10000 microcrater were investigated using binocular microscope techniques on fifteen Apollo 16 rocks: 'crystalline' rocks 60315, 60335, 61156, 62235, 62295, and 68415; 'breccias' 60016, 61015, 61175, 66075, and 69935; and glass surfaces 60015, 60095, 60135, and 64455. Diameter measurements of the central glass-lined pits ( $D_P$ ) and surrounding spall zones ( $D_S$ ) were made. Ratios of spall to pit diameters may range from 3.0 to 4.5 for different rock surfaces.

Crater size distributions obtained for production surfaces confirm and extend to larger crater sizes data published previously. The crater size distribution on lunar rocks in the pit diameter range, 10 to  $1000 \mu$ , is shown to depend on the average angle of impact which is a function of the exposure geometry.

In contrast to results of earlier studies, a wide range of crater densities was observed on relatively heavily cratered surfaces. The highest crater densities observed for lunar breccias are about a factor of 2 higher than that for crystalline rocks, which, in turn, appear up to 4 times more densely cratered than loose regolith in equilibrium.

Analytical models yield the expression for the cumulative equilibrium crater density,  $N_E = AD_S^{-2}$ , which has been adapted to microcratering on lunar rocks. A minimum value for the coefficient,  $A$ , is 0.15 assuming the largest measured spall-to-pit-diameter ratio of 4.5. This minimum is consistent with measurements.

Four independent criteria for recognizing equilibrium populations, (1) absolute crater densities, (2) constant crater densities for different exposure angles, (3) extent of  $D^{-2}$  slope, and (4) erosional state of surface, were applied to nine non-production Apollo 16 rocks, but only populations from two rocks (62235, 66075) satisfied all four criteria and were unambiguously shown to be in an equilibrium state.

Nord, G. L., Lally, J. S., Heuer, A. H., Christie, J. M., Radcliffe, S. V., Griggs, D. T., and Fisher, R. M.: 'Petrologic Study of Igneous and Metigneous Rocks from Apollo 15 and 16 Using High Voltage Transmission Electron Microscopy', *Proceedings of the Fourth Lunar Science Conference, Geochim. Cosmochim. Acta* **1**, Suppl 4, 953-970.

Substructures in plagioclase, pyroxene, and olivine have been studied by high voltage transmission electron microscopy from mare basalts 15555 and 15557, a feldspathic basalt 68415, a troctolite 62295, and a xenoclastic feldspathic basalt 60335. The scale and morphology of the antiphase domain structures in plagioclase in these rocks vary markedly with composition and thermal history. Using these results and similar data from substructures in pyroxene, it is concluded that 15555 and 15557 cooled at a similar rate to 62295 and 68415; 68415 cooled more rapidly than the anorthosite, 15415. The exsolution and M-T APD substructures of the pigeonites of the mare basalts and a poikilitic pigeonite of 60335 are also compared, and indicate that the poikilitic pigeonite cooled more slowly. Inclusions and dislocations in olivine and plagioclase, as well as the mesostasis substructures, are also discussed.

Powell, B. N., Aitken, F. K., and Weiblen, P. W.: 'Classification, Distribution, and Origin of Lithic Fragments from the Hadley-Apennine Region', *Proceedings of the Fourth Lunar Science Conference, Geochim. Cosmochim. Acta* **1**, Suppl. 4, 445-460.

A systematic study of sixteen Apollo 15 soil samples and nineteen 4-10 mm basalt particles from nine sample sites was made. Eight broad groups of lithic types were recognized:  $A_m$ , primary igneous mare-type basalts;  $A_k$ , KREEP basalts with primary igneous textures; B, microbreccias and agglutinates with mare basalt affinity; C, feldspathic microbreccias, including anorthosites, norites (some KREEP), and troctolites; D, complex multigenerational feldspathic microbreccias; E, mixed microbreccias (B + C); F, crystal fragments; and G, glasses and glass-rich particles.

Among mare basalts five specific varieties have been distinguished on the basis of mineralogical, textural, and chemical characteristics (I), pyroxene-rich tridymite gabbros; (II), pyroxene vitrophyres and porphyritic variolitic basalts; (III), olivine-cristobalite basalts; (IV), pyroxene-rich basalts; and (V), olivine-pyroxene vitrophyres.

Population studies on particles in the 0.5-4 mm size range reveal systematic differences among three selenological terranes. Apennine Front samples contain the highest abundances of non-mare (including KREEP) materials and of degraded materials and the lowest abundance of mare materials. By contrast samples from Mare Rille locations are richest in mare materials, including basalts. Ridge or Ray soils have a mixed intermediate character and a relatively high abundance of KREEP basalts.

The population study suggests that the Apennine Front is comprised essentially of pre-Imbrian differentiated (feldspathic) crustal material uplifted by the Imbrium impact. Subsequent gardening produced a local relatively immature regolith. Mare basalts comprise bedrock beneath the mare surface and in Hadley Rille. Several flows of different composition are indicated and type distribution implies some lateral and vertical variation. Non-mare constituents (including KREEP) in the LM soils are probably derived from local bedrock beneath a thin mare surface.

KREEP basalts with primary igneous textures attest to the existence of KREEP magmas and do not require (or suggest) a mixing or hybridization mode of origin. KREEP lavas may underlie the mare surface and be part of a pre-mare crust in this region. At least three different magmas are implied by mare basalt varieties. Although of general mare affinity, and thus distinct from non-mare KREEP, these magmas reflect separate petrogeneses.

Ridley, W. I., Hubbard, N. J., Rhodes, J. M., Weismann, H., and Bansal, B.: 'The Petrology of Lunar Breccia 15445 and Petrogenetic Implications', *J. Geology* **81**, 621-631.

Lunar breccia 15445, collected near the rim of Spur Crater, contains iron-rich olivine and orthopyroxene mineral clasts and two types of white lithic clasts. The dominant type (Type A) is composed principally of anorthite - magnesian orthopyroxene and appears to be a low-pressure cumulate from a magnesian, high-Al basalt. A minor type (Type B) is composed of olivine + chrome pleonaste + aluminous orthopyroxene + minor plagioclase. Type B clasts have affinities to terrestrial spinel peridotites and have a REE pattern unique for the Moon. Considerations of the observed mineralogy



and the trace element geochemistry suggest that garnet was originally a phase in this peridotite but was subsequently lost during subsolidus reequilibration. Hence, Type B clasts provide indirect evidence for the existence of garnet in the lunar interior.

Schneider, E., Storzer, D., Hartung, J. B., Fechtig, H., and Gentner, W.: 'Microcraters on Apollo 15 and 16 Samples and Corresponding Cosmic Dust Fluxes', *Proceedings of the Fourth Lunar Science Conference, Geochim. Cosmochim. Acta* 3, Suppl. 4, 3277–3290.

Crystalline, glass, and metal samples from Apollo 15, 16, and Luna 16 missions have been investigated for micrometeorite impact craters using scanning electron microscope and electron microprobe techniques. At magnifications of 10000–20000 the range of crater detection extends down to 0.1  $\mu\text{m}$  diam. All samples show production state crater distributions. Surface exposure ages ranging roughly between 10 and  $10^5$  yr have been determined using the solar flare track method. Crater number densities together with exposure ages allowed a calculation of the flux of micron and submicron sized particles onto the Moon. Within an uncertainty of about a factor of two all samples yield a constant value for the flux of particles. Compared to the trend of the size distribution of larger particles there exists exceptionally large numbers of micron and submicron sized particles, thus suggesting a bimodal size distribution for the interplanetary dust. Neumann bands were found near a 30  $\mu\text{m}$  diam microcrater on a meteoritic Fe–Ni particle which was separated from coarse fines, 60502,17. Laboratory cratering experiments indicated the Neumann bands were produced during the cratering event.

Sclar, C. B., Bauer, J. F., Pickart, S. J., and Alperin, H. A.: 'Shock Effects in Experimentally Shocked Terrestrial Ilmenite, Lunar Ilmenite of Rock Fragments in 1–10 mm Fines (10085,19), and Lunar Rock 60015,127', *Proceedings of the Fourth Lunar Science Conference, Geochim. Cosmochim. Acta* 1, Suppl. 4, 841–859.

Terrestrial ilmenite ( $\text{Il}_{90}\text{Hem}_{10}$ ) was shock loaded at a peak pressure of 75 kbar and examined by reflected-light and transmission electron microscopy. The shocked ilmenite contains minute oriented platelets of a precipitate phase which is a product of shock-induced unmixing. The precipitate phase is probably titanian hematite epitaxially oriented on (0001) of the ilmenite host. Microtextural relationships indicate that ilmenite may deform by two distinct crystallographic modes during a shock event, viz., by twinning initially on (0001) and, in the latter stages at higher temperatures, by twinning on rhombohedral planes (probably  $\{10\bar{1}1\}$ ). Optically resolvable shock-induced twins in ilmenite develop at peak pressures between 35 and 75 kbar. Preliminary powder neutron diffraction data from experimentally shocked ilmenite are consistent with the presence of iron-rich epitaxial exsolution domains but may also indicate a small degree of cation disorder.

Ilmenite xenocrysts embedded in glass derived from shock-melted Apollo 11 basaltic breccia show subsolidus reduction to rutile plus metallic iron. This suggests that, under the highly reducing conditions of the lunar environment, subsolidus reduction of ilmenite and ulvöspinel may result from shock-induced transient heating as well as by slow cooling in igneous rocks.

Iron-rich aluminian armalcolite and magnesium-rich chromian ulvöspinel probably co-crystallized early from shock-produced basaltic liquid derived from Apollo 11 breccia. This is the most iron-rich armalcolite reported thus far; the spinel is remarkable because it contains the molecular end member  $\text{Mg}_2\text{TiO}_4$ .

The interior of lunar rock 60015 has an anorthositic composition and consists of highly deformed euhedral to anhedral plagioclase containing shock lamellae set in an intergranular and interstitial network of fine-grained feathery plagioclase aggregates. The latter is interpreted as a shock-induced melt derived from the deformed plagioclase. The rock was probably formed either by shock-lithification and partial melting of plagioclase crystals of the regolith or by shock-induced partial melting of a porous anorthositic breccia.

Tittmann, B. R., Housley, R. M., and Cirlin, E. H.: 'Internal Friction of Rocks and Volatiles on the Moon', *Proceedings of the Fourth Lunar Science Conference, Geochim. Cosmochim. Acta* 3, Suppl. 4, 2631–2637.

Internal friction quality factors  $Q$  up to 2200 have been observed in a strongly outgassed terrestrial analog of lunar basalt. This was accomplished by successively cycling a bar shaped sample vibrating in its fundamental longitudinal mode at 15 kHz to higher and higher temperatures in a vacuum between  $10^{-7}$  and  $10^{-8}$  torr. After each cycle,  $Q$  measured at room temperature in the vacuum was observed to decrease with time suggesting that gas re-absorption was taking place even at these low pressures.

A study of the effect of exposing a sample to a variety of gases and vapors showed that of the volatiles most likely to be present in the lunar environment  $H_2O$  was by far the most effective in lowering  $Q$ .

The fact that only a very small amount of volatile material is required to lower the  $Q$  of rocks suggests that with further study of the loss mechanism, the lunar seismic  $Q$  values may be used to place strong constraints on the outgassing history of the Moon and on any possible prehistoric lunar atmospheres.

Todd, T., Richter, D. A., and Simmons, G.: 'Unique Characterization of Lunar Samples by Physical Properties', *Proceedings of the Fourth Lunar Science Conference, Geochim. Cosmochim. Acta* 3, Suppl. 4, 2639-2662.

The measurement of compressional velocity, shear velocity, static compressibility, and thermal expansion of (1) a suite of shocked rocks from the Ries impact crater in Germany, (2) a suite of samples cracked by thermal cycling to high temperatures, (3) many terrestrial igneous rocks, and (4) lunar basalts, gabbroic anorthosites, and breccias, indicate that shock metamorphism is the primary cause for values of physical properties of lunar rocks being different from their intrinsic values. Large scale thermal metamorphism, thermal cycling between temperatures of lunar day and night, large thermal gradients, or thermal fatigue could possibly cause minor cracking in the top few centimeters of the lunar regolith, but are probably not important mechanisms for extensively changing values of physical properties of lunar rocks.

Values of physical properties as functions of depth or radial distance from the center of large impact craters reflect the intensity of the shock event. The profile for seismic velocity vs depth over the first 25 km of the Moon indicates decreasing shock metamorphism with depth. A depth of 25 km probably represents the maximum depth of shock metamorphism or the depth at which shock-produced microfractures are closed or annealed.

Warren, N., Trice, R., Soga, N., and Anderson, O. L.: 'Rock Physics Properties of Some Lunar Samples', *Proceedings of the Fourth Lunar Science Conference, Geochim. Cosmochim. Acta* 3, Suppl. 4, 2611-2629.

Linear strains and acoustic velocity data for lunar samples under uniaxial and hydrostatic loading are presented. Elastic properties are presented for 60335,20; 15555,68; 15498,23; and 12063,97. Internal friction data are summarized for a number of artificial lunar glasses with compositions similar to lunar rocks 12009, 12012, 14305, 15021, and 15555. Zero porosity model-rock moduli are calculated for a number of lunar model-rocks, with mineralogies similar to Apollo 12, 14, and 16 rocks.

Model-rock calculations indicate that rock types in the troctolitic composition range may provide reasonable modeling of the lunar upper mantle. Model calculations involving pore crack effects are compatible with a strong dependence of rock moduli on pore strain, and therefore of rock velocities on nonhydrostatic loading. The high velocity of rocks under uniaxial loading appears to be compatible with, and may aid in, interpretation of near-surface velocity profiles observed in the active seismic experiment. High values of lunar  $Q$  are compatible with results for glass and with recent measurements on rocks.

Wosinski, J. F., Williams, J. P., Korda, E. J., and Geiger, G. A.: 'Glass and Devitrified Zones on Lunar Breccia Rock 15286,3', *Proceedings of the Fourth Lunar Science Conference, Geochim. Cosmochim. Acta* 1, Suppl. 4, 383-388.

Optical and scanning electron microscopy examination of lunar breccia rock 15286,3 indicates considerable devitrification in the glass phase adjacent to the breccia. The glass contains voids, metallic spheres, and four phases in the devitrification region. Four distinct phases are evident in the breccia. An estimation of the chemical composition of the various phases was made by X-ray energy dispersion analysis. Optical properties were determined wherever possible to help identify selected phases.

The data suggest that the glass was formed by meteorite impact; regions of homogeneous and heterogeneous glass were produced; the glass remained at low viscosity (800 to 1000 P) long enough for devitrification; and the metallic phase did not nucleate crystallization in the glass phase.

## 12. Photometry of the Moon

Adams, J. B. and McCord, T. B.: 'Vitrification Darkening in the Lunar Highlands and Identification of Descartes Material at the Apollo 16 Site', *Proceedings of the Fourth Lunar Science Conference, Geochim. Cosmochim. Acta* 1, Suppl. 4, 163-177.

Soil samples from the Apollo 16 site were separated magnetically into nearly pure fractions of glass-bounded aggregates (agglutinates), and agglutinate-free fractions. Agglutinates are typically darker than the parent soil due to the presence of iron and titanium ions in the glass, and the occurrence of finely disseminated Fe metal and other opaques. The build-up of agglutinates in a maturing soil provides an effective mechanism for lowering the albedo. It is proposed that this is the principal age-darkening mechanism on the lunar surface. The spectral reflectance properties of the agglutinate-free fractions and of the bulk soils indicate two compositional end members corresponding to anorthositic breccia and darker breccias. These compositional end-members can be distinguished in spectral reflectance curves of 20 km areas measured by Earth-based telescopes of Descartes and Cayley formations, respectively. It is concluded that Descartes material was sampled at North Ray Crater, Stone Mountain, and perhaps at several subsurface localities elsewhere. Considering isotopic age data for samples from North Ray Crater, the Descartes Highlands may consist of the oldest rocks yet sampled from the Moon.

Birkebak, R. C. and Dawson, J. P.: 'Solar Albedo and Spectral Reflectance for Apollo 15 and 16 Lunar Fines', *Proceedings of the Fourth Lunar Science Conference, Geochim. Cosmochim. Acta* 3, Suppl. 4, 2447-2452.

The spectral directional reflectance of Apollo 15 and 16 fines were obtained for bulk densities of approximately 1000 and 1600 kg m<sup>-3</sup>. The solar albedo as a function of angle of illumination was calculated from these results. Comparison of solar albedos show that Apollo 11, 12, and 15 soils fall into one group and the Apollo 14 and 16 soil results into a second group corresponding to mare or lunar highland materials.

Bowell, E., Dollfus, A., Zellner, B., and Geake, J. E.: 'Polarimetric Properties of the Lunar Surface and Its Interpretation. Part 6: Albedo Determinations from Polarimetric Characteristics', *Proceedings of the Fourth Lunar Science Conference, Geochim. Cosmochim. Acta* 3, Suppl. 4, 3167-3174.

Optical polarization results for 35 lunar samples from Apollos 11 to 15 and from Lunas 16 and 20 are analyzed in terms of 2 relationships: (1) Lunar fines (with the exception of 15401,62), and also the lunar surface itself, show an inverse linear relationship between geometric albedo and the maximum value of polarization, thereby providing a method of determining albedos. Lunar rocks and breccias do not usually fit this relationship. (2) All lunar samples, and all observations of atmosphereless objects in the solar system, show an inverse linear relationship between geometric albedo and the slope of the polarization curve for small positive values of polarization. This enables albedos (and hence diameters) to be determined for objects where the polarization curve is only observable for small phase angles, even when these objects cannot be resolved telescopically.

Egan, W. G. and Hilgeman, T.: 'Optical Constants for Terrestrial Analogs of Lunar Materials', Rm-574J.

Representative terrestrial analogs of the dominant lunar constituents plagioclase feldspar and pyroxene were selected. The refractive, absorption and scattering components were determined separately in the range from 0.33 to 2.3  $\mu$ . A newly developed theory was employed to separate the absorption from the scattering based on thin section total reflectance and transmission measurements. The selected minerals were bytownite (Minnesota) and augite (Ontario, Canada); a comparison of their absorption peaks with those inferred from reflectance measurements on lunar samples reveal comparable bands at 2.0, 1.3, 1.0 to 0.9, 0.6  $\mu$  and the UV. The similarities indicate that the optical constants reasonably characterize the lunar surface material. Another result is the introduction of plagioclase as a possible candidate material causing the 0.6  $\mu$  feature in asteroids and in the interstellar medium.

Evsyukov, N. N.: 'Physical Nature of the Lunar Albedo', *Solar System Res.* 7, 58-63.

The normal albedo map for the visible lunar hemisphere obtained by the author is used to check various assumptions on the physical nature of the albedo. It is concluded that the most probable explanation of the variations in the lunar albedo is that they are due to variations in the composition of lunar rocks.

Fastie, W. G.: 'Special Report; Diffuse Reflectivity of the Lunar Surface', NASA-CR-128546.

The far ultraviolet diffuse reflectivity of samples of lunar dust material is determined. Equipment for measuring the diffuse reflectivity of materials (e.g. paint samples) is already in existence and requires only minor modification for the proposed experiment which will include the measurement of the polarizing properties of the lunar samples. Measurements can be made as a function of both illumination angle and angle of observation.

Gal'perin, B. O., Golubev, V. A., and Martynyuk, A. I.: 'Photoelectric Observations of the Total Lunar Eclipse of January 30, 1972', *Solar System Res.* 7, 110-111.

The photoelectric equipment used to record the integrated brightness during lunar eclipses is described. Observations of the total eclipse of January 30, 1972, in two wavelength regions are reported.

Geake, J. E., Walker, G., Telfer, D. J., Mills, A. A., and Garlick, G. F. J.: 'Luminescence of Lunar, Terrestrial and Synthesized Plagioclase Caused by  $Mn^{2+}$  and  $Fe^{3+}$ ', *Proceedings of the Fourth Lunar Science Conference, Geochim. Cosmochim. Acta* 3, Suppl. 4, 3181-3189.

Luminescence emission spectra have been obtained for 24 different samples of lunar fines, rocks, and breccias, using proton or electron excitation. A representative selection is shown. Plagioclase is the main luminescent component, and its dominant emission is a  $Mn^{2+}$ -activated peak at about 5600 Å. Lunar samples differ from similar terrestrial materials mainly in the strength of their near-infrared emission; this is dominant for most terrestrial plagioclases, but is weak or absent for lunar materials. By doping pure synthesized plagioclase we now have experimental confirmation that this emission is probably due to activation by  $Fe^{3+}$ . The weakness of this emission from lunar samples may be due to oxygen scarcity at formation giving dominant  $Fe^{2+}$ , which quenches luminescence.

Lucchitta, B. K.: 'Photogeology of the Dark Material in the Taurus-Littrow Region of the Moon', *Proceedings of the Fourth Lunar Science Conference, Geochim. Cosmochim. Acta* 1, Suppl. 4, 149-162.

Regional relations and characteristics of the dark material as observed on photographs of the Taurus-Littrow region of the Moon are reviewed to provide a background for interpretations of its nature and origin. The dark material seems to be a surficial deposit that covers mare and highland areas near the southeastern edge of the Serenitatis Basin. The age of the dark material, as deduced from photogeologic analysis, is ambiguous: contact relations near its western edge suggest that it is older than the central light basalts of Mare Serenitatis; evidence elsewhere indicates that it may be younger. The origin of the dark material is also uncertain, and the following alternate hypotheses are briefly considered: (1) thick regolith, (2) dark impact ejecta, (3) pyroclastic blanket, or (4) a material of different origin in different places.

Schmitt, H. H.: 'Lunar Mare Color Provinces as Observed on Apollo 17', *Geology* **2**, 55.

Four major and several minor mare color provinces exist between longs 20°W and 90°E on the Moon. These provinces were clearly visible to the unaided eye during the Apollo 17 mission when viewed from distances up to a few thousand kilometers. It is probable that the mare color provinces correlate with rather specific compositional differences between mare surfaces.

### 13. Thermal Emission of the Lunar Surface

Clark, S. P.: 'Lunar Thermal Measurements in Conjunction with Project Apollo', (Final Report) NASA-CR-136035.

Problems related to the feasibility of measuring lunar heat flow at the lunar surface are analyzed, and the findings which required that a drill be developed for lunar use are discussed. Numerical simulations were made of the in situ measurement of lunar thermal conductivity using a circular ring source of heat. The results of these simulations formed the basis for the criteria used in designing a subsurface thermal probe for ALSEP. Preliminary analyses are presented on the data obtained from the Apollo 15 and 17 missions.

Keihm, S. J. and Langseth, M. G.: 'Surface Brightness Temperatures at the Apollo 17 Heat Flow Site: Thermal Conductivity of the Upper 15 cm of Regolith', *Proceedings of the Fourth Lunar Science Conference, Geochim. Cosmochim. Acta* **3**, Suppl. 4, 2503–2513.

Lunar surface brightness temperatures derived as part of the Apollo 17 heat flow experiment are reported. Night-time surface temperatures, calculated from the data provided by two thermocouples suspended about 15 cm above the lunar surface, are used to determine the conductivity profile of the upper 15 cm of regolith at the ALSEP site. The surface reaches a maximum temperature of 384 ( $\pm 6$ )K at lunar noon and cools to a minimum temperature of 102 ( $\pm 1\frac{1}{2}$ )K at the end of the lunar night. The night-time cool-down curve is best fit by an essentially two-layer conductivity model of the lunar regolith. Conductivities of the order of  $1.5 \times 10^{-5} \text{ W cm}^{-1} \text{ K}^{-1}$  are postulated for a 2 cm porous surface layer overlying more compact regolith material with conductivities in the range of  $1.0\text{--}1.5 \times 10^{-4} \text{ W cm}^{-1} \text{ K}^{-1}$  between 2 and 15 cm.

A mean surface temperature of 216 ( $\pm 5$ )K is deduced from the thermocouple data. The 256K temperature measured by the probe sensors at 130 cm thus indicates that a large mean temperature gradient exists at the Apollo 17 site. A strongly temperature-dependent thermal conductivity, at least in the upper few centimeters, accounts for the large mean temperature gradient. A ratio of radiative to conductive heat transfer = 2.0 at 350K is required for at least the upper few centimeters to produce the observed mean temperature gradient.

Murdock, T. L.: 'Measurements of Infrared Radiation from Mercury and the Moon', Ph.D. Thesis, Minnesota Univ., Microfilms, Order No. 73-10611.

The 2.3 to 18  $\mu$  infrared radiation from the planet Mercury and the 2.3 to 8.6  $\mu$  infrared radiation

from the Moon studies are presented. Experimental results are compared with predictions based on a smooth spherical black body model and it is found that neither object radiates like the model and, although they are not identical. Mercury and the Moon are quite similar.

#### 14. Electromagnetic Properties of the Moon

Butler, R. F.: 'The Effect of Neutron Irradiation on Remanent Magnetization in Iron and Kamacite', Ph.D. Thesis, University Microfilms, Order No. 72-30602.

Natural remanent magnetization in Apollo 11 and 12 lunar samples and in most chondritic meteorites is carried by iron or kamacite. In order to determine whether cosmic-ray exposure is an important variable in formation of remanent magnetization in these rocks, the effects of proton and neutron irradiation on magnetic properties of iron and kamacite were investigated. Radiation damage theory indicates that the secondary fast neutron flux is more effective in producing lattice damage than is the primary proton flux. Two theoretical models of the effects of neutron irradiation on remanent magnetization and coercivity are developed. One model involves the pinning of domain walls by irradiation produced crystal defects. The preferred model involves the production of a uniaxial anisotropy by point defects introduced during irradiation.

Chung, D. H. and Westphal, W. B.: 'Dielectric Spectra of Apollo 15 and 16 Lunar Solid Samples', *Proceedings of the Fourth Lunar Science Conference, Geochim. Cosmochim. Acta* 3, Suppl. 4, 3077-3091.

The dielectric constants, losses and AC-conductivities of lunar samples 15065,27, 15459,62, 15555,88, 15415,57, 60015,29, 60315,34 61016,34, and 62235,17 as they are measured over a range of frequencies from 100 Hz to 10 MHz and temperatures from 77K to 473K by two-terminal capacitance substitution methods are presented. The dielectric spectra of lunar gabbroic basalts are typified by the dielectric behavior of samples 15065 and 15555, showing complex relaxation processes which are both frequency- and temperature-dependent. Such feldspar-rich crystalline lunar basalts like samples 15459, 62235, and 60015 showed essentially the same dielectric relaxation mechanisms which are also a function of both frequency and temperature with a very broad relaxation frequency distribution. The nature and a detailed process of these relaxation mechanisms are not yet understood and as more experimental data become available these mechanisms may be separable in terms of a DC-conductivity and dielectric relaxation mechanisms. Highly-brecciated lunar sample, 60315, exhibits rather an unusual dielectric behavior which is dependent upon on field-strength. Incorporating information on the chemical and physical structure of this sample, we have attributed the observed electrical properties to effects arising from numerous particles of metallic free-iron and other opaque alloys dispersed along mineral boundaries.

Cisowski, S., Fuller, M., Rose, M. E., and Wasilewski, P. J.: 'Magnetic Effects of Experimental Shocking of Lunar Soil', *Proceedings of the Fourth Lunar Science Conference, Geochim. Cosmochim. Acta* 3, Suppl. 4, 3003-3017.

Lunar soil samples from 65901,10 have been experimentally shocked at approximately 50, 75, 100, and 250 kbar, using the flying plate technique. On recovery, all samples were found to be lithified. In the 50 kbar sample some shock melting was evident, but other regions were undeformed. The range of shock effects are comparable with those found in some lunar breccias. In the 250 kbar sample, large amounts of glass were produced by the shock. Some of this glass was clear, and some contained fine particles which appear to be both magnetic  $\alpha$ -iron and non-magnetic  $\gamma$ -iron.

The magnetic characteristics of the soil were changed by the shock experiments. In the low shock range, the coercivity ( $H_c$ ) and saturation isothermal remanent magnetization ( $IRM_s$ ) increased. In the higher shock range, magnetic viscosity increased, but coercivity ( $H_c$ ) and  $IRM_s$  were similar to those of the control material. The 100 kbar sample exhibited anisotropy of  $IRM_s$ .

Shock remanent magnetization (SRM) was acquired as the result of the shock loading. The max-

imum value, which was that of the 50 kbar sample, was  $10^{-3} \text{ G cm}^3 \text{ g}^{-1}$ . Assuming a linear dependence of SRM upon field for a given shock pressure, this would give rise to remanence of  $10^{-4}$  and  $10^{-5} \text{ G cm}^3 \text{ g}^{-1}$  in fields of  $10^3 \gamma$  and  $10^2 \gamma$  respectively. The direction of SRM was not simply related either to the field in which the samples were shocked nor to the fields in which they were recovered. SRM acquired in the low shock range was stable in direction during AF demagnetization. However, SRM acquired in the 100 and 250 kbar experiments changed in direction during AF demagnetization. The remanence acquired in 100 kbar shock has distributed blocking temperatures.

It is concluded that shock remanent magnetization (SRM) is a relatively efficient mechanism of magnetization and should not be discounted as a source of lunar NRM. SRM may also account for the NRM of certain meteorites. Indeed SRM could be a relatively common phenomena in the early solar system being produced in planetesimal collisions as well as by meteoroid impact phenomena.

Collinson, D. W., Stephenson, A., and Runcorn, S. K.: 'Magnetic Properties of Apollo 15 and 16 Rocks', *Proceedings of the Lunar Science Conference, Geochim. Cosmochim. Acta* 3, Suppl. 4, 2963–2976.

The remanent magnetism of samples of Apollo 15 and 16 rocks has been measured and its characteristics studied. The stable remanence, which is found in most of the samples, is carried by iron and in some cases has the properties of a thermoremanence. One of the Apollo 16 samples has provided an exceptionally high estimate of the field in which it acquired its magnetism. A detailed study has been made of the homogeneity of magnetization in a breccia, and the rock magnetism and magnetic mineralogy of some of the samples is described.

Dunlop, D. J.: 'Theory of the Magnetic Viscosity of Lunar and Terrestrial Rocks', *Rev. Geophys. Space Phys.* 11, 855–901.

Lunar materials exhibit two distinct types of viscous or time-dependent magnetic behavior. Igneous rocks and largely recrystallized breccias, whose magnetic properties are due to multidomain iron, typically have weak magnetic viscosity, but decay persists for very long times following even a brief exposure to a field. Lunar soils and low metamorphic grade breccias, which contain an important fraction of metallic iron of singledomain and superparamagnetic size, generally acquire an anomalously strong viscous remanence, whose decay time is about equal to the time of exposure to the field. Four theories of magnetic viscosity are reviewed in this paper in an attempt to interpret the very different viscous properties of these two types of rocks. The Richter and Néel theories are appropriate to soils and low-grade breccias, whereas igneous and recrystallized rocks are better described by the multidomain theories of Néel and Stacey. Both the Stacey and Néel theories correctly predict logarithmic magnetic viscosity, in spite of the fact that the central role played by the internal demagnetizing field in multidomain grains is ignored in Néel's formulation. This apparent paradox has been resolved. Analysis of the particularly simple case of a two-domain particle shows that the distribution of asymmetrical nonidentical potential barriers required by Néel is automatically generated from the simpler distribution of symmetrical identical barriers proposed by Stacey through the action of the demagnetizing field. Experimental evidence on many facets of viscous magnetization, from terrestrial as well as lunar materials, is reviewed in detail before a final evaluation of the various theories is made. One interesting conclusion is that the magnetic viscosity of multidomain particles, although relatively weak, is still too strong to be explained by displacements of entire domain walls. Either displacements of small wall segments or rotation of pseudo-single-domain moments could account for the enhancement of magnetic viscosity in these particles.

Dunlop, D. J., Gose, W. A., Pearce, G. W., and Strangway, D. W.: 'Magnetic Properties and Granulometry of Metallic Iron in Lunar Breccia 14313', *Proceedings of the Fourth Lunar Science Conference, Geochim. Cosmochim. Acta* 3, Suppl. 4, 2977–2990.

Based on a detailed study of time-dependent or viscous remanence (VRM), thermoremanence (TRM) and magnetic granulometry of soil breccia 14313, single-domain particles of iron 100–200 Å

in size are proposed as the major carriers of natural remanence (NRM) in this rock. The VRM of 14313 is unusually intense and exhibits a logarithmic time decrease of VRM which ceases fairly abruptly after a time about equal to the original exposure to the field, unlike crystalline rocks and high-grade breccias whose logarithmic decay persists to extremely long times. The partial TRM spectrum reveals both a high-blocking-temperature fraction, scarcely affected by AF demagnetization to 1000 Oe, and an unusual concentration of blocking temperatures just above room temperature. The former fraction would contribute a very hard and stable component to any NRM of lunar origin, but the latter fraction, which accounts for the pronounced VRM of 14313 and undoubtedly has imparted a large viscous NRM component in the Earth's field, is also surprisingly hard. A substantial portion (20–40%) is not demagnetized by an 800 Oe field. Metallic iron in a single-domain state is the only plausible carrier of such hard remanences and magnetic granulometry using partial TRM data indicates that two distinct populations are involved. The first consists of 120–200 Å roughly equidimensional particles. The number of particles of volume  $v$  in this population varies as  $v^{-1.8}$ , in good agreement with the  $v^{-2}$  dependence found by Stephenson for an Apollo 11 soil, and the distribution appears to peak in the superparamagnetic range below 100 Å. The second population contains elongated particles  $\leq 100$  Å in size, whose microscopic coercive forces are distributed right up to 10000 Oe, the shape anisotropy limit for single-domain needles of iron.

Dyal, P., Parkin, C. W., and Daily, W. D.: 'Surface Magnetometer Experiments: Internal Lunar Properties', *Proceedings of the Fourth Lunar Science Conference, Geochim. Cosmochim. Acta* 3, Suppl. 4, 2925–2945.

Magnetic fields have been measured on the lunar surface at the Apollo 12, 14, 15, and 16 landing sites. The remanent field values at these sites are respectively 38 $\gamma$ , 103 $\gamma$  (maximum), 3 $\gamma$ , and 327 $\gamma$  (maximum). Simultaneous magnetic field and solar plasma pressure measurements show that the remanent fields at the Apollo 12 and 16 sites are compressed and that the scale size of the Apollo 16 remanent field is  $5 \leq L < 100$  km. The global eddy current fields, induced by magnetic step transients in the solar wind, have been analyzed to calculate an electrical conductivity profile. From nightside data it has been found that deeper than 170 km into the Moon, the conductivity rises from  $3 \times 10^{-4}$  mhos  $m^{-1}$  to  $10^{-2}$  mhos  $m^{-1}$  at 1000 km depth. Analysis of dayside transient data using a spherically symmetric two-layer model yields a homogenous conducting core of radius  $0.9 R_M$  and conductivity  $\sigma = 10^{-3}$  mhos  $m^{-1}$ , surrounded by a nonconducting shell of thickness  $0.1 R_M$ . This result is in agreement with the conductivity profile determined from nightside data. The conductivity profile is used to calculate the temperature for an assumed lunar material of peridotite. In an outer layer ( $\sim 170$  km thick) the temperature rises to 850–1050K, after which it gradually increases to 1200–1500K at a depth of  $\sim 1000$  km. From lunar hysteresis curves it has been determined that the global relative magnetic permeability is  $\mu/\mu_0 = 1.029_{-0.019}^{+0.024}$  for the whole Moon. This permeability indicates that the Moon responds as a paramagnetic or weakly ferromagnetic sphere.

Dyal, P., Parkin, C. W., and Daily, W. D.: 'Surface Magnetometer Experiments: Internal Lunar Properties', NASA-TM-X-62278.

Magnetic fields have been measured on the lunar surface at the Apollo 12, 14, 15, and 16 landing sites. The remanent field values at these sites are respectively 38 $\gamma$ , 103 $\gamma$  (maximum), 3 $\gamma$ , and 327 $\gamma$ . Simultaneous magnetic field and solar plasma pressure measurements show that the remanent fields at the Apollo 12 and 16 sites are compressed and that the scale size of the Apollo 16 remanent field is  $5 < \text{or} = L < 100$  km. The global eddy current fields, induced by magnetic step transients in the solar wind, were analyzed to calculate an electrical conductivity profile. From nightside data it was found that deeper than 170 km into the Moon, the conductivity rises from 0.0003 mhos  $m^{-1}$  to 0.01 mhos  $m^{-1}$  at 1000 km depth. Analysis of dayside transient data using a spherically symmetric two-layer model yields a homogeneous conducting core of radius  $0.9 R$  and conductivity  $\sigma = 0.001$  mhos  $m^{-1}$ , surrounded by a nonconducting shell of thickness  $0.1 R$ . This result is in agreement with a nonconducting profile determined from nightside data. The conductivity profile is used to calculate the temperature for an assumed lunar material of peridotite. In an outer layer the temperature rises to 850 to 1050K, after which it gradually increases to 1200 to 1500K at a depth of approximately 1000 km.



Fenner, M. A., Freeman, J. W., and Hills, H. K.: 'The Electric Potential of the Lunar Surface', *Proceedings of the Fourth Lunar Science Conference, Geochim. Cosmochim. Acta* 3, Suppl. 4, 2877-2887.

Acceleration and detection of the lunar thermal ionosphere in the presence of the lunar electric field yields a value of at least +10 v for the lunar electric potential for solar zenith angles between approximately 20° and 45° and in the magnetosheath or solar wind. An enhanced positive ion flux is observed with the ALSEP Suprathermal Ion Detector when a pre-acceleration voltage attains certain values. This enhancement is greater when the Moon is in the solar wind as opposed to the magnetosheath.

Goldstein, B. E.: 'Observations of Electrons at the Lunar Surface', *J. Geophys. Res.* 79, 23-39.

Observations of electrons at the Apollo 12 and 15 sites by the Alsep Solar Wind Spectrometer experiments showed qualitative differences. In the geomagnetic tail the Apollo 15 instrument provided measurements of lunar photoelectron flux from 5 to 40 eV; at 20 eV the flux was  $2 \times 10^6$  el (cm<sup>2</sup> s eV ster)<sup>-1</sup>. The estimated height-integrated conductivity of the photoelectron layer is  $10^{-4}$  to  $10^{-5}$  ohm<sup>-1</sup>. A theoretical model, ignoring the magnetic field, indicates that most solar wind electrons should reach the lunar surface; a lunar surface potential at the subsolar point of +5 to -3 V is calculated. At the Apollo 15 site (6-γ local magnetic field) electron densities and temperatures agree with this model. At the Apollo 12 site (38-γ local field) energetic nonsymmetric electron fluxes are observed. The data support a local space charge separation and a magnetic field of 5 km scale size or less. Downwardmoving solar wind electrons require a balancing current due to upward-moving lunar photoelectrons; this suggests that the less energetic lunar photoelectrons should decrease electron pressure on magnetic field lines connected to the Moon. When the magnetic field and solar wind velocity are approximately parallel, a solar wind density enhancement upstream of the Moon is required for pressure balance.

Griscom, D. L., Friebele, E. J., and Marquardt, C. L.: 'Evidence for a Ubiquitous, Sub-Microscopic 'Magnetite-Like' Constituent in the Lunar Soils', *Proceedings of the Fourth Lunar Science Conference, Geochim. Cosmochim. Acta* 3, Suppl. 4, 2709-2727.

Electron spin resonance (ESR) has been employed in a study of the ferromagnetic constituents of a wide variety of soils from six samples regions of the Moon as well as glasses made to simulate lunar compositions. The technique is most sensitive to both highly spherical particles of Fe metal  $\lesssim 320$  Å and equant particles of magnetic. A significant result has been that 'magnetite-like' phases (magnetic iron spinel) precipitated in and on simulated lunar glasses as a result of sub-solidus oxidation yield room-temperature ESR spectra virtually identical with the line shape predicted for spherical, single domain particles of metallic Fe. It is shown that such 'magnetite-like' phases can nevertheless be distinguished from metallic iron on the basis of the temperature dependence of the ESR intensity. Thus, the ESR spectrum of a 2-mg separate of green glass balls from 15426,78 is interpreted as arising *entirely* from 'magnetite-like' phases of the same genre as those produced in the laboratory. The total 'magnetite' concentration in this specimen is estimated to be ~0.01 wt. %.

Well established methods (e.g., computer simulation) and a variety of innovative techniques have been used to partially disentangle the effects of metallic iron and 'magnetite' in the other samples. It is inferred that all sub-mm fines samples examined may contain "magnetite-like" components in amounts ranging up to ~0.4 wt. %, roughly in proportion to the soil maturity. The probable morphologic expressions of these phases are suggested by scanning electron micrographs of the (sub-microscopic) laboratory analogs. Preliminary static magnetic studies of these synthetic 'magnetite-like' precipitates indicate that lunar 'magnetites' of similar origin may be important carriers of natural remanent magnetism.

Ivanov, N. A. and Panov, T. N.: 'Magnetic Lunar-Solar Variations, According to the Data of Vysokya Dubrava Observatory', *Geomagn. Aeron.* 13, 415-418.

Lunar-solar daily variations are investigated as a function of the seasons and of the phases of the Moon using harmonic analysis. It is found that the lunar-solar daily variation substantially reduces the daily variation of  $Z$ .

Katsube, T. J. and Collett, L. S.: 'Electrical Characteristics of Apollo 16 Lunar Samples', *Proceedings of the Fourth Lunar Science Conference, Geochim. Cosmochim. Acta* 3, Suppl. 4, 3101–3110.

Electrical parameters of 1 fine sample (66041) and 4 rock samples (60025, 62295, 66055, and 68815) from Apollo 16 flight have been measured over the frequency range from  $10^2$  to  $1.8 \times 10^8$  Hz. The purpose of these measurements is to accumulate data on the electrical characteristics of various rocks, to extend the frequency range of measurement, and to obtain data with sufficient accuracy to characterize the general trend of the electrical parameters. General trends of the 4 samples 66041, 60025, 62295, 66055, and 68815 are similar to previous measurements by various scientists. The real relative permittivity ranges from 5 to 7 and shows little variation with frequency. The parallel resistivity decreases with frequency and the dissipation factor generally decreases with frequency but shows a minimum and a maximum at about  $10^5$ – $10^7$  Hz, for certain samples. The breccia sample 66055,7 shows electrical characteristics that are unusual for a lunar sample in many ways.  $K'$  is about 10 at  $10^2$  Hz, and levels off at 3.7 from frequencies above  $3 \times 10^5$  Hz. The parallel resistivity is about  $3 \times 10^7$  ohm-m at 10 Hz, and decreases to about  $3 \times 10^4$  ohm-m at  $1.8 \times 10^8$  Hz. This parallel resistivity at the lower frequencies is perhaps the lowest ever reported for lunar rocks.  $D$  is about 0.6 at  $10^2$  Hz and decreases to about 0.001 at  $1.8 \times 10^8$  Hz. These trends for real relative permittivity, parallel resistivity and dissipation factor at the lower frequency resemble a terrestrial pyroxene or serpentinite. The electrical parameters of this rock seem to have a close relation to the apparent matrix of the specimen at the lower frequencies. These parameters at the higher frequencies seem to be related to the true matrix of the sample.

Katsube, T. J. and Collett, L. S.: 'Electrical Characteristics of Rocks and Their Application to Planetary and Terrestrial EM-Soundings', *Proceedings of the Fourth Lunar Science Conference, Geochim. Cosmochim. Acta* 3, Suppl. 4, 3111–3131.

It is essential to have a good understanding of the conductive and dielectric mechanism of the rocks in order to lay a basis for future planetary and terrestrial and EM-sounding. There has been a rapid increase of data on electrical measurements for lunar and terrestrial rocks over the last few years. Based on these data it is possible to characterize the trends for real relative permittivity, parallel resistivity, and dissipation factor for many rocks over the frequency range from about 1.0 to  $10^8$  Hz. These trends suggest that from a macroscopic view grain boundaries, insulating and low resistivity minerals are important elements in determining the conductive and dielectric mechanism of rocks in general. There are cases where the dielectric relaxation are also thought to be of importance. At frequencies below the critical frequencies, the effect of insulating materials and grain boundaries vertical to the electric current are important for dry rocks, and the effect of the grain boundaries parallel to the current is dominant for rocks which contain water or other liquids. At frequencies above the critical frequency, the effect of low resistive minerals may be dominant for dry rocks and low porosity moist rocks. These studies on the conductive and dielectric mechanism indicate that, (1) there is a possibility for radar techniques to be useful in detecting conductive materials, (2) information on the content and conductivity of moisture or other liquids contained in the rocks might be obtained by a combination of LF and HF electromagnetic sounding methods, and (3) there are indications that grain boundaries and critical frequency concepts apply to rocks at elevated temperatures.

Manka, R. H. and Michel, F. C.: 'Lunar Ion Energy Spectra and Surface Potential', *Proceedings of the Fourth Lunar Science Conference, Geochim. Cosmochim. Acta* 3, Suppl. 4, 2897–2908.

The acceleration model for lunar ions and the resulting ionosphere dynamics are reviewed briefly. An application is made to lunar atmosphere trapped in the surface fines, and the enhancement in the  $Ar^{40}/Ar^{36}$  ratio in samples from the Apennine Front compared to the adjacent mare is calculated

to be  $\sim 2.0$ . The predicted lunar ion energy spectra is shown and found to agree well with Suprathermal Ion Detector measurements; from this spectra, the neutral atmosphere scale height can be studied and the neutral atmosphere number density is found to be  $1$  to  $3 \times 10^5 \text{ cm}^{-3}$  at the sunrise and sunset terminators. The lunar surface potential is calculated and is found to be several volts positive over much of the sunlit face of the Moon but to go tens of volts negative at the terminator.

Meyer, J. W., Baker, R. H., and Johnson, L. B.: 'Surface Electrical Properties Experiment Study Phase; Volume 1', (Final Report), NASA-CR-128918.

The evolution of a conceptual design of the flight hardware for the surface electrical properties experiment (SEP), the definition of requests for proposals, the analysis of proposals submitted by prospective flight hardware subcontractors, and recommendations for the flight configuration to be implemented are discussed. Initial efforts were made to assess the electromagnetic environment of the SEP experiment. An EMI receiver and tri-loop antenna were constructed and tests of opportunity were performed with a lunar roving vehicle. Initial analyses were made of data from these tests with support from this contract, analyses which were continued in depth under the hardware contract.

Meyer, J. W., Baker, R. H., and Johnson, L. B.: 'Surface Electrical Properties Experiment Study Phase; Volume 2', (Final Report), NASA-CR-128919.

The choice of an antenna for a subsurface radio sounding experiment is discussed. The radiation properties of the antennas as placed on the surface of the medium is examined. The objective of the lunar surface electrical properties experiment is described. A numerical analysis of the dielectric permittivity and magnetic permeability of a subsurface domain is developed. The application of electromagnetic field measurements between one or more transmitting antennas and a roving receiving station is explained.

Meyer, J. W., Baker, R. H., and Johnson, L. B.: 'Surface Electrical Properties Experiment Study Phase; Volume 3', (Final Report), NASA-CR-128920.

The reliability and quality assurance system and procedures used in developing test equipment for the Lunar Experiment projects are described. The subjects discussed include the following: (1) documentation control, (2) design review, (3) parts and materials selection, (4) material procurement, (5) inspection procedures, (6) qualification and special testing, and failure modes and effects analysis.

Nagata, T.: 'Piezo-Remanent Magnetization of Lunar Rocks', *Pure Appl. Geophys.* **110**, 2022–2030.

Characteristics of the piezo-remanent magnetization (PRM) of lunar rocks are particularly interesting in comparison with the PRM of terrestrial rocks, because ferromagnetic constituents in lunar materials are metallic iron grains whose average magnetostriction coefficient ( $\lambda$ ) is negative. Experimentally observed characteristics of the PRM of lunar rocks are substantially the same as those of the PRM of terrestrial rocks and magnetites, in which  $\lambda$  is positive. These experimental results indicate that the acquisition mechanism of PRM is due to a non-linear superposition of the magnetoelastic pressure upon the magnetostatic pressure on both sides of the  $90^\circ$  domain walls in ferromagnetic particles, as suggested by Nagata and Carleton.

Nagata, T., Fisher, R. M., Schwerer, F. C., Fuller, M. D., and Dunn, J. R.: 'Magnetic Properties and Natural Remanent Magnetization of Apollo 15 and 16 Lunar Materials', *Proceedings of the Fourth Lunar Science Conference, Geochim. Cosmochim. Acta* **3**, Suppl. 4, 3019–3043.

The basic magnetic characteristics and the intensity and stability of the natural remanent magnetization of five Apollo 15 materials (15058, 15418, 15495, 15555, and 15556) and eight Apollo 16 materials

(60255, 60315, 65010, 66055, 66095, 67455, 68415, and 68815) have been examined. The anorthositic highland materials containing only 4–9% of FeO have a considerably smaller paramagnetic susceptibility in comparison with the lunar mare materials.

The ferromagnetic constituent in all these highland materials including igneous rocks consists of both essentially pure metallic iron and a considerable amount of kamacite. An appreciable fraction of the ferromagnetic metal grains are in the form of extremely fine particles which behave superparamagnetically or even pseudo-paramagnetically at room temperature. Hence their saturation remanent magnetization and coercive force increase considerably with decreasing temperature down to 4.2K, continuously in some samples and discontinuously in others. The smallest estimated size of the fine particles is 40 Å or less in mean diameter.

The natural remanent magnetization (NRM) of Apollo 15 and 16 rocks seems to be composed of a soft component and a hard and stable component. The soft component can be demagnetized easily by AF-fields of 15–30 Oe rms and sometimes its direction is much different from that of the stable component, so that the soft component can be regarded as a result of magnetic contamination. The intensity and direction of the stable component of NRM is approximately invariant against AF-demagnetization up to 200 Oe rms or more. It seems that rocks with large remanence coercive force can maintain a larger and more stable remanent magnetization. The intensity of the stable NRM obtained as a result of magnetic cleaning amounts to  $(0.9\text{--}11) \times 10^{-6}$  emu gm<sup>-1</sup>. These stable NRM's can be attributed to the thermoremanent magnetization acquired in a magnetic field of 800–3000 γ or to the piezoremanent magnetization acquired by a uniaxial compression of 50 Kbar in a field of 200–400 γ.

Olhoeft, G. R., Strangway, D. W., and Frisillo, A. L.: 'Lunar Sample Electrical Properties', *Proceedings of the Fourth Lunar Science Conference, Geochim. Cosmochim. Acta* **3**, Suppl. 4, 3133–3149.

Electrical conductivity and dielectric constant measurements have been performed in vacuum on solid and soil samples over a wide range of temperatures and frequencies. The temperature dependence and the frequency response of the dielectric properties together with the temperature dependence of the DC conductivity have permitted us to propose a mathematical model describing the mechanisms controlling the electrical properties. In general, each lunar sample has several distributed mechanisms, each mechanism dominant in a particular temperature range.

Parkin, C. W., Dyal, P., and Daily, W. D.: 'Iron Abundance in the Moon from Magnetometer Measurements', *Proceedings of the Fourth Lunar Science Conference, Geochim. Cosmochim. Acta* **3**, Suppl. 4, 2947–2961; also NASA-TM-X-62279.

Apollo 12 and 15 lunar surface magnetometer data with simultaneous lunar orbiting Explorer 35 data are used to plot hysteresis curves for the whole Moon. From these curves a whole Moon permeability  $\mu = 1.029^{+0.024}_{-0.019}$  is calculated. This result implies that the Moon is not composed entirely of paramagnetic material, but that ferromagnetic material such as free iron exists in sufficient amounts to dominate the bulk lunar susceptibility. From the magnetic data the ferromagnetic free iron abundance is calculated. Then for assumed compositional models of the Moon the additional paramagnetic iron is determined, yielding total lunar iron content. The calculated abundances are as follows: ferromagnetic free iron,  $5 \pm 4$  wt.%; total iron in the Moon,  $9 \pm 4$  wt. %.

Pearce, G. W., Gose, W. A., and Strangway, D. W.: 'Magnetic Studies on Apollo 15 and 16 Lunar Samples', *Proceedings of the Fourth Lunar Science Conference, Geochim. Cosmochim. Acta* **3**, Suppl. 4, 3045–3076.

The magnetic properties of lunar samples are almost exclusively due to rather pure metallic iron. The mare basalt contains about 0.06 wt. % Fe, the soils 0.5–0.6 wt. %, and the breccias 0.3–1.0 wt. %. Most of the additional iron in the soils and breccias is believed to be the result of reduction processes operating on the lunar surface. Whereas the total metallic iron content of the soils from all landing sites is rather constant, the Fe<sup>0</sup>/Fe<sup>++</sup> ratio and the average iron grain size increases with the age of

the landing site reflecting increasing maturity. The crystalline rocks studied from Apollo 16 have highly variable, but generally, very high metallic Fe content (up to 1.7 wt. % Fe). It is suggested that these rocks are either breccias or igneous samples which have been severely thermally metamorphosed in a highly reducing environment. Many lunar basalts and breccias contain a magnetization which is stable against AF demagnetization, although results on an Apollo 12 sample returned to the Moon with the Apollo 16 mission show that the samples can acquire a strong isothermal remanence during handling. A conglomerate test on 16 surface oriented samples shows that their stable remanent magnetization was acquired before they were last put on the lunar surface. The stable magnetization of mare basalts is typically  $1-2 \times 10^{-6}$  emu  $\text{gm}^{-1}$ . The stable component in breccias varies over a wide range but there is a class of breccias with a stable remanence of about  $1 \times 10^{-4}$  emu  $\text{gm}^{-1}$ .

Rao, K. S. R. and Reddy, S. J.: 'Variation of Lunar and Solar Geomagnetic Tides with Sunspot and Geomagnetic Activity', *Pure Appl. Geophys.* **111**, 2291–2299.

Solar and lunar geomagnetic tides in  $H$  at Alibag have been determined by spectral analysis of discrete Fourier transforms following the method of Black and the well-known Chapman-Miller method. The seasonal variation in  $L_2(H)$  is opposite to that in  $L_2(D)$ , with maximum in the  $d$  season and minimum in the  $j$  season. In both  $H$  and  $D$  the enhancement due to sunspot activity is larger in lunar tide than in solar tide. Surprisingly, the enhancement due to magnetic activity is greater in  $L_2(H)$  than in  $S_1(H)$ , while the contrary is true for declination. It is inferred that there is a local time component of the storm time variation contrary to the view expressed by Green and Malen. The enhancements in amplitudes  $L_2$  and  $S_1$  in  $H$  and  $D$ , due to sunspot activity and due to magnetic activity, have been separated. The results show that the amplitude at zero sunspot number increases with magnetic activity in all the four parameters, while the enhancement due to sunspot activity at different levels of magnetic activity decreases with increase of  $K_p$ . But if both  $K_p$  and  $R$  are increasing, when  $K_p$  increases enhancement due to  $R$  decreases and when  $R$  increases enhancement due to  $K_p$  decreases.

Rastogi, R. G.: 'Lunar Effects in the Counter Electrojet Near the Magnetic Equator', *J. Atmospheric. Terrest. Phys.* **36**, 167–170.

The examination of  $H$  magnetograms of Huancayo for the period, 1948–1971, has shown that the negative effects on the daily variation of  $H$  occur primarily in the morning hours around 07 hr and in the evening between 15 and 17 hr. The occurrence of the evening event is maximum around lunar ages 1.4 and 13.4 hr or around lunar times 2.2 and 14.2 hr. The occurrence of the morning events is maximum around lunar ages 4.8 and 16.8 hr or around lunar times 2.3 and 14.3 hr. These lunar times correspond to that of maximum negative effect in  $H$  due to lunar tidal wave. These counter electrojet effects are suggested to be due to the superposition of lunar semi-diurnal wave over the solar daily wave of  $H$ . The late appearance of sporadic- $E$  in the morning or the earlier disappearance of  $E_s$  in the evening is due to these counter electrojet events, when the ionospheric currents over the equatorial regions are reversed to westward direction during the daylight hours.

Rich, F. J., Reasoner, D. L., and Burke, W. J.: 'Plasma Sheet at Lunar Distance: Characteristics and Interactions with the Lunar Surface', *J. Geophys. Res.* **78**, 8097–8112.

The plasma sheet at lunar distance is investigated with the use of data from the charged particle lunar environment experiment (CPLLE), complemented with data from the Explorer 35/ARC magnetometer. It is shown that the presence of the lunar surface does not appreciably affect measurements of the plasma sheet characteristics by the lunar-based CPLLE instrument. In particular, the lunar surface generally does not shadow plasma sheet particles. This may be due to rapid random passage ( $> 40 \text{ km s}^{-1}$ ) of magnetotail field lines with respect to the lunar surface or to diffusion of plasma sheet electrons into the flux tubes in contact with the lunar surface. The plasma sheet is generally observed as a rapid increase in observed particle fluxes and a simultaneous decrease in

field strength. Analysis of the CPLEE data shows that, for the plasma sheet at lunar distance, typical quiet time parameters are  $n = 0.10 \pm 0.05 \text{ cm}^{-3}$ ,  $kT_e = 200 \pm 50 \text{ eV}$ , and  $kT_i = 2.5 \pm 0.75 \text{ keV}$ . The typical ranges for the parameters are  $0.05\text{--}0.20 \text{ cm}^{-3}$  for  $n$ ,  $175\text{--}325 \text{ eV}$  for  $kT_e$ , and  $1\text{--}5 \text{ keV}$  for  $kT_i$ . The typical total (plasma plus magnetic) energy density is in the range  $150\text{--}350 \text{ eV cm}^{-3}$ . A statistical analysis of the CPLEE data shows that the plasma sheet in the midnight sector has a thickness of  $5 R_E \pm 2 R_E$ . Geomagnetic activity reduces the probability of encounters between the moon and the plasma sheet. This finding is consistent with the concept that geomagnetic activity increases the variance of the plasma sheet from its average location and/or decreases its thickness.

Russell, C. T., Coleman, P. J., Lichtenstein, B. R., Schubert, G., and Sharp, L. R.: 'Subsatellite Measurements of the Lunar Magnetic Field', *Proceedings of the Fourth Lunar Science Conference, Geochim. Cosmochim. Acta* 3, Suppl. 4, 2833–2845.

The Apollo 15 subsatellite magnetometer data have been used to map the lunar magnetic field over a narrow band of the lunar surface. Within this band the magnetic field is generally stronger and more variable over the farside highlands than the nearside maria. The correspondence between the strong variable lunar field regions and the source regions for limb compressions suggests that limb compressions arise as the result of the deflection of the solar wind just upstream of the terminator by the lunar magnetic field. Using this apparent relationship between field strength and limb compressions source regions, we deduce that the field strength in the northern farside highlands is not as strong as in the southern hemisphere at similar longitudes. This agrees with Apollo 16 subsatellite measurements in the northern hemisphere but closer to the equator.

Fourier analysis of the orbital plane components of the lunar magnetic field at 100 km altitude places an upper limit of  $2.1 \times 10^{18} \text{ G-cm}^3$  on the present day lunar magnetic dipole moment in the orbital plane. If the total magnetic dipole moment is parallel to the rotation axis of the Moon, this measurement places an upper limit of  $4.4 \times 10^{18} \text{ G-cm}^3$  on the lunar moment. This is  $5 \times 10^{-8}$  of the Earth's magnetic moment.

Simultaneous measurements of the interplanetary magnetic field obtained by Explorer 35 and the Apollo 15 subsatellite above the dayside hemisphere are essentially identical. Thus, both instruments are measuring the undisturbed interplanetary field. Exceptions to this rule occur near the lunar limbs where the occasional occurrence of limb compressions and the possible influence of upstream wave phenomena cause differences between the two sets of data. Thus, if the regions of the terminators and of the lunar cavity are avoided the subsatellite magnetometer measurements can be used as a measure of the driving function in lunar conductivity studies.

Schubert, G., Schwartz, K., Sonett, C. P., Colburn, D. S., and Smith, B. F.: 'Lunar Electromagnetic Scattering. II: Magnetic Fields and Transfer Functions for Parallel Propagation', *Proceedings of the Fourth Lunar Science Conference, Geochim. Cosmochim. Acta* 3, Suppl. 4, 2909–2923.

Magnetic field and transfer function amplitudes, resulting from a transverse electromagnetic wave in the interplanetary medium scattering from the Moon and its diamagnetic cavity, are presented. Calculations are made using the asymmetric scattering theory of Part I for a spherical two-layer model of the lunar electrical conductivity profile and a nonconducting cylindrical model of the downstream lunar plasma void. Both the field and transfer function magnitudes are calculated as functions of position on the surface of the Moon for frequencies relevant to the observations of the lunar surface and orbiting magnetometers. The amplitudes of the magnetic field components on the cavity boundary are also computed as functions of frequency and distance downstream from the lunar limb. Comparisons of the results are made with those of (1) spherically symmetric descriptions of lunar electromagnetic scattering, (2) the quasistatic approximation to asymmetric scattering theory, and (3) observations of the scattering phenomenon by lunar surface and orbiting magnetometers. The quasistatic approximation qualitatively accounts for all aspects of the scattering process except for the propagating cavity surface wave and the interference of different orders of multipole response at high frequency. Asymmetric scattering theory can apparently explain the many features of lunar induction observed by the Apollo and Explorer magnetometers. The numerical finite difference calculation of Riesz *et al.* for scattering from a cylindrical Moon-slab cavity model is either in error or does not describe scattering from a spherical Moon-cylindrical cavity model.

Schwerer, F. C., Huffman, G. P., Fisher, R. M., and Nagata, T.: 'Electrical Conductivity of Lunar Surface Rocks at Elevated Temperatures', *Proceedings of the Fourth Lunar Science Conference, Geochim. Cosmochim. Acta* 3, Suppl. 4, 3151–3166.

The electrical conductivity of several lunar surface rocks has been measured in the temperature range 20–850°C in atmospheres adjusted to be either reducing or oxidizing with respect to the original material. Specific samples studied were from an Apollo 11 breccia (10048) and from a basalt and a recrystallized breccia from the Apollo 15 suite (rocks 15555 and 15418, respectively). Similar measurements were made for several terrestrial pyroxenes. For all samples studied, the electrical conductivity was observed to depend in a complex fashion on the furnace atmosphere and prior thermal history; however, the data obtained for specified sets of conditions were reproducible. Data for lunar samples measured under potentially reducing conditions were similar to those measured during the initial heating of the samples and are presented as representative of the pristine Apollo material. The conductivity values measured under these conditions indicate that some of the returned lunar rocks are among the least electrically conducting natural bulk materials reported. Mössbauer spectroscopy ( $\text{Fe}^{57}$  indicator) was used to characterize the dependence of the electrical conductivity on furnace atmosphere, and the results support the expectation that the conductivity of the anhydrous silicate phases is influenced principally by the concentration, oxidation state, and distribution of multivalent cations, most notably iron. The distribution of iron among various mineral phases and oxidation states for several Apollo 16 samples was determined by Mössbauer spectroscopy.

Tsay, F.-D.: 'Relaxation Times of Remanent Magnetisation in Lunar Fines', *Nature Phys. Sci.* 246, 76–77.

On the basis of the observed equivalence between  $H_{RC}$  and  $2K_1/M_s$  for the Apollo 11–16 fines, it seems that the bulk of metallic Fe particles in the lunar fines are essentially spherical and have a short remanent relaxation time. These spherical metallic Fe particles could account for the apparently low blocking temperature observed for the unstable components of the NRM detected in the returned lunar samples. In view of the ease with which the ESR technique can distinguish between shape and crystalline anisotropy effects, it seems that the technique is particularly valuable for identifying the carriers of various NRM components having differing degrees of thermal stability.

## 15. Exploration of the Moon by Spacecraft

Alekseyev, V., Lebedev, L., and Narimanov, G. S.: 'For Lunar Rock', NASA-TT-F-14983.

A discussion is reported of the spaceflights by Soviet devices to the Moon and the results of the research which they carried out on the lunar surface. The work performed by the Lunokhod-1 is described and the results of an analysis of the samples of lunar rock brought back to Earth by the Luna-16 are presented. Data are included on the flight of the Luna-20 station which brought material from the lunar mountains.

Buck, S. W.: 'Traverse Gravimeter Experiment', (Final Report), NASA-CR-128948.

A semiautomatic self-leveling lunar gravimeter has been designed for the Apollo 17 mission. This traverse gravimeter, which is completely self-contained and powered by an internal battery, was used to measure gravity at predetermined stops along the route of the Lunar Rover Vehicle. The gravity sensor is a vibrating string accelerometer (VSA) enclosed in a temperature-controlled oven and gimballed leveling assembly. This instrument is capable of resolving gravity differences as small as 0.035 mgal (1 mgal =  $0.001 \text{ cm s}^{-2}$ ) on the Moon and yet also is able to measure the Earth's gravity field of 980000 mgals. Twenty-two measurements were taken on the Moon during the Apollo 17 mission, during which the VSA temperature never varied more than 0.005°C. The flight results indicate an instrument accuracy of better than 2 mgal.

Bulekov, V. P., Graf, L. É., Dryuchenko, D. D., Zakhar'ev, B. V., Motovilov, É. A., Smorodinov, M. I., Strellov, Yu, N., and Shvarev, V. V.: 'Soil Sampling on the Lunar Surface with the Automatic Lunar Station Luna 20', *Cosmic Res.* **11**, 406–409.

On February 14, 1972, the Soviet automatic station Luna 20 was launched towards the Moon. The main goal of the experiment conducted with this station was the delivery of soil from a lunar mare region. Therefore, Luna 20 was supplied with soil-collection apparatus and on the lunar landing stage the return rocket was deployed which delivered the collected soil to the Earth.

Dunkin, J. H., Pekar, P. R., Spadoni, D. J., and Stone, C. A.: 'Cost Estimation for Unmanned Lunar and Planetary Programs', NASA-CR-131897.

A basic model is presented for estimating the cost of unmanned lunar and planetary programs. Cost data were collected and analyzed for eight lunar and planetary programs. Total cost was separated into the following components: labor, overhead, materials, and technical support. The study determined that direct labor cost of unmanned lunar and planetary programs comprises 30% of the total program cost. Twelve program categories were defined for modeling: six spacecraft subsystem categories (science, structure, propulsion, electrical power, communications, and guidance and integration, test and quality assurance, launch and flight operations, ground equipment, systems analysis and engineering, and program management). An analysis showed that on a percentage basis, direct labor cost and direct labor manhours compare on a one-to-one ratio. Therefore direct labor hours is used as the parameter for predicting cost, with the advantage of eliminating the effect of inflation on the analysis.

Gurshtein, A.: 'The Achievements of Lunokhod-2', *New Scientist* **61**, 190–192.

A year ago, the Soviet Union's second automatic lunar rover – Lunokhod-2 – landed in a border area of the Moon where lunar mare meets upland relief. Despite working actively for some four lunar days only, compared to the ten lunar days of Lunokhod-1, the second vehicle made many successful measurements.

NASA, L. B. Johnson, Space Center: 'Apollo 17 Mission Report', NASA-TM-X-69292.

Operational and engineering aspects of the Apollo 17 mission are outlined. The vehicle configuration was similar to those of Apollo 15 and 16. There were significant differences in the science payload for Apollo 17 and spacecraft hardware differences and experiment equipment are described. The mission achieved a landing in the Taurus-Littrow region of the moon and returned samples of the pre-Imbrium highlands and young craters.

Muehlberger, W. R. and Wolfe, E. W.: 'The Challenge of Apollo 17', *Amer. Scientist* **61**, 660–669.

The contribution of the last manned lunar landing to the knowledge of the Moon's geological history is outlined.

Mundt, F. D., Schreyer, J. M., and Wampler, W. E.: 'Apollo Lunar Sample Return Container', Oak Ridge Y-12 Plant, Tenn.

A description is given of the design and manufacture of Apollo lunar sample return containers and their associated sample collection devices. The containers were successful in providing adequate storage and protection for lunar samples and maintained these samples in a near-lunar environment during their travel to the Earth.



NASA, L. B. Johnson Space Center: 'Apollo 17 Mission 5-Day Report', NASA-TM-X-69527.

A five day report of the Apollo 17 mission is presented. The subjects discussed are: (1) sequence of events, (2) extravehicular activities, (3) first, second, and third lunar surface extravehicular activity, (4) transearth extravehicular activity, (5) lunar surface experiments conducted, (6) orbital science activities, (7) spacecraft reentry and recovery.

Nishioka, K., Arno, R. D., Alexander, A. D., and Slye, R. E.: 'Feasibility of Mining Lunar Resources for Earth Use: Circa 2000 AD; Volume I: Summary', NASA-TM-X-62267.

The feasibility of obtaining lunar minerals for terrestrial uses is examined. Preliminary results gave indications that it will not be economically feasible to mine, refine, and transport lunar materials to Earth for consumption. A broad systems approach was used to analyze the problem. It was determined that even though the procedure was not economically advisable, the concept for the operations is technically sound.

Nishioka, K., Arno, R. D., Alexander, A. D., and Slye, R. E.: 'Feasibility of Mining Lunar Resources for Earth Use: Circa 2000 AD; Volume 2: Technical Discussion', NASA-TM-X-62268.

The technologies and systems required to establish the mining base, mine, refine, and return lunar resources to Earth are discussed. Gross equipment requirements, their weights and costs are estimated and documented. The operational requirements are analyzed and tabulated. Diagrams of equipment and processing facilities are provided.

Vinogradov, A. and Surkov, Yu.: 'Current Achievements in Astronautics', NASA-TT-F-14929.

Soviet automatic stations carried out a wide range of investigations of Mars and Venus. Luna-20 brought soil from the continental region of the Moon back to Earth. The Prognoz satellites are on 24-hr watch along the Earth. A number of important agreements were reached between the U.S.S.R. and the U.S.A. in the area of the investigation of space. This collection, basically compiled from materials published in the central printing office, discusses these achievements and the commentaries of well-known Soviet scientists.